SAE Baja: Suspension, Steering, & Brakes

Report 2

Colby Brett, Rear Suspension Design and Manufacturing Specialist, Website Designer

Jose Avitia, Budget Liaison, Rear Suspension Asst.

James Cole, Front Suspension Lead, Engineering Calculations Proofreader

Jakob Martinez, Steering Lead

James Sundeen, Sub-Team Lead, Suspension Design

Marc Angelo Maquiling, Brake Lead, Front Suspension Asst., Finance Co-Lead

Fall 2025-Spring 2026

Instructor: David Willy

DISCLAIMER

This report was prepared by students as part of a university course requirement. While considerable effort has been put into the project, it is not the work of licensed engineers and has not undergone the extensive verification that is common in the profession. The information, data, conclusions, and content of this report should not be relied on or utilized without thorough, independent testing and verification. University faculty members may have been associated with this project as advisors, sponsors, or course instructors, but as such they are not responsible for the accuracy of results or conclusions.

EXECUTIVE SUMMARY

The suspension system of an off-road vehicle is crucial to its overall performance, handling, and long-term durability. In the Baja SAE competition, students are challenged to design and manufacture a vehicle capable of navigating rugged terrain, absorbing harsh impacts, and maintaining stability across a wide range of dynamic events that test every subsystem. Achieving efficient and effective performance requires close coordination between the suspension, steering, and braking subsystems to ensure predictable maneuverability, consistent wheel control, and driver safety. This report summarizes the design improvements made after the initial prototype iteration and presents the analyses and calculations that guided the updated suspension design.

The current steering knuckle design achieves a factor of safety of 5, exceeding the engineering requirement of 3 and providing a strong margin for off-road loading conditions. In this iteration, the team is implementing a two-stage portal hub design to increase ground clearance and reduce drivetrain loading through staged gear reduction. The knuckle geometry has been refined to ensure proper integration with the portal hub assembly and surrounding suspension components, supporting improved durability, reliability, and predictable handling while simplifying overall assembly.

The updated front control arm design was analyzed under four times the static load to simulate competition conditions, yielding factors of safety as low as 1.23, above the required 1.2. Design improvements include shifting the upper arm closer to the chassis for increased shock clearance and integrating the Heim joint mounting points into an outer member, resulting in a stronger and more efficient assembly. These changes enhance durability, clearance, and overall suspension performance.

Additional engineering analyses were completed to validate the rack-and-pinion steering system under a worst-case crash load of 2,928 lbf per tie rod. Euler buckling calculations for the 14-in 6061-T6 aluminum tie rods established a required inner diameter of 0.667 in, and the selected 0.652-in inner diameter meets this requirement while remaining in the elastic buckling range. Thread-shear evaluation of the 3/8-24 Heim joints produced a factor of safety of 10.24, confirming sufficient load capacity. A static FEA showed a maximum deformation of about 0.9 in at the tie-rod ends under extreme loading, consistent with elastic bending. Initial prototyping also identified the steering rack being installed upside-down, prompting a correction and improving alignment for subsequent iterations

The rear suspension control arms were revised after the first prototype showed they were too long to meet competition regulations, with each arm shortened by 2.5 in to comply. ANSYS simulations were performed to evaluate deformation and stress under combined loads of 1,287 lbf applied at the knuckle connections. The maximum deformation observed was 0.5 in for the lower arm and 0.4 in for the upper arm, occurring near the knuckle connections. These results confirm that the redesigned rear control arms meet performance requirements while maintaining structural integrity.

The current brake design requires 2579.37 lbf of clamping force to lock out the brakes with piston diameters of 3.96 and 2.64 for front and rear, respectively. These results are taken from an analysis of the brake systems that incorporated worst-case scenarios into the calculations to allow for margins in the design. From visual inspection of the current inboard design of the brake system, the integration of the rotor-caliper assembly into the toe box with the differential is

not feasible due to spatial limitations, as the brake would protrude outside of the allotted space. Further reconfiguration of the allotted pistons and an introduction of an outboard installation of the caliper-rotor assembly must be investigated and tested due to the limitation discovered from the additional mathematical calculation and physical modeling.

TABLE OF CONTENTS

Contents

Disclaimer i
Executive Summary ii
Table of Contents iii
1 Background 5
1.1 Project Description 5
1.2 Deliverables 5
1.3 Success Metrics 5
2 Requirements 3
2.1 Customer Requirements (CRs) 3
2.2 Engineering Requirements (ERs) 4
2.3 House of Quality (HoQ) 6
3 Research Within Your Design Space 8
3.1 Benchmarking 8
3.2 Literature Review 8
3.3 Mathematical Modeling 17
4 Design Concepts 27
4.1 Functional Decomposition 27
4.2 Concept Generation 27
4.3 Selection Criteria 32
4.4 Concept Selection 35
5 Schedule and Budget 42
5.1 Schedule 42
5.2 Budget 43
5.3 Bill of Materials 44
6 Design Validation 45
6.1 Failure Modes and Effects Analysis 45
6.2 Initial Prototyping 49
6.3 Other Engineering Calculations 54
6.4 Future Testing Potential 65
7 Conclusion 67
8 References 68
9 Appendices 74
9.1 Appendix A: VSusp 74
9.2 Appendix B: FMEA Charts 76
9.3 Appendix C: MATLAB Code 79
9.4 Appendix D: Optimum Kinematics 85
9.5 Appendix E: Bill of Materials 89

1 BACKGROUND

This chapter of the report will go over the suspension team's role withing the NAU SAE Baja capstone. It introduces the project's purpose, scope, and key objectives for the team The sections that follow include a project description, the expected deliverables, and the success metrics that define a successful project. Together these sections establish the understanding of the team's goals, design approach, and criteria for defining a successful project.

1.1 Project Description

The suspension sub-team within the NAU Baja capstone is responsible for the vehicles' handling, driver control, and dynamic stability of the vehicle. The suspension sub-team consists of different sub-systems which include steering, brakes, and suspension design. Each of these sub-systems play a crucial role in the vehicles performance in the competition. The Society of Automotive Engineers (SAE) challenges students to apply the knowledge to design and manufacture an off-road capable vehicle. This project is important because it not only test the knowledge of the students on the topic but also puts us in an environment we would see in the real-world, collaborating with different teams, meeting strict deadlines and standards.

The NAU SAE Baja team was allocated $5,000 from a donation made from GORE for any purchasing, registration, and R&D costs for the whole team. A big part of this project is to so fundraising. The team plans to do some fundraising to cover the costs of the suspension sub-team which is about $4,000.

1.2 Deliverables

There are numerous deliverables that the suspension team has the responsibility of completing. A large portion of the deliverables are centered around progress presentations and prototyping. A major deliverable for the suspension team for the current cycle is the progress presentation of the suspension, steering, and brake design. Theoretical testing through rough calculations was used to determine the feasibility of the designs presented by the suspension team. Through these calculations, the preliminary final design of each of the components of the suspension assembly can be chosen for further testing and prototyping. The prototyping of the chosen components for the suspension system allows for greater analysis of each part as they interact with the whole system, which allows for problems to be seen and answered before the team moves on design finalization and manufacturing cycle. These deliverables can help determine the direction of the team and the accuracy of the team's design in relation to the customer, engineering, and competition requirements.

1.3 Success Metrics

The success of the Suspension, Steering, and Braking sub team will be evaluated using a variety of tools such as Optimum Kinematics and ANSYS. These two software programs will allow us to validate our designs through various simulations that will allow us to design our failure points into the bolts used for mounting with a minimum safety factor of 1.3 of a maximal load case. Therefore, when something breaks in competition it will be in a place that is relatively easy to fix. In the first semester. Success will be having a functioning assembly of the suspension system tested in ANSYS to find the current failure points and how we can address those points.

1.3.1 Testing

Optimum Kinematics Testing
Vehicle Simulation Software (VSS) data will be used to verify camber, caster, toe, and roll center behavior throughout the full suspension travel range.
Target: Achieve consistent camber gain and minimal bump steer across suspension articulation.
Reference: Insert VSS output values.

ANSYS Static, Buckling, and Vibration Analysis

Suspension:
Identify maximum stress regions and design failure points at mounting bolts and control arm joints.
Success Criterion: All critical stress values remain below the material yield stress with a factor of safety ≥ 2.0.

Steering:
Conduct buckling analysis of tie rods and perform vibrational mode analysis to ensure driver-perceived vibration is minimized.
Success Criteria: First natural frequency exceeds engine vibration frequency range; mounting brackets maintain full structural integrity under cornering and impact loads.

Braking System:
MATLAB simulation evaluates braking force under various load conditions.
Success Criteria: System achieves required deceleration with calculated brake-line pressure corresponding to realistic driver pedal input.

1.3.2 Results (Preliminary Measured Values)

Suspension Travel: 12.5 inches measured at the wheel under full compression and rebound.

Camber Range: 0° to −4°; with an ideal operational camber angle of −1° to −2° for travel between 3–9 inches.

Braking Clamping Force: Achieved lockout of brakes using estimated vehicle parameters.

Kinematic Consistency: No measurable bump steer or interference throughout travel

Structural Integrity: All analyzed components meet FEA safety factors and vibrational limits for Baja terrain loading.

2 REQUIREMENTS

This chapter presents the customer requirements and engineering requirements for the baja suspension sub teams. The customer requirements are primarily made from the SAE Baja competition rules and team expectations, ensuring that the vehicle meets all safety, performance, and durability standards for competition. The engineering requirements translate the customer requirements into quantifiable design targets. Each requirement is expressed using measurable parameters to guide design and verify systems are working as intended.

2.1 Customer Requirements (CRs)

2.1.1 Front suspension

1. Simplicity: The design of the suspension arms must be designed in a way that does not burden the manufacturer, with minimal unique parts and simple geometry.
2. Affordability: The front suspension components must be cost-effective, without diminishing the structural integrity or performance of the system.
3. Reliability: Components must be able to consistently handle the rigorous conditions that they will be subject to throughout the competition.
4. Durability: Must be able to withstand the high dynamic loads experienced throughout the competition. The design should ensure long-term structural integrity throughout the life of the vehicle.

2.1.2 Rear suspension

1. Simplicity: Designs must be manufactured with minimal parts and be easy to install or replace
2. Affordability: Each part of the member must have efficient material use while not sacrificing structural integrity or performance
3. Reliability: Components must handle all the rigorous conditions throughout the competition
4. Durability: The system must be able to withstand the high dynamic loads seen in the competition while also being able to handle the continual load of the car.

2.1.3 Steering

1. Responsive Handling: The driver should be able to make quick and precise steering inputs
2. Reliability: The steering must function consistently throughout all competition events without failure.
3. Lightweight design: Should not significantly increase the vehicles overall weight.

4. Durability: Must be able to withstand continuous vibrations, dynamic loads, and impacts without failure.
5. Safety: No binding, jamming, or excessive play that could cause loss of control
6. Ease of Maintenance: Easy to inspect, replace, or adjust components with limited time

2.1.4 Brakes

1. Simplicity: Simple installation and maintenance of the whole brake assembly
2. Durability: Brake assembly to last through testing, trials, and competition course with no substantial changes or repairs, lasting through different loads, vibration, and different elements
3. Compactness: Brake assembly must not obstruct with other major onboard systems – differential casing, constant velocity boot, etc. – and must provide enough ground clearance and clearance for frame assembly
4. Lightweight: Brake assembly to provide major changes to the overall unsprung mass of the vehicle while providing the required performance and reliability
5. Safety: Brake assembly to provide more adequate brake torque on rotors that locks all four wheels of the vehicle at any given time, with minimal to no obstruction from the elements

2.1.5 Knuckles

1. Simplicity: Simple manufacturing, assembly and installation of the front and rear knuckles while also having a mirrorable design
2. Durability: The design must be strong enough to handle any load without any malfunctions through the entire competition
3. Compact: Small designs to fit within the diameter of the wheel but also create distance between the members of the double wishbone suspension

2.2 Engineering Requirements (ERs)

2.2.1 Front suspension

1. Minimal use of unique parts - ≤ 4

   To keep the design simple and to make the most of symmetry between the front and rear suspension systems, the number of unique parts must be less than or equal to four.

2. Suspension travel - 12”-15”

   The front suspension shall provide a wheel travel of 12”-15”, measured from the center of the wheel, to ensure adequate ground clearance and performance without diminishing vehicle stability.

3. Design failure points to be at the bolts for ease of repair

The assembly should be designed so that, if failure were to occur, it would occur at the bolts rather than the members, for ease of repair/replacement.

2.2.2 Rear suspension

1. Minimal use of Unique parts
    a. Use symmetry for the left and right sides of the car
2. 12”-15” of travel measured from the center of the wheel
3. Design failure points are at the bolts connecting the heim joints to the knuckle and frame for easy repair

2.2.3 Steering

1. Maximum Steering Effort - $\leq 30\ lbs$

    The maximum force required by the driver to turn the steering wheel under static or low-speed conditions. This ensures comfortable, responsive control during tight maneuvers.

2. Minimum Turning Radius - $\leq 7\ ft$

    The vehicle must be able to achieve a turning radius that is no greater than 7 ft, ensuring maneuverability through slaloms, hairpin turns, and obstacle courses.

3. Lock-to-Lock Rotation - $\leq 360°$

    The steering wheel must be able to go from lock-to-lock steering positions under 360 degrees. This allows for sufficient range for sharp turns and obstacle avoidance in the tight course sections.

4. Steering wheel play - $\leq 10°$

    The steering wheel free play before wheel response should be under 10 degrees. Limiting steering play ensures accurate driver input and improves steering precision.

2.2.4 Brakes

1. 4-wheel lockout

    All four wheels of the vehicle must stop spinning under hard braking conditions and static tests.

2. One Primary Hydraulic System

    The brake assembly must have one primary hydraulic system that controls and locks all four wheels of the vehicle. The system must also provide friction brakes to all four wheels.

3. Two Independent Hydraulic Systems

    The brake assembly must contain two independent hydraulic systems for redundancy, where if one of the two hydraulic systems fails, the other system could still provide sufficient braking on two wheels of the vehicle.

4. Minimum of 450 lbf on the Brake Pedal

   The brake pedal must withstand a minimum of 450 lbf of force applied; if using two pedals, both pedals shall withstand 2000 Newtons of force each. Locking of all the wheels must be done with one foot; if using two pedals, the pedals must be close enough in proximity for one foot to lock all wheels.

2.2.5 Knuckle

1. Max Member Connection Distance of 6 inches

   With the addition of portal hubs connecting to the knuckle designs, the knuckle must be raised to create space for the gear reduction. Since the wheel is only 10 inches in diameter, the knuckle must fit within half of the wheel. To limit the space taken by the knuckle design, the gap between the connection points of the suspension members should be as small as possible.

2. Factory of Safety ≥ 3

   A large factory of safety is needed to ensure the knuckle design will not be a failure point within the car.

2.3 House of Quality (HoQ)

Figure 2.3-1 displays the quality function deployment (QFD) of the suspension system, relating the customer and engineering requirements to each other in terms of their correlation with each other. Scores and appropriate weightages were assigned to determine each of the criterion's relevance to the suspension team's goals.

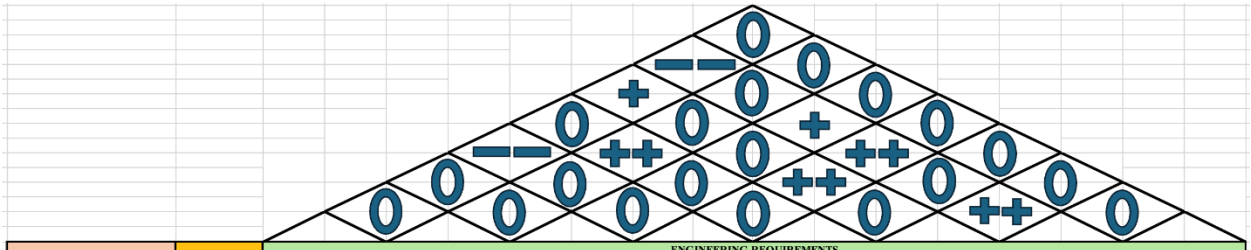

CUSTOMER REQUIREMENTS	WEIGHTAGE	ENGINEERING REQUIREMENTS							
		Maximum Steering Effort	Minimal Unique Parts	Suspension Travel (Front/Rear)	Turning Radius (Front and Rear)	Average Repair Time	Lock to Lock Rotation	Steering Wheel Play	Minimum Brake Pedal Force
Light Weight	5	1	3	1	1	1	1	1	1
Safety	5	3	1	9	9	1	3	3	3
Simple	3	3	9	3	3	9	1	1	1
Serviceable	3	1	9	3	1	9	1	1	1
Compactness	2	3	3	9	3	3	1	3	1
Affordable	2	3	3	1	1	1	1	1	1
Reliable	4	9	3	9	9	1	9	9	9
Durable	4	3	3	9	1	1	3	3	3
Responsive Handling	3	9	1	1	9	1	9	9	3
Importance Weight		119	113	163	137	83	105	109	87
Relative Importance Weight		12.99%	12.34%	17.79%	14.96%	9.06%	11.46%	11.90%	9.50%
Measurement Unit		lbs	N/A	inches	feet	minutes	Degrees	Degrees	Newtons
Target Value		30	4	12-15	7	20	360	10	2000

Figure 2.3-1: Quality Function Deployment of the Suspension System

The customer requirements were given a weight on a scale of 1-5 based on how relevant they are to achieving our design goals with 5 being the most relevant and 1 being the least relevant. Each engineering requirement was correlated to one another in the correlation matrix on the top of the QFD, with a 0 representing correlation, a + representing a positive correlation, and

a – representing a negative correlation. A double positive or double negative represents a strong correlation in their respective matters. The importance weight of each engineering requirement was calculated, and the suspension travel of the suspension arms was seen to be the most important while the average repair time was seen to be the least important.

3 Research Within Your Design Space

3.1 Benchmarking

To guide the design and performance goals of our suspension system, benchmarking of the current state of the art for Baja suspension design was conducted. This process involved observing and studying the suspension subsystems of leading Baja teams to identify proven designs. The schools selected for benchmarking were Cornell University, ETS Montreal, and Johns Hopkins University, each recognized for their consistent superior performance in previous SAE Baja competitions. The results of this benchmarking serve as a foundation for setting our own design targets and ensuring that our vehicle exceeds the performance from last year's vehicle.

3.2 Literature Review

3.2.1 Colby Brett

Race Car Vehicle Dynamics

Race car vehicle dynamics Chapter 17 applies to the design of the suspension system as it explains the differences between the different types of suspensions and important factors to consider when designing a suspension system. This chapter also includes some important calculations to do that will impact the design of the suspension system.

Double Wishbone Suspension: Precision and Performance

F. Luo Double wishbone suspension shows the advantages of utilizing a double wishbone suspension system in both the front and rear on an offroad vehicle. The advantages are the simplicity of a double wishbone will keep maintenance relatively simple. A double wishbone will also give more adjustability to camber caster and tow; this will allow us to tune the suspension to run optimally for our car.

Design and calculation of double arm suspension of a car

D.J B & S.P. R this provides CAD-based design equations for double wishbone systems. Including the distribution of force and stress calculations, this applies directly to our team because it gives us the framework for validating our designs.

Vehicle Body Roll and Vehicle Dynamics

Abe, M., Vehicle body roll and vehicle dynamics discuss the effects of the body roll and how it affects the stability of the vehicle. This will be very applicable to our team, and our application of the body roll balance will be most evident in the rock crawl event.

Spring spacing, Roll Stiffness and Transverse Weight Transfer

Hathaway, D., spring spacing, roll stiffness, and transverse weight transfer, this article explains how spacing the springs will affect the body roll stiffness and the lateral load transfer. Our team will need to consider many factors when selecting springs and how the load will be

distributed throughout the car. For example, cars with high-horsepower motors will induce a great amount of torque, and to compensate for the torque, stiffer springs may be selected on one side of the car.

Understanding Spring Rate: Calculations & Selection Guide for Car Suspension

This article acts as a guideline for how to choose the proper springs for your car. This article also breaks down how to calculate the spring rate and how the terrain can affect the choice in springs.

Design and Analysis of Double Wishbone Suspension System using FEA and MATLAB

This source gives a path to follow on how to run additional calculations that verify our designs by utilizing the methods described and using the same programs. The choices made on boundary conditions are insightful and helped me choose the boundary conditions for my analysis.

Optimizing Vehicle Handling with Trailing Arms

This article discusses how suspension tuning enhances the stability and performance of vehicles. The impacts, effects, and relations of trailing arms are also introduced. This article also goes over the different kinds of adjustments and techniques regarding the tuning of the trailing arms.

Design and Calculation of Double Arm Suspension of a Car

Talks about how the increase in the width of the connection points of an A-arm to the frame can change the loads on the connection points and can allow for increased shear force on the bolts. This will directly affect our design since the A-arms on the rear suspension will not be symmetrical.

SAE AISI 4130 Chromoly Steel: Properties, Composition, and Applications

This resource gives the standards of the steel tubing used in our design.

3.2.2 Jose Avitia

Vehicle Dynamics: Theory and Applications

Chapter 7 examines various suspension system configurations and analyzes their critical role in vehicle performance, ride comfort, and handling characteristics. The chapter covers necessary design parameters such as spring rates, damping coefficients, roll centers, and their effects on vehicle stability during cornering and rough terrain navigation. This chapter covers multiple suspension systems, and their purpose, which helped me learn of the options available for our project, as well as the benefits from each.

Suspension Geometry and Computation

This book examines suspension geometry and steering systems, covering both single-arm and double A-arm suspension configurations with detailed computational methods for analyzing

their kinematic behavior. It provides extensive discussion on suspension points, control arm geometry, instant centers, and camber change characteristics throughout suspension travel. The text includes practical design guidelines and calculation procedures for determining optimal pickup points and linkage geometry to achieve desired handling characteristics. This source was particularly helpful for designing geometry for double arm on Chapter 12, as well as camber angle explanation and calculations on Chapter 7.

Active Suspension for a Baja SAE car

This technical report documents the design and implementation of an active suspension system for Cornell University's Baja SAE vehicle, focusing on real-time damping control using sensors and microcontrollers. The author describes the hardware selection process, sensor integration, control algorithm development, and field-testing results comparing active versus passive suspension performance on rough terrain. This source provides a practical case study of implementing electronic suspension control in a Baja application.

Baja SAE Semi-Active Suspension Final Design Review Report

This technical report discusses the design and implementation of a semi-active damper system for a Baja SAE vehicle at Cal Poly San Luis Obispo. The team developed a control algorithm, designed the electrical system for damper actuation, and constructed a test setup to validate prototype performance under simulated racing conditions. This source is particularly valuable to my project as it provides a recent, practical implementation example of an adjustable suspension system for Baja competition.

Zips SAE Baja Brakes and Throttle System

This technical report examines the brake system design, manufacturing processes, and performance analysis for the University of Akron's Baja SAE vehicle. It details the hydraulic brake system component selection, pedal assembly design, brake line routing, and mounting bracket fabrication, along with stopping distance testing results. The report includes CAD models, manufacturing drawings, and safety analysis demonstrating compliance with SAE Baja rules. The manufacturing techniques and rules compliance discussion provide useful context for my overall vehicle systems integration approach.

Design of a suspension system

This article presents a systematic suspension design methodology, progressing from customer needs analysis through Quality Function Deployment (QFD) to engineering requirements definition and component interface analysis. The source outlines a structured approach for translating vehicle performance objectives into specific suspension design parameters such as ride frequency, damping ratios, and geometry constraints. This online resource provides a useful framework for organizing my design process and ensuring that requirements are addressed.

4130 Steel (AISI, ASTM, UNS)

This webpage provides material property data for 4130 chromoly steel, including chemical composition, mechanical properties, and physical properties. This reference supplies

the material specifications needed for designing the suspension of A-arm beams using 1" 4130 chromoly tubing. The yield and tensile strength values will be used in stress analysis calculations to ensure adequate safety factors under bending and impact loads during Baja racing conditions. Additionally, these material properties will serve as the baseline data for comparing theoretical calculations against experimental results during physical testing of the fabricated suspension beams later in the project.

VSusp: Vehicle Suspension Geometry

This website provides a 2-D simulation of the suspension geometry, allowing you to specify the dimensions of your suspension system, from wheel sizes to frame and arm lengths. This source is particularly valuable for initial geometry calculations with visual aid options.

Optimum Kinematics: Suspension and Design Analysis

This student version of the software program allows modeling and simulation for the suspension system to evaluate performance under different motions. This source provides analysis that can validate our suspension system design for the SAE Baja competition.

2026 Baja SAE Rules

The official rules for the SAE Baja 2026 competition. This source helps us ensure our team is in compliance with design constraints and safety requirements for the competition.

3.2.3 James Sundeen

Design for Manufacturing and Assembly of a BAJA Steering Knuckle

This was used as a design example of a specific steering knuckle. This knuckle was built using steel, and each part was welded together to speed up the manufacturing process. The issue with the interior section of the knuckle is that there is not much room for any cv axle and it will not work with the proposed portal hubs. Many modifications will have to happen to a new knuckle design to incorporate the addition of portal hubs.

Structural Analysis of Steering Knuckle

This analyzes the forces applied to a steering knuckle and how they could bend the knuckle. This knuckle is a standard steering knuckle for a sedan so the force analysis numbers must be modified to the needs of our vehicle. This source was used to find the force analysis that will proposedly be on our steering knuckle.

Topology Optimization of Steering Knuckle Structure

This was used as an example of a topology optimization for the designed steering knuckle. This source shows how material within the model causes a buildup of weight and can be removed while maintaining structural integrity. The current tests for this did not remove much material from the design of the steering knuckle. This will change when the addition of the portal hub casing is added to the new model.

Static Load Simulation of Steering Knuckle for a Formula Student Race Car

This was like other sources used for the force analysis, but it had differed from the analysis of a standard sedan. This analysis has more extreme conditions since it is a formula car but the comparison between the predicted load equations was useful.

Design and Structural Analysis of Steering Knuckle for An Electric All-Terrain Vehicle

This source was used as great inspiration for the design of the steering knuckle used in the project. This vehicle was extremely like ours and had the same force load locations. This source also included material choice analysis of the knuckle design to understand how the materials changed the stress points.

SAE Baja Front Suspension

This is a report on the front suspension system of the SAE Capstone project at George Washington University. This report goes over their complete front suspension system which includes their member design choice and their required camber and caster. Their knuckle design was quite small and would not work with the force loads of the NAU vehicle. The focus of this source is how to connect the knuckle to the front members and how to get the correct camber required in the wheels.

2013 Baja Car Rear Suspension Redesign

This is a report on the rear suspension system of the SAR Capstone project at the University of Cincinnati. This covers how a car must keep its roll center close to the center of gravity and it reviews what designs could assist with the issue. It talks about 3 different suspension system designs and the pros and cons of using them. It also shows how the knuckle design of the car varies with each of the suspension designs.

AMSQQA200/8A

This standard is a specification that covers the requirements for aluminum alloy 6061 to be produced extrusion. The knuckle design plans to use this material so it is important to know the tensile strength, yield strength, heat treatment, quality requirements and inspections that happen when making the material.

Steering Knuckle Design & FEA Simulation

This video is a tutorial on the setup of FEA on a steering knuckle. This source has a quick review of the steps to apply loads and set up a mesh onto a geometry. It also shows the details of stress throughout the part. This source is a good reference on how to remember to use a FEA program again.

Structural Analysis of a Knuckle of a Student Car using Altair Inspire

This video is a long tutorial on the setup of FEA on a steering knuckle. This setup uses loading points instead of placing the loads onto the geometry. It then connected the loading points throughout the areas where the loads would be placed on the geometry. This example is more detailed in how the load cases would be on a knuckle design. This source was used to improve the accuracy on the part.

3.2.4 Jakob Martinez

W. F. Milliken and D. L. Milliken, Race car vehicle dynamics. Warrendale, Pa, U.S.A.: SAE International, 1995. Chapter 19

This chapter in this book provides an analysis of vehicle behavior and its relation to steering. This source explains steering geometry and handling tradeoffs, providing an insight for selecting the geometry of the steering system.

UC SAE Baja Steering Rack Design and Analysis

This student report provides practical insight into the design process, analysis, and testing of a steering rack developed for a Baja SAE vehicle. This source also provides detailed reasoning and analysis on important parts of a steering assembly that can guide the development of the steering rack. This source also acts as guidance on analyzing steering forces, minimizing play, and FEA analysis.

A Study of Ackerman Steering and Its Applicability to SAE Mini Baja

This study provides analysis Ackermann steering for an SAE Mini Baja car which demonstrates how corrected geometry can reduce tire scrub and improve maneuverability. Although the study was done for a Mini Baja car, the same knowledge and equations are still applicable in the steering system design for our vehicle's steering system. Providing valuable guidance for optimizing steering performance and dimensions for critical parts.

2017 Bearcats Baja SAE – Steering System

This student report gives a breakdown of steering system components in a baja vehicle, offering insight into the layout and force analysis for the steering system.

EXPERIMENTAL RIG STUDY ON RESISTANCE FORCES IN CAR STEERING SYSTEM WITH RACK AND PINION

This source was an experimental study of a rack and pinion steering, which gives a breakdown of resistance forces and component loads. This study identifies how factors like alignment and load affect steering effort and efficiency. These insights help our team reduce steering resistance and improve responsiveness of our vehicles steering systems design.

Design and Analysis of an Ackermann Steering system for an Off-Road Electric Vehicle

This report presents a comprehensive analysis of the steering geometry for an SAE e-Baja vehicle, explaining in detail it's design, key components, and overall performance. It also includes mathematical calculations used to determine the optimal Ackermann geometry, along with Finite Element Analysis (FEA) simulations to evaluate stress distribution throughout certain steering components. This source provides valuable insight into both the theoretical and practical parts if steering design.

SAE J670_202206

This standard defines common terminology for passenger cars and light cars for suspension. This standard is relevant to the steering of our vehicle because it ensures constant

communication and accurate interpretation of the vehicles steering. By adhering to these definitions, the team can maintain clarity in analyzing steering geometry and handling.

Steering Shaft and U-Joint Selection Guide

This article outlines key guidelines for selecting and routing steering shafts and U-Joints. It explains spline sizing, Maximum allowable joint angles, and when to use support bearings to avoid binding. It also compares shaft types and provides practical recommendations for designing a safe, reliable steering linkage.

Analysis of Steering System in FSAE Vehicle

This paper presents the design and analysis of an FSAE race car steering system, focusing on optimizing Ackermann geometry and evaluating components through FEA. The authors model the steering assembly in SolidWorks, test rack and pinion Strength in ANSYS, and verify steering behavior through LOTUS simulations. The study Shows how proper geometry and component sizing improve steering response, reduce steering effort, and enhance stability for a lightweight formula style vehicle.

D.O.T Standard 49 CFR §393.209 — Steering Wheel Systems

This standard sets safety requirements for commercial vehicle steering systems, limiting steering wheel lash based on wheel diameter and steering type to ensure precise control. It mandates that the steering wheel, column, joints, and gearbox be securely mounted, free of cracks, wear, or loose components. Overall, the regulation ensures steering integrity and consistent handling.

Shigley's Mechanical Engineering Design

Chapter four of the textbook explains the buckling behavior of long, slender columns and details how the Eulers column equation is used to determine critical loading conditions and appropriate column dimensions. This analysis includes material properties, geometric factors, effective length, and end conditions to evaluate when a column becomes unstable. This source is crucial in being able to calculate the diameter and material needed for the tie rod to perform effectively.

3.2.5 Marc Angelo Maquiling

Race Car Vehicle Dynamics.

Chapter 20 of *Race Car Vehicle Dynamics* provides an investigation into race braking systems through the analysis of proper weight balancing, pressure distribution, and breaking effects on pedal distance. This resource provides a good material for baseline research into the brake assembly and brake physics in the context of racing, outside of commercial applications.

Brake Design and Safety.

This resource provides an analysis on the feasibility of Driveshaft Mounted brakes, their effects on brake temperature, and the regulations and standards governing such brakes. This is a

good resource for inboard brake assemblies, and the complexities involved in such systems which allow for a deeper understanding of the current direction of the current inboard brake design.

Design and analysis of Double Piston Brake Caliper for SAE baja vehicle

This resource provides an analysis on double piston brake caliper for Baja specific purposes. This analysis on this resource provided insights into a double piston brake caliper's braking performance and heat dissipation, while also providing an analysis on the weight addition and reliability of the brakes in a Baja race environment.

"Going rock crawling?," PowerStop Brakes

This resource provides an analysis on different brake pads, and brake rotors for outdoor driving purposes, as well as the importance of proper brakes for offroad elements. The analysis imparted in this document allows for a greater understanding of the offroad vehicle brake assemblies and provides a guide to balance offroad brake performance and cost.

Design and Analysis of Braking System for BAJA Al-Terrain Vehicle

This resource provides an analysis of brake components and their significance to the overall performance of the brake system design under offroad conditions. Each significant component was investigated to provide an insight into their effect on performance while subjected to SAE Baja rules and conditions.

Fundamentals of Brake Design

This resource provides an analysis on the fundamentals of brakes such as the relationship between foot pressure and brake force, thermodynamic effects, causes of brake wear and break noise and the effects of friction coefficient. This document provides information that allows for an effective analysis and testing of the brake assembly design, and how to rectify issues commonly present on brake systems.

Brake System Regulations and Standards Review and Comparison Focused on Europe, NA and SA Markets

This resource provides a comparative review of brake system regulation and standards present in Europe, NA, and SA market. The standards imparted in document highlights how each region conducts their manufacturing and regulation on commercial brake assemblies, providing an analytical inquisition on how to properly manufacture brake assemblies in an offroad context by interpolating the data presented in the document.

Shigley's Mechanical Engineering Design

Chapter 16 of this source provides an in-depth analysis of a vehicle's brake system. The analysis included an investigation of the forces, pressures, and geometry involved in brake calculations. These investigations were modified for the team's specific use case.

Wilwood.com

This resource provides different types of calipers, rotors, and brake pads that can be used as a reference for analysis. Dimensions, geometry, and coefficient of friction were taken and input

for analysis with respect to the vehicle's use case, allowing for greater accuracy in the calculations and justification of choices.

The Motor Carrier Safety Planner

This resource provides braking standards for commercial vehicles. The standards presented in this resource allow for an in-depth analysis of the team's braking system, and allow for corrections to be made in areas that may have been overlooked, such as making sure that the brake hoses are not interrupted and bent above standards.

Code of Federal Regulation

This resource provided insight into the regulations and standards surrounding the hydraulic systems of brakes. This resource provides, but is not limited to, brake hydraulic system design standards, brake terms definitions, and hydraulic brake design requirements. The modification of the information contained within this resource allows for refinement of the current brake design.

3.2.6 James Cole

Race Car Vehicle Dynamics

Chapter 21 of the book, *Race Car Vehicle Dynamics*, goes in depth on approximate methods on how to calculate properties of suspension springs, focusing on spring rate and maximum stress. The suspension springs that this source covers are torsion springs, coil springs, and leaf springs.

Tires, suspension and handling

Chapter 5 of this book provides an analysis on suspension characteristics, specifically wheel rate and spring rate. This source also explains load transfer and the distribution of vertical forces throughout suspension systems.

Of Springs and Dampers

This source goes in depth on what wheel rate is, providing equations and definitions to help explain clearly. This source also gives real-life examples of when wheel rate may be used and gives numerical values to help understand what reasonable ranges to expect.

Design of Double Stage Springs for Baja SAE Type Vehicles

This article provides information on the design methodology of double stage springs specific to Baja SAE. This source proposes substituting linear springs with double stage springs and provides testing procedures and results to compare and contrast the two types of springs. They provide graphics that better show the results of the tests that were conducted.

International Journal of Creative Research Thoughts (IJCRT)

This article provides a more in depth analysis of the double wishbone suspension system with detailed calculations on relative parameters. They explain that the double wishbone system provides enhanced handling, stability, and performance in high-performance vehicles. The article mainly focuses on the design and analysis of a suspension system that incorporates these A-arms.

The Science of Suspensions: How They Work and Why They Matter

This blog provides an easy to understand explanation of what a suspension system does and how the system works fundamentally. They go over some of the main relative terms in a suspension system such as a spring rate and damping, as well as the future developments that may be made in suspension technology.

Springs and Spring Suspensions

This resource explains the standards specifically related to the spring components of suspension systems. This article is from the Society of Automotive Engineers (SAE) and mainly goes over the chief factors that affect the riding quality of a motor vehicle such as spring deflection and amplitude.

Shigley's Mechanical Engineering Design

Chapter 3 of this textbook focuses on load and stress analysis of members of simple geometry. Particularly, section 10 of this chapter dives into normal stresses for beams in bending, providing guidance for any simple stress calculations that may need to be performed on the front suspension members. This chapter also includes example problems to aid readers in any calculations that they may be performing, along with proper definitions of relevant variables.

Stress Analysis of a Suspension Control Arm

This document covers a more realistic approach to the stresses acting on control arm members, providing a finite element approach to solving for the stresses. They explain how the mesh that was used was created and provide a color coded stress distribution for an ease of visual observation.

Measurement of Vehicle and Suspension Parameters for Directional Control Studies

This standard goes over the measured parameters that are used in the simulation of directional control performance in the linear range. They also explain how these parameters can be used for other simulations such as vehicle and suspension characterization and comparison, suspension development and optimization, and the processing of road test data.

3.3 Mathematical Modeling

This chapter presents the mathematical models and equations used to analyze and design the suspension system for our Baja vehicle. The modeling is organized by subsystem - suspension, steering, and brakes – and shows the calculations and methods applied by each team member. These equations form the foundation for the design process and guide our design processes.

3.3.1 Wheel Rate – James Cole

The following calculations go over the wheel rate, Kw, of the springs used in a suspension system, with relative numbers coming from previous iterations of Baja vehicles. The spring rate, Ks, was assumed to be around 110 lbf/in while the motion ratio, MR, was assumed to

be 0.7, which is a standard value used in Baja vehicles. A standard spring angle, θ, of 30 degrees and spacing on track T, S/T, of 0.7 was used for an ease of calculations. The spacing on the track is used when wheels are raised, such as during the rock crawl in the competition. The following calculation utilizing the spacing on the track assumes only one wheel is raised.

$$K_w = (MR * \cos(\theta))^2 * K_s$$

$$K_w = \frac{1}{2} * K_s * (1 + (S/T)^2)$$

After plugging in the relative values, we get an initial wheel rate of around 40.43 lbf/in, and a wheel rate of around 81.95 lbf/in when one wheel is raised. These values essentially mean that when 40.43 pounds of force are applied to the wheel, the suspension system is compressed by 1 inch. This definition of the wheel rate makes it clear as to why it is higher when one wheel is raised, as the force applied to the wheels is distributed to three of the wheels as opposed to four.

3.3.2 Front Suspension – James Cole

The following calculations go over a stress analysis on the individual components of a standard A-arm, a laterally offset A-arm, and a longitudinally offset A-arm. For an ease of calculation, the middle member of the arm is neglected. The arms are considered to be hollow tubing with an outer diameter, D, of 1 inch and an inner diameter, d, of .87 inches. The weight acting on each individual member is derived from the total weight of last year's car, to get a weight, W, of 32.5 lbf acting on each member. The length of each arm is considered to be 16 inches with an additional 2.5 inches added due to the offsets. The distance from the outer edge of the member to the neutral axis is half of the outer diameter, or 0.5 inches. In order to find the stress (σ), the second moment of area (I) of a hollow circular cross-section must be found along with the bending moment (M) acting on each member.

$$I = \frac{\pi}{64} * (D^4 - d^4)$$

$$M = W * L$$

$$\sigma = \frac{M * c}{I}$$

After plugging in the necessary values, we get a second moment of area of around 0.021 in^4, with a bending moment of 520 lbf*in, 601.25 lbf*in, and 601.25 lbf*in for the standard, lateral, and longitudinal A-arms respectively. The values for the lateral and longitudinal members are of equal values because the offsets for each are considered to be of the same amount. Proceeding with calculations, the stress acting on each member comes out to be 12,401.42 psi, 14,339.14 psi, and 14,339.14 psi for the standard, lateral, and longitudinal members respectively. The material that is being used to manufacture these members is 4130 chromoly steel which has a yield strength of 66,700 psi. Comparing the stress acting on each different member to the yield strength of the material, any one of these designs would be sufficient to be used in the suspension system that is being designed.

3.3.3 Rear Suspension – Colby Brett

Roll stiffness is important because we must balance the cornering stability of the wheels while maintaining a constant path of articulation. Since our vehicle will be competing in events such as a rock crawl the roll stiffness may be on the softer side to ensure tire contact through the uneven terrain but stiff enough to prevent the car from rolling over. Adjustments can be made in the wide of the A arms, increasing the length will increase the roll stiffness quadratically, which will need to be accompanied by the appropriate adjustments to the spring rate to retain articulation.

$$K_w = wheel\ Rate$$

$$k_w = \frac{k_{spring}}{MR^2} \approx 81.95 lbs/in \qquad MR = \frac{Wheel\ travel}{Spring\ travel}$$

$$K_{\phi f} = 2k_{wf}\left(\frac{t_f}{2}\right)^2\left(\frac{\pi}{180}\right) \qquad Assume\ K_{\phi f} = K_{\phi r}$$

$$\left(\frac{t_f}{2}\right)^2\left(\frac{\pi}{180}\right) = \Delta Z = Vertical\ displacement$$

$$t_f = track\ width = 50in$$

$$K_{\phi f} = 1787.9\ \frac{lbf\text{-}in}{\deg} \qquad K_{\phi}^{total} = 2\,K_{\phi f} = 149\,\frac{ft\text{-}lb}{\deg}$$

Figure 3.3.3-1: Calculation of the roll stiffness

3.3.4 Rear Suspension Geometry/Camber Angle – Jose Avitia

The rear suspension geometry was analyzed in conjunction with camber angle behavior to determine the optimal control arm dimensions and mounting locations needed to achieve a target static camber angle between -1° and -2°. Negative camber refers to the inward tilt of the tire at the top, which improves cornering performance by maximizing the tire contact patch during turns when the vehicle body rolls outward. The geometric analysis examined multiple interrelated parameters including upper control arm length, lower control arm length, vertical and horizontal separation between frame mounting points, tire diameter and width, steering knuckle dimensions, and wheel offset. These parameters collectively determine the suspension's kinematic behavior and the resulting camber characteristics throughout the suspension travel range. Originally these were the formulas used in our calculations Figure 3.3.4-1, and Figure 3.3.4-2 [11].

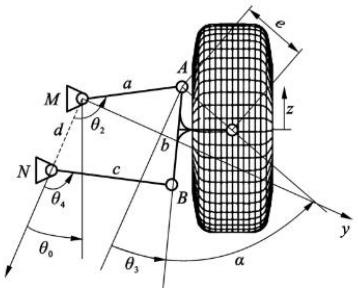

Figure 3.3.4-1: Double A-Arm Suspension Geometry.

$$\theta_3 = 2\tan^{-1}\left(\frac{-E \pm \sqrt{E^2 - 4DF}}{2D}\right)$$

where

$$D = \frac{c^2 - d^2 - a^2 - b^2}{2ab} - \frac{d}{a} + \left(1 + \frac{d}{b}\right)\cos\theta_2$$

$$E = -2\sin\theta_2$$

$$F = \frac{c^2 - d^2 - a^2 - b^2}{2ab} + \frac{d}{a} - \left(1 - \frac{d}{b}\right)\cos\theta_2$$

Figure 3.3.4-2: Camber Angle Calculation Equations.

VSusp ("Vehicle Suspension") was utilized to analyze the suspension geometry and determine the optimal configuration to achieve the target camber angle [18] (Appendix 9.1.). Manually calculating how different control arm lengths, mounting positions, and component dimensions affect suspension behavior would be extremely time-consuming. VSusp automates these calculations and visualizes how geometric changes impact camber angle, roll center height, steering axis inclination, and scrub radius. This enabled rapid design iteration to optimize the suspension while balancing camber requirements with structural and packaging constraints.

While this was an improvement over manual calculations, the 2-D VSUP could still not calculate the specific dimensions of individual A-arm lengths. Because of this, I utilized the Optimum Kinematics program.

Optimum Kinematics is computer-aided software for suspension design and analysis [19] (Appendix 9.4). The suspension was designed in the program using a double A-arm with a single coil-over shock. It's setting up the connecting points in a coordinate system, where the X, Y, and Z coordinates can be arranged as you prefer. For the analysis, I chose the X coordinates to run from side to side of the car, with the origin at the car's center, positive to the right and negative to the left. The Y coordinates increase from bottom to top, with the origin at ground level. The Z coordinate runs from front to back; the wheel's center is at the origin, with positive toward the front of the car and negative toward the rear. The connecting points are where the A-arms connect to the frame and to the knuckle, which are chosen as coordinate points (Figure 9.4-2).

Once the suspension design was set up at Optimum Kinematics, a series of simulations could be run in the program. There are four main motions for the simulations. The first is heave, which is the movement of the wheels up and down in reference to the frame, for example, going over a bump. Second is roll, one side of the tires moves up while the other side moves down, for example, when turning. The third one is pitch, which is when the front wheels move up and the rear move down in relation to the frame or vice versa, for example, when breaking or accelerating. The last one is steering, which causes the wheels to change direction and can make them move up and down.

The simulations are set up in multiple steps; the analysis has 20 steps. Where the data for different results is given, such as camber angle, toe angle, steer angle, toe distance, wheel position, and others. For this analysis, the focus is on the camber angle, but many of the other results will be important throughout the project.

The first motion analysis was for Heave motion (Figure 9.4-3), which shows the progression of the camber angle over the 20 simulation steps. It shows a starting camber angle of 0.0° (Step 0), which serves as the reference point for the design camber of -1.469°. The angle then reaches 1.226° (Step 5), indicating the wheel tilts outward (more upright), resulting in an absolute camber angle of -0.24°. Then comes back down to -0.376° (Step 13), equivalent to an absolute camber angle of -1.85 °. At the end, it returns to 0.0° (Step 20). This shows that the suspension will return to its original position. The heave motion simulation shows very stable camber angles, with a maximum absolute change of 1.226° from the original angle. With an average of only 0.21° and a standard deviation of 0.483°, it demonstrates that the suspension stays very close to the desired camber angle during heave motion.

Roll was the second motion analysis (Figure 9.4-4), which evaluated the camber angle through roll conditions on a 20-step simulation. Starting from the 0.0° (Step 0) reference position on the left wheel, it increases to 0.127° (Step 5), while the right wheel reaches -0.077° (Step 5). They went in the opposite direction during the roll motion, as expected. Then, as the roll motion reverses, the left wheel reaches -0.078° (Step 15) and then goes to 0.117°. The camber angle deviation was very minimal on both sides during the roll, indicating good suspension geometry and better grip.

On the third test, the pitch motion analysis (Figure 9.4-5) was performed, during which the front and rear move up or down in opposite directions, such as during breaking or acceleration. In this case, both left and right rear wheels maintained symmetry throughout the simulation. With a maximum deviation of -0.0178° (Step 3), the rear suspension showed an almost negligible change in camber angle throughout the simulation. This ensures effective tire traction during braking and acceleration.

The steering motion analysis (Figure 9.4-6) was the last motion test done with Optimum Kinematics. Throughout the 20 steps, both left- and right-wheel camber angles remain constant at 0.0°. which reflects perfect camber stability. This shows a very stable rear suspension, and shows there is no steering on the rear axle. Although more testing will be needed on both the rear and front suspension as a whole to obtain more results for the front suspension.

Overall, the Optimum Kinematics simulations confirmed that our suspension geometry achieves the desired camber angles with minimal changes across all motion tests. This validates our design and will ensure good tire performance and handling during the Baja SAE competition.

3.3.5 Steering – Jakob Martinez

The following calculations go over fundamental steering aspects required to design an effective and reliable steering system. Some key aspects addressed include Ackermann angles, full steering stroke, steering wheel angle, and the gear ratio of the steering box. As the project progresses, these calculations will change as the project progresses over time.

Ackermann Steering

The calculations below are the updated calculations to determine the Ackermann steering angles of the steering rack that will be used. They define the relationship between the inner (θ_i) and outer (θ_o) front wheels during a turn to ensure both follow concentric paths, reducing tire scrub and improving cornering.

$$tan(\theta_i) = \frac{L}{R - \frac{W}{2}} = 49.3^{\circ} \quad tan(\theta_o) = \frac{L}{R + \frac{W}{2}} = 28.9^{\circ}$$

Variables used

L = 63 in (wheelbase)

W = 60 in (Updated Width)

R = 84 in (Turning radius)

Full Stroke

The following calculations below determine the full stroke of the steering rack, which defines the total linear travel needed to achieve the desired wheel lock angles on both sides, ensuring the vehicle can reach its maximum turning capability.

$$\Delta x_{one\ side} = 2.5\ in$$

$$\Delta x_{Full} = (2)(2.5\ in) = 6.4$$

Variables used

$$\Delta x_{one\ side} = Linear\ rack\ travel\ for\ one\ lock\ (in)$$

θ_i = Inner wheel angle (°)

Steering Wheel Angle

The calculations below show the updated steering wheel angle, which represents the total rotation required to turn the front wheels from lock to lock. The previous lock-to-lock angle was 733.4°, and the new value of 540° reflects a 26.4% improvement.

$$\theta_{wheel} = 2 * \theta_{sw,center} = 540^{\circ}$$

$$\theta_{sw,center} = 0.75 * 360^{\circ} = 270^{\circ} \textit{ (Steering wheel rotation to one lock)}$$

Variables used

$$\theta_{wheel} = \textit{ Total steering wheel rotation from lock to lock}$$

$$\theta_{sw,center} = (\textit{Steering wheel rotation to one lock}$$

Gear Ratios

The calculations below present the updated values used to determine the steering box gear ratio, which relates the rack's linear travel to the pinion's rotation. Compared to the previous gear ratio of 3.15 $^{in}/_{rev}$, to the new ratio of 3.33 $^{in}/_{rev}$ there is a slight improvement.

$$Gear\ Ratio = \frac{Linear\ travel\ of\ rack\ (in)}{Pinion\ rotation\ (rev)} = 3.33\ {}^{in}/_{rev}$$

Variables used

$$Linear\ travel\ of\ rack = 5\ in$$

$$Pinion\ rotation = 1.5\ revs$$

3.3.6 Knuckle Static Force Analysis and Buckling – James Sundeen

These calculations are a prediction of what forces the car will handle based upon the data from last year's car. These calculations use the weight of last year's car to be 520 pounds and the hopeful loading case of an even weight spread between the front and back wheels. The load cases calculated were on the Hub in the X, Y and Z directions. These forces are from braking, cornering and bump loads. The equations used and the found forces are shown below:

$$Bump = 2mg = \ 260.1lbf$$

$$Cornering = 2mg = \ 260.1lbf$$

$$Braking = mg = \ 130\ lbf$$

There were initial calculations for the forces on the brake caliper mounts and the moment seen at the specific mounts, but this is no longer needed. The brakes have been moved off the knuckle and are now inboard so there will be no issues with mounting the portal hubs. The predicted distance from the caliper mounting point and knuckle is 0.31 inches. The formulas and found data are shown below:

$$Braking\ Force\ on\ Caliper = \frac{1.5mg}{2} = \ 97.5lbf$$

$$Moment\ at\ Caliper\ Mounts = \ Braking\ Force * \ D = 30.7\ lbf * in$$

To better represent intense load cases on the knuckle design, it is more effective to enlarge the forces for the testing of the knuckle design. A larger load case is used to show where the weak points of the design are. This can also be treated as a worst case scenario, and it is better to be prepared for total failure of the part.

For testing a bump force of 2248 pound force or 10000 Newtons is applied to understand the weak points of the design. These load cases were used in the ANSYS software Mechanical ADPL 2025 and SolidWorks. ANSYS is a finite element analysis software used to analysis the structure integrity on the design. The process involves loading the geometry into the software and applying loads to the points on the geometry that are expected to have them. The analysis happens by showing the stress points on the created mesh across the geometry. This process can be used to identify weak points. An analysis was done on the first design ever design and it shows the weak point at the sharp curve of the knuckle member connections.

3.3.7 Dynamic Brake Analysis – Marc Maquiling

The following calculations provide an analysis and reference point on the forces involved in braking, focusing on the dynamic analysis on distance, time, and clamping force requirements. Although the vehicle is still in the initial stages of the design process, the calculations presented could be augmented according to the changes with the vehicle specifications. The calculations are also baseline calculations that could be modified to match the brake requirements further along with the design process.

The reaction distance, $d_{reaction}$, can be determined by multiplying the initial velocity, V_i, and the reaction time, $t_{reaction}$.

$$d_{reaction} = V_i * t_{reaction}$$

The total distance required for braking, d_{total}, can be determined by adding the brake distance, d_{brake}, and the reaction distance, $d_{reaction}$.

$$d_{total} = d_{brake} + d_{reaction}$$

The relation between target velocity, V_o, the initial velocity, V_i, acceleration, or in this case deceleration, a, and brake distance, d_{brake}, can be used to analyze the brake requirements of the vehicle. By setting the target velocity to 0, the relationship between deceleration and brake distance can be interpolated.

$$V_o^2 = V_i^2 + 2 * a * d_{brake}$$

The total time for braking, t_{total}, can be determined through the relationship between the initial velocity, V_i, the deceleration, a, and the reaction time, $t_{reaction}$.

$$t_{total} = \left(-\frac{V_i}{a}\right) + t_{reaction}$$

Figure 3.3.7-1 shows how the total breaking distance affects the deceleration and the braking time of the vehicle, respectively. The figure reveals that as the breaking distance

requirement decreases, the deceleration required from the brakes also decreases exponentially, approaching a limit at some deceleration. The figure also highlights the linear relationship between braking distance and braking time, describing that as the distance required for braking increases, the time needed for braking also increases. These relationships can be used later on the finalization of the brake assembly design to choose the appropriate brake system that satisfies the braking requirements derived from these formulas.

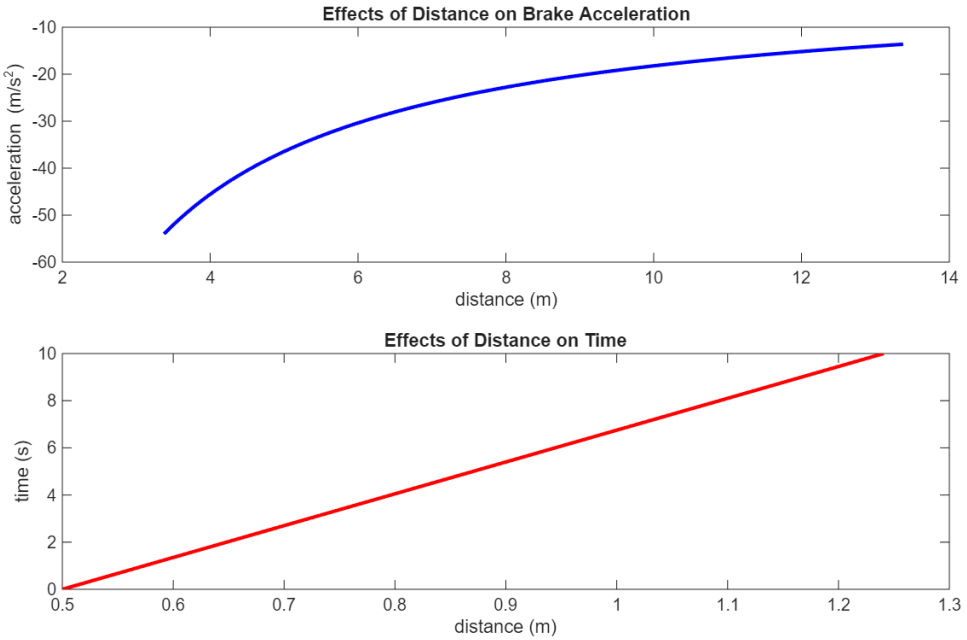

Figure 3.3.7-1: Brake Distance Effects on Deceleration and Time

The clamping Force, F_c, can be determined through its relationship between the load on the wheel, W, of approximately 578 N, the tire radius, r_t, of approximately 0.292 m, the effective disk radius, r_e, which is approximately $\frac{1}{5}$ of the tire radius, and the number of pads, N, which is two pads for each caliper-rotor assembly.

$$F_c = \frac{W * r_t}{\mu * r_e * N}$$

Figure 3.3.7-2 displays how the clamping force requirement to lockout a wheel of a tire changes as a function of the brake's rotor. It can be derived that the force requirement has an inverse relationship with the rotor diameter, and that as the rotor diameter increases, the clamping force requirement decreases. As the design of the vehicle finalizes, this relationship could be refined and be used to determine other parts of the brake assembly such as pedal pressure, hydraulic pressure requirements, and brake torque calculations that can help shape the type, size, and brake forces of the brake assembly.

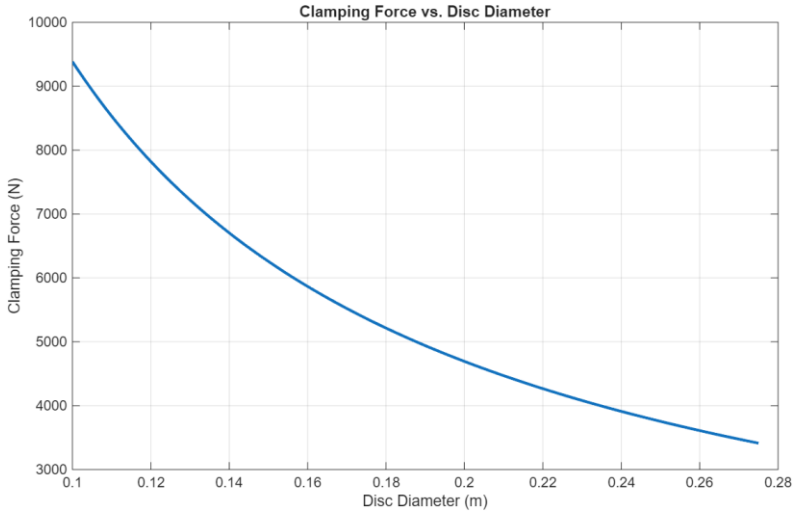

Figure 3.3.7-2: Clamping Force for Tire Lockout as a function of Rotor Diameter

4 Design Concepts

4.1 Physical Decomposition

The decomposition model represents a tree of all the parts that must be manufactured or acquired to make the sub-system operational. It also reveals how complicated each sub-assembly can be and how there needs to be precise planning to make each sub-system work together. The model is broken into 3 sections inside of the suspension category. The Steering and Wheels and Brakes sections do not have a break down since all the parts make up the full assembly. The suspension system has a breakdown because the assemblies have specific parts or areas. The function decomposition is shown below in Figure 4.1-1.

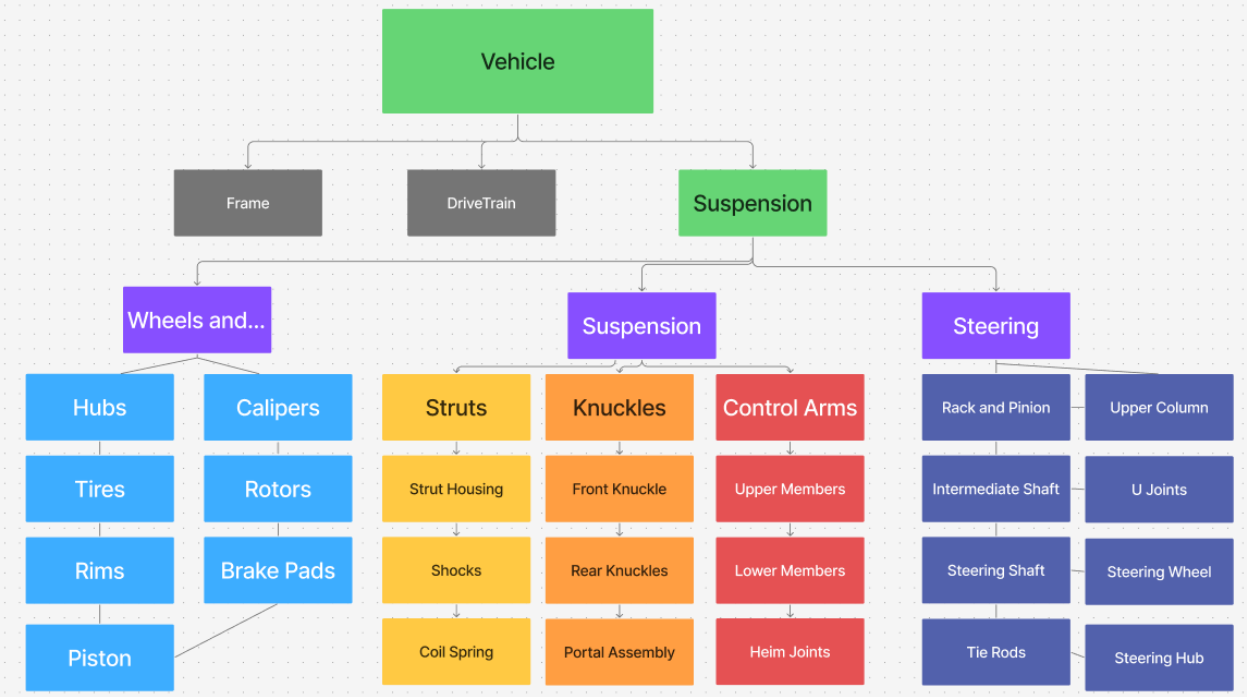

Figure 4.1-1: Physical Decomposition Model

4.2 Concept Generation

4.2.1 Front Suspension – James Cole

The front suspension system considered three different types of A-arms to be used in the final design. These designs are a standard A-arm, a laterally offset A-arm, and a longitudinally offset A-arm. Concept 1 shown in Figure 4.2.1-1 shows the standard A-arm which provides balanced geometry and a simpler design while having the con of tight spacing between the wheel and chassis.

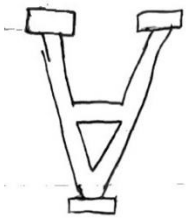

Figure 4.2.1-1: Standard A-arm

Concept 2 shown in Figure 4.2.1-2 shows the laterally offset A-arm which provides an improved clearance between the wheel and chassis while having more complex geometry, creating a weak point at the bend, and requiring more material to manufacture.

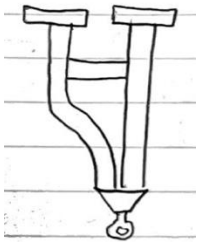

Figure 4.2.1-2: Laterally Offset A-arm

Concept 3 shown in Figure 4.2.1-3 shows the longitudinally offset A-arm which provides further improved clearance as compared to the laterally offset arm as both outer members have offsets while the lateral arm only has one arm with an offset. This arm also comes at the cost of having complex geometry, creating weak points at the bends, and requiring more material to manufacture.

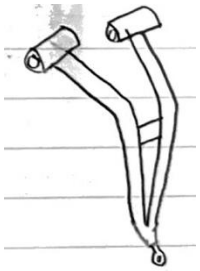

Figure 4.2.1-3: Longitudinally Offset A-arm

4.2.2 Rear Suspension – Jose Avitia, Colby Brett

The rear suspension system design required careful consideration of control arm geometry, mounting configuration, and kinematic behavior. Three primary concepts were developed for the rear suspension control arm members, each offering different advantages in terms of packaging, performance, and manufacturability. These concepts varied in mounting point locations, member lengths, and spatial orientation.

Concept 1 (Wide Mounting Configuration) features control arms with widely spaced mounting points on the frame, creating a broad attachment base for improved load distribution. The

asymmetric arm lengths provide ample clearance for drive shaft routing and shock absorber mounting.

Figure 4.2.2-1: Wide Mounting Configuration

Concept 2 (Narrow Mounting Configuration) features control arms with closely spaced, symmetrical mounting points near the vehicle centerline, creating a compact packaging envelope. The equal-length upper and lower control arms simplify manufacturing and enable longer suspension travel while reducing material usage. Figure 4.2.2-2.

Figure 4.2.2-2: Narrow Mounting Configuration

Concept 3 (Variable Height Extended Members) features control arms extending at varying heights from the horizontal plane, creating three-dimensional geometry. This configuration optimizes camber and roll center characteristics but increases binding risk and manufacturing complexity. Figure 4.2.2-3.

Figure 4.2.2-3: Variable Height Extended Members

4.2.3 Steering – Jakob Martinez

For the steering system there was a few different systems that the team could've chosen, those being rack and pinion, power steering, and drive by wire. The rack and pinion system as show in the sketch below was considered for its lightweight, simple, and inexpensive design, as

well as its reliability. However, it requires higher steering effort from the driver and can be less comfortable for longer operations.

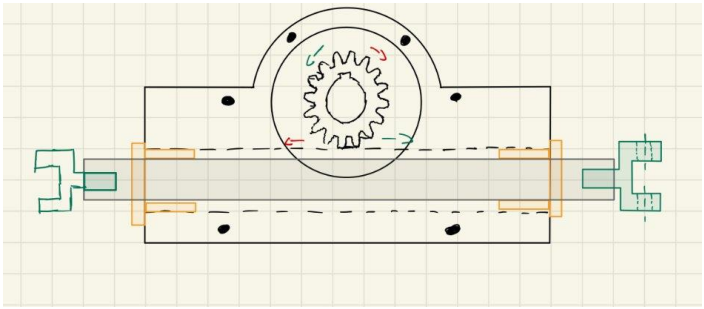

Figure 4.2.3-1: Sketch of Rack and Pinion system

Power steering offers reduced driving effort, smoother operation, and is widely used in most vehicles today. But it comes with some drawbacks such as added weight, higher cost, greater design complexity, and the potential for fluid or electrical issues. The figure below is a sketch of the system.

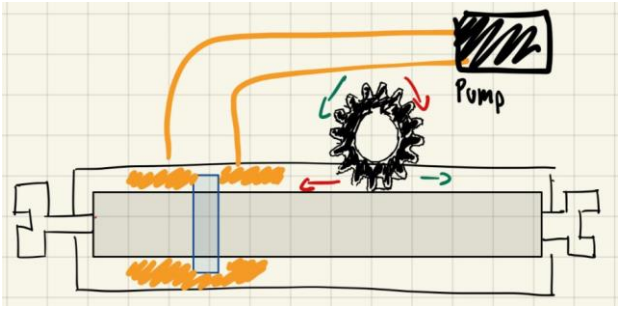

Figure 4.2.3-2: Sketch of Power Steering system

Lastly, drive by wire steering provides advantages like the removal of mechanical linkages, tunable performance, and flexible orientation options. The drawbacks to this system being that it is significantly more expensive, electronically complex comma and introduces a higher risk of system failure. Below are sketches of each steering system. The figure below is a sketch of the drive by wire system.

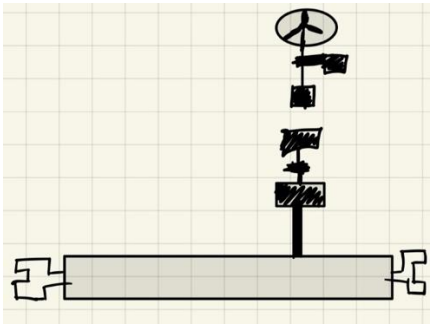

Figure 4.2.3-3: Sketch of Drive by Wire system

4.2.4 Brake Rotor – Marc Angelo Maquiling

Three different types of brake rotors were investigated and analyzed to determine the right rotor to satisfy the customer and engineering requirements. The three different types of rotors investigated were the solid rotor, vented rotor, and slotted and drilled rotor.

The solid rotor has a simple, cheaper, and built for the element design. This provides a great advantage for simple outdoor usage and can provide adequate breaking for a fraction of the price in comparison to the different rotors. Despite the pros, the solid rotor's low fade resistance, unsuitability for heavy load braking, and high temperature warping may prove to be a challenge in racing applications.

Figure 4.2.4–1: Solid Rotor Design

The vented rotor design provides an increase in strength, greater cooling, and an increased fade resistance in comparison to the solid rotor design. It can provide an advantage in the context of racing for brakes. However, the increased weight, increased price, slight increase in complexity, and the availability to trap debris could provide a challenge incorporating the vented rotor for the brake assembly.

Figure 4.2.4–2: Vented Rotor Design

The slotted and vented rotor design provides greater cooling for the brake assembly, and higher fade resistance which can result in greater durability. However, the steep increase in price, greater increase in weight, easily damageable by terrain, and the allowability for debris due to the design can prohibit a team from having improved race performance.

Figure 4.2.4–3: Slotted and Drilled Rotor Design

4.2.5 Knuckle – James Sundeen

There were 3 main designs for the knuckles with the steering knuckles for the front suspension system taking the lead in development. The 3 designs differ by geometry and member mounting locations. The two leading designs had similar mounting locations that were extended outward from the wall of the design where the third design had the top member mounting point right above the bearing hole. The third design was removed because there was suspect stress that could deform the bearing hole and cause the axle to spin improperly. The two main designs are shown in the figures below:

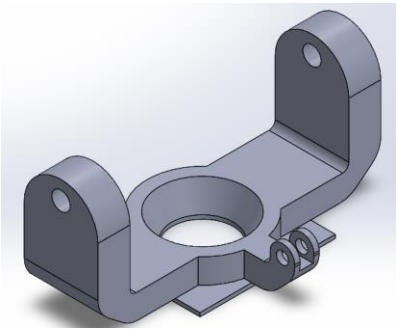

Figure 4.2.5-1: Squared Knuckle

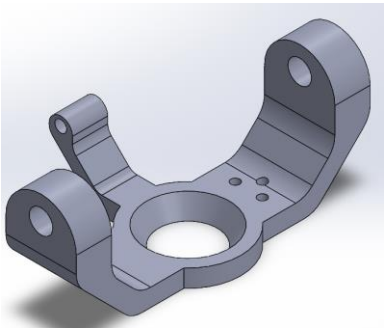

Figure 4.2.5-2: U Shaped Knuckle

Design 1, seen in Figure 4.2.5-1, had the ability to be easily produced since the geometry was so simple. The design was not space efficient because the shape did not account for the distance between the center and the wheel. Design 2, seen in Figure 4.2.5-2, is space efficient since it has arms that move diagonally out to both spread the load and reach further out the wheel rim. The design does have more complicated geometry so it would be harder to manufacture.

4.3 Selection Criteria

The selection criteria for each sub-system was developed based on engineering requirements and quantifiable calculations to make sure that all generated concepts met the projects performance expectations. By comparing each concept against measurable criteria, the team was able will be able to identify the best design that balances performance and durability.

4.3.1 Front Suspension – James Cole

The selection criteria used to determine which A-arm to proceed with for the final front suspension system were complexity, cost, spacing, weight, strength, and factor of safety. These criteria were chosen as they were deemed to be the most relevant towards our design goals. Each criterion was also given weight based on their relative importance towards those design goals. Complexity can be quantified by the number of unique parts that are used in each arm, cost can be quantified by the dollar amount of each arm, weight can be quantified by the number of pounds making up each arm, strength can be quantified by the ultimate tensile strength of the material being used, and the factor of safety can be quantified by the ratio of the stress acting on each member with the yield strength of the material being used.

4.3.2 Rear Suspension – Jose Avitia

The rear suspension concept selection was conducted using a weighted decision matrix to objectively evaluate the design alternatives against key engineering requirements. Six primary criteria were established based on the project's technical specifications, manufacturing constraints, and competition requirements. The evaluation criteria include manufacturability, cost, complexity, weight, strength, and factor of safety. Each criterion was assigned a weight reflecting its relative importance to overall suspension performance and project success.

4.3.3 Steering – Jakob Martinez

The selection criteria for the steering system were based on engineering requirements such as steering effort and steering wheel play. Steering effort ensures that the driver can comfortably even maneuver the vehicle over extended periods of time without excessive fatigue which is critical for the endurance challenge. Steering wheel play can have a large impact on the performance of the whole vehicle. It is vital that the amount of steering wheel play is kept to a minimum to have precise steering.

4.3.4 Knuckle – James Sundeen

The knuckle designs were similar in geometry so buckling tests were done to understand the deformation that would occur and if the designs were effective. From testing both the front and the rear designs, the deformation of each design was almost identical. The designs differed in deformation by less than 1 percent. The testing for the front and rear knuckles are shown below in Table 4.3.4-1. Figure 4.3.4-1 through Figure 4.3.4-4 show the stress concentration on each of the knuckles.

Table 4.3.4-1: FEA Analysis for the Knuckle Design

	Design 1	Design 2
Front Suspension	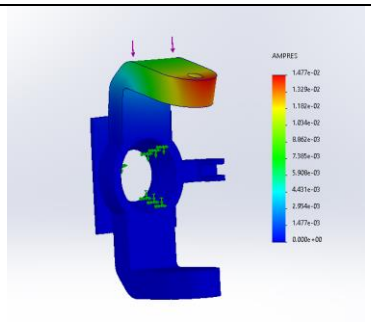 **Figure 4.3.4-1**	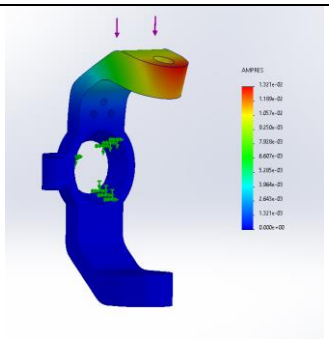 **Figure 4.3.4-2**
Rear Suspension	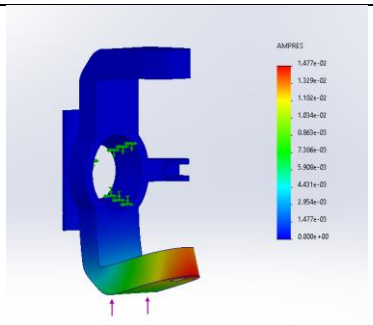 **Figure 4.3.4-3**	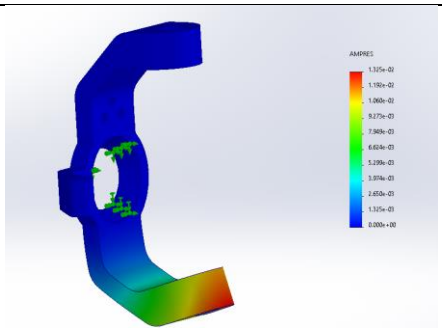 **Figure 4.3.4-4**

This test showed that both designs were effective, but it could not determine if one design was better than the other. The next set of evaluation was a decision matrix. This matrix had criteria for cost, complexity, weight, strength, manufacturability, and factors of safety with the criteria being ranked highest to lowest in that order. Each design was scored in those criteria and multiplied by the weight to make a total score for the design.

4.3.5 Brakes – Marc Maquiling

The selection design for the brake rotor design was based on the customer and engineering requirements presented earlier. Keeping the diameter, force, number of pads, and material equal, each of the rotor were compared using a design matrix. Each criterion was given a weight and scored respectively to reflect their relevance to the overall goal. The cost, fade resistance, weight, complexity, size, and offroad resistance of each rotor were compared to come with a preliminary final rotor design for purchasing for the brake assembly.

4.4 Concept Selection

4.4.1 Front Suspension – James Cole

The decision matrix that was used to determine which A-arm to proceed with in the final front suspension system is shown below in Table 4.4.1-1. Each type of arm was given a score from 1-5 based on how well they accomplish each criterion, with 5 being the best and 1 being the worst. Each score was multiplied by the weight of each criterion, which were averaged to get a total weighted score for each arm. Comparing the total weighted score of each arm, it can be seen that Concept 3, the longitudinally offset arm, is the best design choice for the front suspension system. This is mainly due to the spacing that this arm provides, as each arm was seen to be sufficient in terms of strength, as seen in the mathematical modeling for front suspension.

Table 4.4.1-1: Front Suspension Decision Matrix

Criteria	Weight	A-arm	Lateral Offset	Longitudinal Offset
Complexity	15%	4	3	3
Cost	15%	4	4	4
Spacing	30%	3	4	5
Weight	20%	4	3	3
Strength	15%	4	3	3
Factor of Safety	5%	5	5	5
Total Weighted Score		3.75	3.55	3.85

Although the longitudinally offset arm was determined to be the best option, as seen in Table 4.4.1-1, the offset it provided was not as necessary as the one provided by the laterally offset arm. The offset provided by this lateral arm creates space for the shocks to be connected from the frame to the front lower arms. Due to this fact and the observation that this arm also takes stress levels far below the yield strength of the material, this design is chosen. Since this offset is only necessary for the front upper arm, the front lower arm is designed as a standard A-arm for an increase in strength, as there is no bend that creates a weak point in this design. The CAD model of the laterally offset A-arm is shown in Figure 4.4.1-1, with the standard lower arm

shown in Figure 4.4.1-2. The CAD drawings of both arms are also shown in Figures 4.4.1-3 and 4.4.1-4, with relevant dimensions and notes labeling important components of the arms.

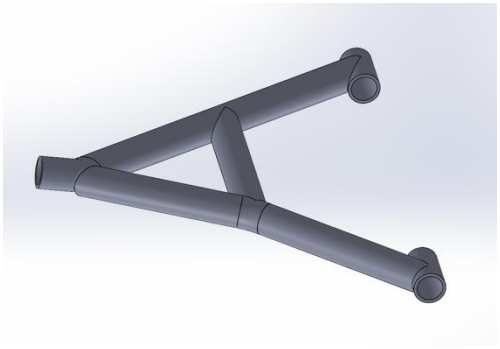

Figure 4.4.1-1: CAD Model of Front Upper Laterally Offset A-arm

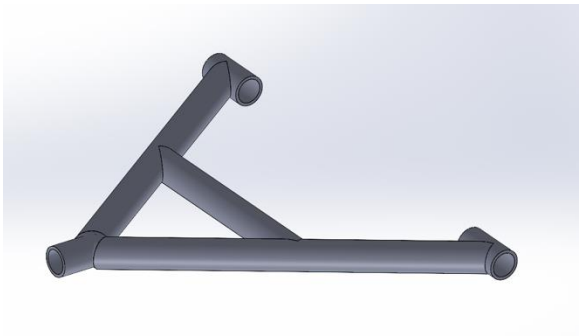

Figure 4.4.1-2: CAD Model of Front Lower A-arm

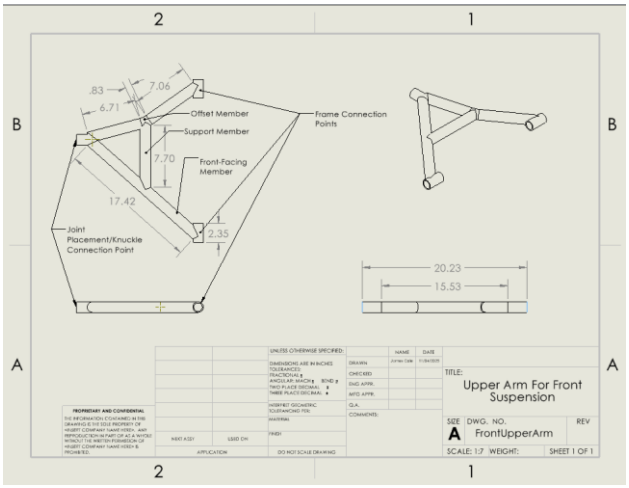

Figure 4.4.1-3: CAD Drawing of Front Upper Laterally Offset A-arm

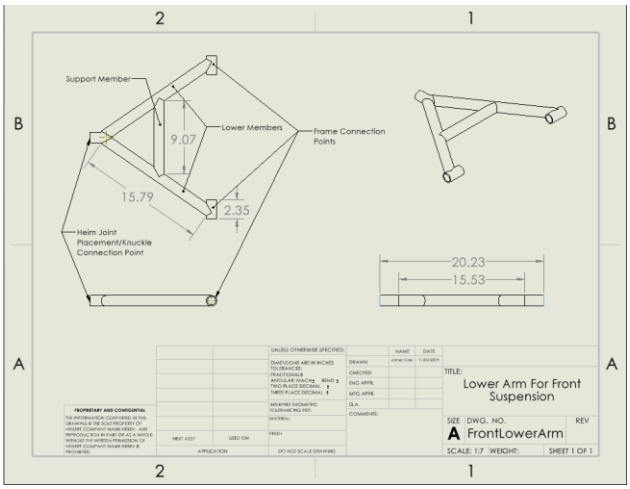

Figure 4.4.1-4: CAD Drawing of Front Lower A-arm

4.4.2 Rear Suspension – Jose Avitia

A weighted decision matrix was used to objectively evaluate rear suspension design alternatives against engineering requirements. The methodology involved preliminary screening to eliminate infeasible concepts, establishing quantifiable evaluation criteria, assigning importance weights to each criterion, and scoring designs on a consistent scale. Weighted scores were summed to compare designs, with the final selection validated against all engineering requirements as shown in Table 4.4.2-1. Design 3 (Variable Height Extended Members) was eliminated due to binding risk and manufacturing complexity, leaving Design 1 and Design 2 for formal evaluation.

Table 4.4.2-1: Rear Suspension Decision Matrix

		Design 1		Design 2	
Criteria	Weight	Score	Weighted	Score	Weighted
Manufacturability	0.15	2	0.3	4	0.6
Cost	0.3	2	0.6	3	0.9
Complexity	0.05	3	0.15	2	0.1
Weight	0.2	4	0.8	4	0.8
Strength	0.15	4	0.6	4	0.6
Factor of Safety	0.1	3	0.3	4	0.4
	0.95		2.75		3.4

Design 2 (Narrow Mounting Configuration) was selected based on its superior weighted score (3.4 vs. 2.75). The symmetric design with equal-length control arms (18.2-inch upper, 19.0-inch lower) offers better manufacturability, 15-20% material savings, and higher factor of

safety (1.70). Potential drivetrain clearance concerns will be addressed through detailed 3D modeling, making Design 2 the optimal balance between performance and fabrication feasibility. Figure 4.4.2-1 shows a CAD model of our final concept selected.

Figure 4.4.2-1: Proof on Concept Model of Rear Members

4.4.3 Steering – Jakob Martinez

In order to select the most optimal steering system for our vehicle, a weighted decision matrix was used. Each concept was scored against what the most important criteria for a steering system. After summing up each designs scores with their weights, the rack and pinion design received the overall highest score. The decision matrix that was used is shown below.

Table 4.4.3-1: Steering Decision Matrix

Criterion (Weight)	Weight	Manual R&P	Power-Assist R&P	Steer-by-Wire
Cost	25%	5	3	2
Weight / Packaging	10%	5	3	4
Steering effort	15%	2	5	5
Responsiveness / Driver Feel	15%	5	4	3
Safety & Reliability	20%	4	4	2
Complexity / Maintainability	15%	5	3	2
Total Weighted Score		4.35	3.65	2.8

Figure 4.4.3-2 below shows the updated CAD design of the steering box assembly.

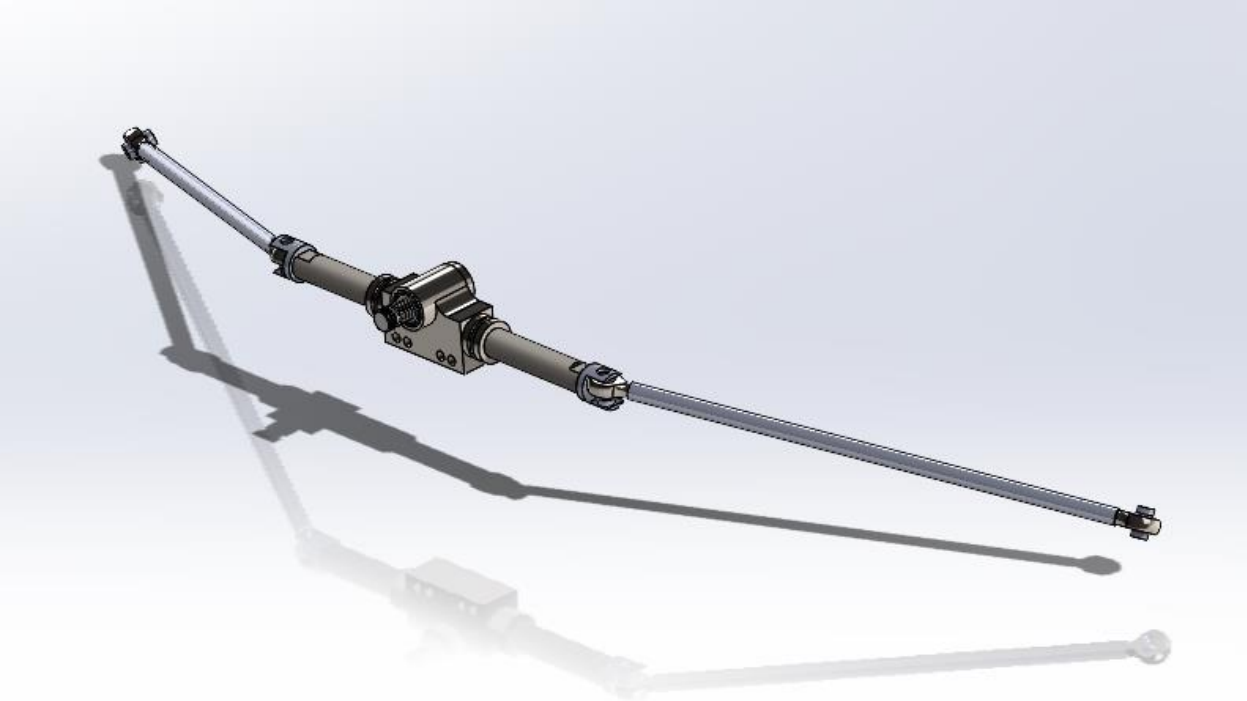

Figure 4.4.3-2: Updated CAD Assembly of Steering System

4.4.4 Knuckle – James Sundeen

The weighted decision matrix was used to eliminate one of the designs. With the scoring being weighted and summed up, Design 2 has a lead of 16% which led to it being chosen as the selected design. The decision matrix to choose the design is shown below in Table 4.4.4-1:

Table 4.4.4-1: Knuckle Design Decision Matrix

		Design 1		Design 2	
Criteria	Weight	Score	Weighted	Score	Weighted
Manufacturability	0.15	3	0.45	2	0.3
Cost	0.3	2	0.6	4	1.2
Complexity	0.2	4	0.8	2	0.4
Weight	0.2	2	0.4	5	1
Strength	0.1	4	0.4	4	0.4
Factor of Safety	0.05	5	0.25	3	0.15
	1		2.9		3.45

Future designs will have portal hub casings as the main body of the knuckle design with the parts of the knuckle stemming from the back of the casing. For now, the designs are shown in

the following figures. Figure 4.4.4-1 is the front right steering knuckle. Figure 4.4.4-2 is the front left steering knuckle. Figure 4.4.4-3 is the rear knuckle for both sides.

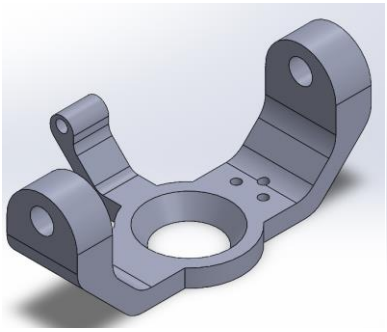

Figure 4.4.4-1

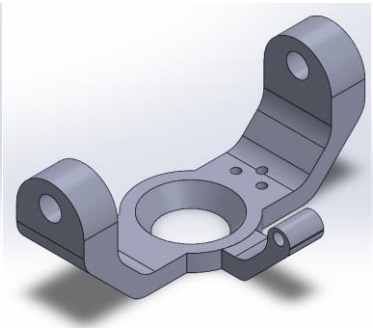

Figure 4.4.4-2

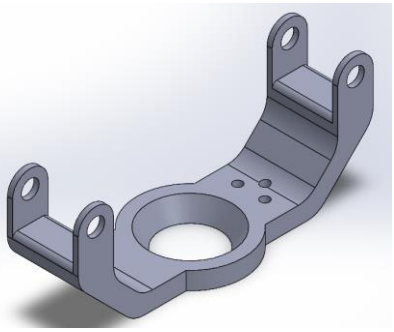

Figure 4.4.4-3

4.4.5 Brakes – Marc Maquiling

A weighted decision matrix was used, as shown in Table 4.4.5–1 to compare each rotor design to determine which design was optimal in achieving the presented customer and engineering requirements. Each design was scored from 1 to 5, 1 being the worst and 5 being the greatest. The weighted scores were then summed and compared to determine which design suited the criteria the most. As displayed on Table 4.4.5–1, the solid rotor design was chosen as the final preliminary final design for the brake assembly.

Table 4.4.5–1: Weight Rotor Design Matrix

CRITERIA	WEIGHT (%)	SOLID ROTOR		VENTED ROTOR		DRILLED AND SLOTTED	
		SCORE	WEIGHT	SCORE	WEIGHT	SCORE	WEIGHT
COST	20	5	1	3	.6	2	.4
FADE RESISTANCE	15	3	0.45	4	.6	5	.75
WEIGHT	10	3	.3	2	.2	1	.1
COMPLEXITY	20	5	1	3	.6	1	.2
SIZE	20	4	.8	3	.6	2	.4

OFFROAD RESISTANCE	15	5	.75	3	.45	1	.15
TOTAL			4.3		3.05		2

The solid rotor design was chosen to be the preliminary final design of the brake assembly due to mainly its simplicity, cost, and complexity. However, further analysis, testing, and verification are required to determine wither the chosen rotor design can withstand the harsh offroad environment of the racecourse. Different designs could also be chosen after testing and simulation, such as a combination of vented and slotted, to accommodate the terrain presented in the racecourse.

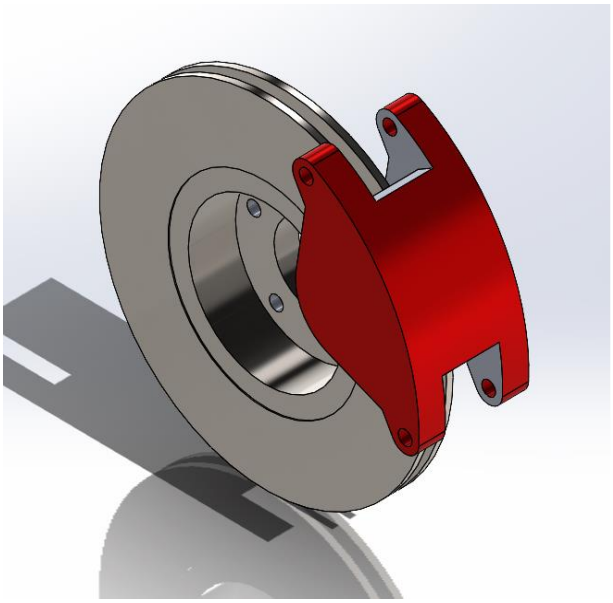

Figure 4.4.5–1: Solid Rotor and Caliper Housing Assembly.

5 SCHEDULE AND BUDGET

5.1 Schedule

The Gantt chart shows the current progress of this semester's suspension sub-team for the Baja SAE Capstone. Most of the documentation tasks have been completed and the designs are nearly complete. Some final design changes must be made, and materials need to be ordered to begin manufacturing before the semester ends. More funding must be acquired before the semester ends as well.

Figure 5.1-1: Gantt Chart with Current Semester and Future Work

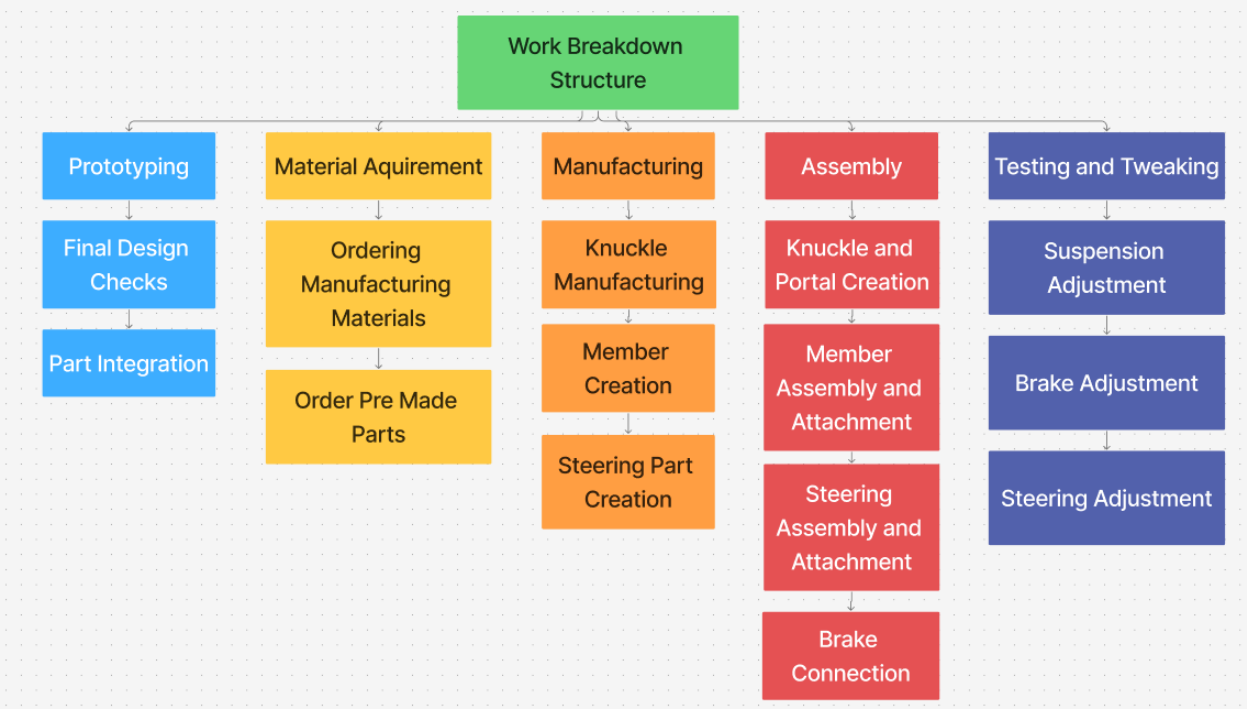

Figure 5.1-2: Work Breakdown Structure

The break down is divided into 5 sections being prototyping, material acquirement, manufacturing, assembly and the testing. The prototyping section should be editing the first prototype to answer any questions that remained unanswered. This should also be another time to check the integration of the other sub systems of the vehicle. The material acquirement should happen once any designs are completely finalized. This includes ordering any material needed for the manufacturing process or ordering off the shelf parts that will be used in the design. The manufacturing section comes with the finalized design. This should also be happening as part of the prototyping since some material has already been obtained. The assembly section will come when the vehicle's sub systems can all start to be put together. This includes creating the suspension sub systems as well as integrating them with the drivetrain team and attaching everything to the frame. The testing and tweaking will happen after full assembly of the car and there can be a true stress test of the car. That will be the first opportunity to adjust the suspension, brake and steering systems on the car.

5.2 Budget

The total budget for our sub-team is $8,966.61. Material costs are $3,714.77, including prototype and final design components. Competition expenses total $5,251.84, covering SAE registration ($1,850), membership fees for 6 team members ($240), and travel costs including hotel, vehicle rental, and gas. The travel expenses are estimated based on current market prices and may vary.

Table 5.2-1: Budget

Expenses		
Materials	Prototype	$60.00
	Final Design	$3,654.77
SAE Competition	Registration	$1,850
	Membership	$240
	Hotel	$2,000
	Car Rental	$611.84
	Gas	$550
Total		$8,966.61

5.3 Bill of Materials (BoM)

Our Bill of Materials totals $3,714.77 for the suspension, brakes, and steering systems. Key components include Heim joints, aluminum steering knuckle material, 4130 chromoly tubing for the frame and suspension arms, steering rack, bearing, U-joints, four disc brakes, four calipers, and four 23" tires with rims. We also purchased Optimum Kinematics software for design and testing. PVC tubing and wooden dowels were used for prototyping. Some items were donated or are already in stock at the machine shop, reducing our overall costs. We will continue seeking donations or discounts for the remaining materials.

Bill of Materials

Item #	Item Name	Description	Part #	Supplier	Website	Type	Quantity	Unit	Unit Cost	Total	Action
1	Heim Joints	Suspension Member Connection To Front Knuckle	JMX12T	Summit	Link	Component	4	ea	$ 43.99	0	In stock
2	3in x 6in x 48in Alumir	Steering Knuckle Material	F436	MetalsDepot	Link	Raw Material	2	ea	$ 659.20	1318.4	
3	3/4 in Bolts	Suspension Member Connection To Rear Knuckle	G8HB3431	Menards	Link	Component	4	ea	$ 4.35	17.4	
4	Screws	Screws that will attach steering housing to car (comes in pack	90044A129	McMaster-Carr	link	Component	1	ea	$ 10.71	10.71	
5	Steering rack	Steering rack	2932N1	McMaster-Carr	Link	Component	1	ea	$ 150.00	0	Using in house
6	Steering bearing	Bearing that connects to pinion to allow for smooth roation	2780T65	McMaster-Carr	Link	Component	1	ea	$ 38.36	38.36	
7	U - Joints	Steering U-joints				Component	2	ea	$ 50.00	100	
8	Optimum Kinematics	Student edition software for suspension design and analysis		Optimum G	LInk	Software	1	ea	$ 295.00	295	Purchased
9	4130 Chromoly 1.25"x	Chassis & Suspension tubing	CMR1049	Advanced Metal Sales		Raw Material	20	ft	$ 112.93	0	Donated
10	4 x Tires	Tires and rims 23"		BBWheels	link	Finished Good	4	ea	$ 148.47	593.88	
11	4 x Disc Brakes			Point Karting	Link	Finished Good	4	ea	$ 143.12	572.48	
12	4X Calipers			Wilwood	Link	Finished Good	4	ea	$ 171.42	685.68	
13	1" PVC tubing	1 in. x 10 ft. PVC Schedule 40 Tubing DWV Pipe	PVC40 PEPIP	Homedepot	Link	Raw Material	3	ft	$ 8.91	26.73	Purchased by Chasis
14	Vibration-damping bushing	Neoprene Vibration-Damping Bushing, 1.09" Diameter, 140 lbs	8109N14	McMaster-Carr	LInk	Component	2	ea	$ 11.43	22.86	
15	Wooden 3/8 Dowels	Wooden Dowels for temperary tie rods		Home Depot	Link	Raw Material	3	ea	$ 11.09	33.27	Purchased
									Total	3714.77	

Figure 5.3-1: Bill of Materials for Suspension, Breaks, and Steering.

6 DESIGN VALIDATION AND INITIAL PROTOTYPING

6.1 Failure Modes and Effects Analysis (FMEA)

The team conducted multiple Failure Modes and Effects Analysis (FMEA) to systematically evaluate potential failure points in the BAJA vehicle and assess their impact on performance, safety, and reliability. Five separate FMEAs were performed, covering the steering knuckle, front suspension arms, steering system, rear suspension, and brakes. Each analysis identified possible failure modes, their causes, and effects, and assigned severity, occurrence, and detection ratings to prioritize risks. This process allowed the team to implement targeted design improvements and preventive measures, ensuring that critical components meet safety and performance requirements under off-road conditions.

6.1.1 Steering Knuckle

Product Name: NAU SAE BAJA		Development Team: James Sundeen				Page No 1 of 1			
System Name: Suspension						FMEA Number			
Subsystem Name: Knuckles						Date: 11/25/25			
Component Name: Front and Rear Knuckle									
Part # and Functions	Potential Failure Mode	Potential Effect(s) of Failure	Severity (S)	Potential Causes and Mechanisms of Failure	Occurance (O)	Current Design Controls Test	Detection (D)	RPN	Recommended Action
P1: Knuckle/Portal Hub Casing	Deformation/Destruction	Wheel is no longer supported, Car no longer competes	10	Extreme Applied Force/ Crash	3	FEA on Structural Integrity	1	30	Keep Factor of Safety of the design as high as possible to avoid deformation
P2: Bearings	Lock Up/Fall out	Axle or portal gears struggle to spin	5	debris, lack of lube	2	CAD or Visual inspection	5	70	design lock for the bearing to avoid slip and clearance to avoid rub
P3: CV Axles	Deformation/Destruction	Wheel is no longer supported, Car no longer competes	9	Extreme Applied Force/ Crash	1	visual inspection	4	36	keep axles inside of other parts like suspension members and frame supports
P4: Casing Bolts	Shear	Opening or portal hub	7	Debris/ extreme applied force	4	visual inspection	1	28	Change bolts regularly or check regularly for damage after a hit

Figure 6.1.1-1: FMEA of Steering Knuckle

The knuckle design has many parts that connect to it and it is an important structural member to keep the wheel rolling while the car drives. It is also an expensive part, and it is not easily repairable so keeping the part intact is imperative. The knuckle could break or bend under extreme load cases, but a high factor of safety can help to avoid the knuckle from breaking. Another part on the knuckle design that could break is the bearings. The bearings can slip out of their fitting or have debris lodged inside of it. Covers as well as a bearing lock can be used to prevent both issues. The CV axles can also fail but they would fail from an extreme load case as well. The CV axles are protected by other more expendable parts so if an applied force manages to break the axles, then the race is over anyway. The last part that could break are the bolts used for connecting the portal hub cover to the case. These can fail from the debris that will be in the wheel as well as the amount of torque place upon them. Strong bolts could be used as well as replacing the bolts regularly, so the same bolts do not continuously take a force load. Each of these parts has a high risk of causing catastrophic damage to our vehicle but they are all easily preventable and detectable, so the RPN is not high.

6.1.2 Front Suspension

Product Name: NAU SAE BAJA		Development Team: James Cole				Page No 1 of 1			
System Name: Suspension						FMEA Number			
Subsystem Name: Front Arms						Date: 11/04/2025			
Component Name									
Part # and Functions	Potential Failure Mode	Potential Effect(s) of Failure	S	Potential Causes and Mechanisms of Failure	Occurance (O)	Current Design Controls Test	Detection (D)	RPN	Recommended Action
P1 – Upper Arms (Guides Wheel Movement)	Cracking or bending of the pipe, especially at the bend	Change in camber angle, uneven vehicle, less stability, reduced clearance	7	Poor material selection, thi pipes, repeated use, installation errors	4	Visual observation, check mounting points	2	56	Ensure proper installation prior to use, use mathematical modeling to ensure material properties and geometry will suffice
P2 – Lower Arms (Guides Wheel Movement)	Cracking or bending of the pipe	Change in camber angle, uneven vehicle, less stability, reduced clearance	7	Poor material selection, thin pipes, repeated use, installation errors	4	Visual observation, check mounting points	2	56	Ensure proper installation prior to use, use mathematical modeling to ensure material properties and geometry will suffice
P3 – Heim Joints (Increase Range of Motion of Control Arms)	Ball wear, angle of rotation being exceeded	Looseness of the joint, the angle of rotation being exceeded may cause sudden failure	6	Repeated use, harsh use, installation errors, corrosion	6	Visual observation, test the angle of rotation, check for corrosion, audible observation	1	36	Ensure full thread engagement, have frequent inspections, add lubrication

Figure 6.1.2-1: FMEA of Front Suspension

Figure 6.1.2-1 displays the FMEA of the front suspension system which covers potential failures that can occur on the main components of this system along with their causes and ways to avoid them. The components in consideration are the front upper and lower arms, which guide wheel movement, along with the Heim joints that connect these arms to the steering knuckle, which also increase the range of motion of the arms. The control arms could crack or bend, especially the offset upper member at the bent area, due to factors such as poor material selection and installation errors. These failures could lead to the vehicle becoming less stable and changes in the camber angle. The Heim joints on the other hand, could experience ball wear as well as the angle of rotation being exceeded due to repeated and harsh use, which could cause looseness in the joint or sudden failure. To mitigate these failures, mathematical modeling was done to present a stress analysis on these members while comparing the results to the yield strength of the material, ensuring that proper material selection was done and to ensure that no cracking or bending will occur. For the Heim joints, ensuring full thread engagement and having frequent checkups will help in mitigating failure. The risk trade-off analysis that was done considered risk priority numbers (RPN) that were calculated considering the severity, probability, and detectability of the failures. The main risk trade-off that can be noted is adding the risk of the bend in one of the front upper members, which creates a weak point in that arm. This risk was taken to get the trade-off of clearance for the shock placement on the lower arm, which allows for a more compact vehicle.

6.1.3 Steering

Product Name: NAU SAE BAJA		Development Team: Jakob Martinez				Page No 1 of 1			
System Name: Suspension						FMEA Number			
Subsystem Name: Steering						Date: 11/04/2025			
Component Name									
Part # and Functions	Potential Failure Mode	Potential Effect(s) of Failure	S	Potential Causes and Mechanisms of Failure	Occurrence (O)	Current Design Controls Test	Detection (D)	RPN	Recommended Action
P1- Steering Wheel (Provides Driver Input)	Loose or detaches from hub	Loss of driver input (Total loss of steering	10	Insufficient torque on fasteners, worn splines, failed retention pin	2	Visual QA at assembly, Assembly Torque spec	3	60	Desing secure hub/Connection point with steering column
P2 — Steering Column (transmits torque to gearbox)	Shaft fracture or spline connector failure	Loss of torque transmission; possible loss of steering	10	Fatigue f, overload, poor material, defective connection points	3	Material spec & visual inspection; design strength check	4	120	Use strong material, make sure connections are torqued to spec, visual QA during assembly
P3 — Rack & Pinion (converts rotation to linear motion)	Gear wear, excessive backlash, seizure	Increased play , reduced precision , locked steering	9.5	Inadequate lubrication, contamination, incorrect materials for gear/rack, seal failure	4	Verify material strength QA on seals, lubrication during assembly	4	152	Improve material hardness & seals; add dust boots; schedule lubrication, maintenance
P4 — Tie Rods (transfer rack motion to knuckle)	Bending, thread failure, or fracture	Wheel misalignment, reduced control, potential steering loss	9	Impact/overload, improper thread engagement, improper length	3	SOF for design, CAD to ensure proper lengths	4	108	Increase rod diameter for strength; implement inspection intervals
P5 — Heim Joints (rod-end bearings)	Wear, loosening, or excessive play	Steering play, imprecise control, accelerated wear in linkage	7	Poor lubrication, contamination, undersized joint, cyclic wear	5	Selected rod-ends, occasional greasing	6	210	Use sealed or maintenance-free joints; add grease fittings/shields
P6 — Steering Knuckle (wheel pivot interface)	Fracture, bearing failure, or spindle wear	Wheel collapse, total loss of control (safety hazard)	10	Impact damage, poor material, bearing preload loss3	2	Design checks (FEA), bearing selection, visual inspection	4	80	Validate with FEA & proof-load testing; specify impact-tolerant materials

Figure 6.1.3-1: FMEA of Steering System

Our team conducted an FMEA on the BAJA vehicle steering subsystem to identify critical potential failures and evaluate their impacts on safety and performance. Top priority failure modes included loosening or detachment of the steering wheel, shaft fracture in the steering column, and fracture or bearing failure in the steering knuckle, all of which could result in total loss of steering control. Other significant risks, such as gear wear in the rack and pinion, bending or thread failure in the tie rods, and excessive play in the Heim joints could reduce steering precision and vehicle control. To mitigate these failures, our design incorporated strong, fatigue-resistant materials, proper torque specifications, FEA validation, proof-load testing, sealed or maintenance-free joints, improved lubrication, and scheduled inspection intervals. The team also performed a risk trade-off analysis, prioritizing components with the highest Risk Priority Numbers (RPNs) for targeted design improvements while balancing weight, cost, and manufacturability, ensuring a robust and safe steering system.

6.1.4 Rear Suspension

Product Name NAU SAE BAJA						Page No 1 of 1			
System Name Rear Suspension						FMEA Number			
Subsystem Name Control arms and shocks						Date			
Component Name									
Part # and Functions	Potential Failure Mode	Potential Effect(s) of Failure	Severity (S)	Potential Causes and Mechanisms of Failure	Occurance (O)	Current Design Controls Test	Detection (D)	RPN	Recommended Action
LCA	Bending/ Welding failure	Changes to castor, camber& tow	7	Rough impacts at odd angles	2		1	14	Properly install, verify with engineering models
UCA	Bending/ Welding failure	Pipe Bending and Cracking	7	Rough impacts at odd angles	2		2	28	Properly install, verify with engineering models
Heim Joints	Bolt shear/ Ball wear, exceexing max angle of rotation	Shear force. Ball wear	8	Sharp impact forces	5		1	40	Have extra, easy to replace, verify with saftey factor of 1.2
Shocks	Bolt failure	Shear force	8	fatigue/ shear	3		1	24	Have extra, easy to replace, verify with saftey factor of 1.2

Figure 6.1.4-1: FMEA of Rear Suspension System

The FMEA for the rear suspension control arms identifies bending and welding failures in both the lower control arm (LCA) and upper control arm (UCA) as primary risks, mainly caused by rough impacts at odd angles. These failures can alter key suspension geometry such as camber, caster, and toe, or cause structural cracking. Severity is moderate-high (S=7), with low occurrence and good detectability, resulting in RPNs of 14 and 28. Recommended actions focus on proper installation and verification through engineering models. Additional risks include bolt shear and ball wear in Heim joints, as well as bolt failure in shocks, driven by impact forces and fatigue. These components carry higher RPNs (24–40), and the recommended mitigation is to keep spare parts on hand and verify sizing with an adequate safety factor.

6.1.5 Brakes

Product Name: NAU SAE BAJA		Development Team: Marc Angelo Maquiling				Page No 1 of 1			
System Name: Suspension						FMEA Number			
Subsystem Name: Brakes						Date: 11/05/2025			
Component Name									
Part # and Functions	Potential Failure Mode	Potential Effect(s) of Failure	S	Potential Causes and Mechanisms of Failure	Occurrence (O)	Current Design Controls Test	Detection (D)	RPN	Recommended Action
P1- Rotor (Converts Motion to Thermal Energy)	Fading, Warping, Cracking	Reduction of Break Power, Vibration	9	Overheating, Heavy Braking, Terrain, Contamination	4	Visual, Hearing, Braking at Speed, Thickness Check, Heat Measurement	5	180	Wear and Warping Check, Proper Material Choice, QAs
P2 — Caliper (Clamps Pads Into Rotor)	Wear, Sticking, Leaking	Brake Pressure Reduction, Uneven Breaking	9	Poor Maintenance, Corrosion	3	Hearing, Braking at Speed, Leaking Check	3	81	Cleaning, Lubrication, and Checking Actuation
P3 — Caliper Pad (Provides Friction to Stop Car)	Wear and Glazing	Increased Stopping Distance, Disc Damage	9	Damaged Rotor, Heavy Braking	7	Braking at Speed & Static, Hearing, Wear Check	2	126	Checking for Wear, Replace Timely
P4 — Master Cylinder (Provides Hydraulic Pressure to Caliper)	Leaking	Brake Failure, Reduced Pedal Actuation	10	Terrain, Poor Maintenance, Contamination	4	Leak Test, Pressure Check	1	40	Seal and Fluid Checks, Immediately Repair for Any Leaks
P5 — Brake Lines(Carry the Hydraulic Pressure)	Corrosion, Leaking	Brake Failure, Reduced Pedal Actuation	10	Age, Corrosion, Terrain	2	Leak Test, Pressure Test, Visual	1	20	Regular Visual Inspection, Replace Timely
P6 — Brake Pedal (Converts User Force to Brake Control)	Sinking, Bending	Delayed Pedal, Reduced Control	9	Misalignment, Hydraulic Issues, Age	2	Force Input Check, Link Check	3	54	Check links, Adjust for Proper Ergonomics

Figure 6.1.5-1: FMEA of Braking System

The brake system FMEA identifies several high-severity failure modes across critical components. The rotor presents the highest risk due to fading, warping, or cracking from overheating and heavy braking, resulting in reduced braking power and vibration (RPN 180). Brake pads also carry a significant risk (RPN 126) because wear and glazing can increase stopping distance and damage the rotor. Caliper issues such as sticking, leaking, or general wear can reduce brake pressure and cause uneven braking (RPN 81). Hydraulic failures in the master cylinder and brake lines are severe but have lower occurrence and strong detection, leading to lower RPNs of 40 and 20, respectively. Pedal bending or sinking is less likely but still affects braking control (RPN 54). Recommended actions emphasize regular wear checks, leak tests, proper material selection, and timely replacement or repair to ensure reliable braking performance.

6.2 Initial Prototyping

This section outlines the early prototypes developed to explore key design questions and validate assumptions. Each prototype is presented with the specific question it aimed to answer, the insights gained from testing, and how those insights shaped the direction of the design. By breaking down each prototype in this way, we demonstrate how the prototyping process informed our next steps for the manufacturing process.

6.2.1 Steering Knuckle

From the first set of prototypes, there were many answers to the main question of how the knuckle design integrates with the other parts. The knuckle design was effective but there were issues with how parts connected to it as well as fit through it. From a simple test, random cv axles could not fit through the initially design hole. There was also an issue with the Heim joints being in the way of the cv axle placement. The tie rod connection was too close to the cv axle and it was also not the correct geometry. Since Heim joints are currently being used for all the mounting points, there is an issue with the rear knuckle's rotation in an incorrect axis. This will still need to be fixed with a future iteration of the design. Many improvements have been made to the new version of the design. A simple comparison is shown below between Figure 6.2.1-1 and Figure 6.2.1-2.

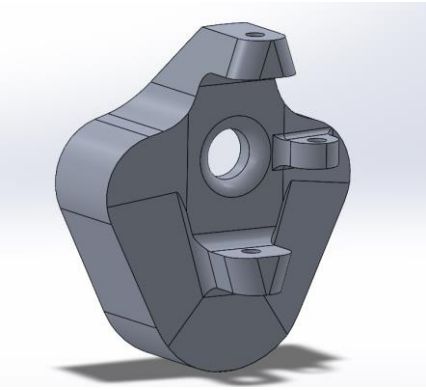

Figure 6.2.1-1: Steering Knuckle V1

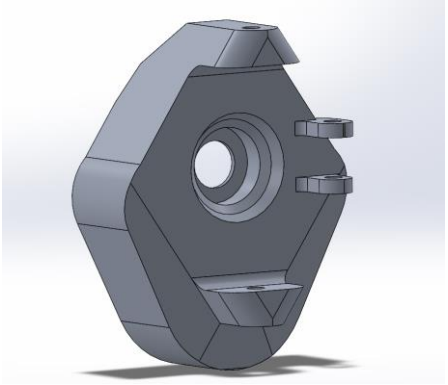

Figure 6.2.1-2: Steering Knuckle V2

6.2.2 Front Suspension

Through the prototyping of the front suspension control arms, the question of what the suspension travel looks like compared to the engineering requirements was trying to be answered. This question was able to be answered by attaching the prototyped control arms to the chassis and measuring the full distance the suspension system moved fully up and down. Figures 6.2.2-1 and 6.2.2-2 showcase the prototyped control arms from different angles.

Figure 6.2.2-1: Prototypes Front Suspension System Connected to Chassis and Knuckle

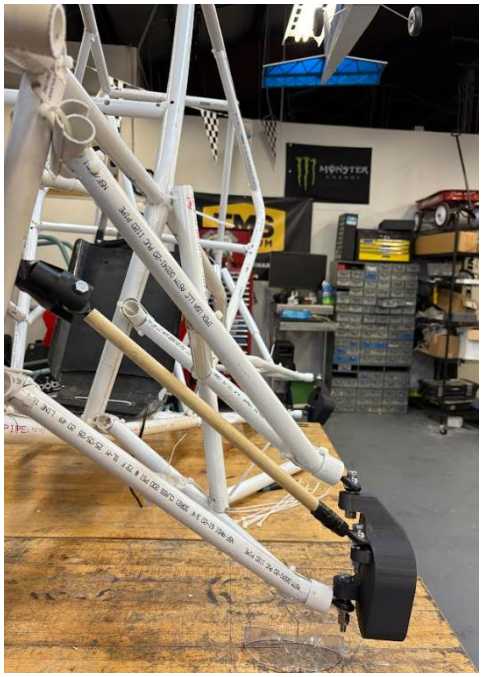

Figure 6.2.2-2: Side View of Prototyped Front Suspension System

The answer to the proposed question was that the front suspension system had a total suspension travel of 13”, which is within the 12”-15” range given in the engineering requirements. This answer led to the conclusion that the design process was going in the right direction, but some changes that had to be made were noticed. As seen in Figure 6.2.2-1, the shock has little to no clearance with the upper control arm due to the offset in the right member being closer to the knuckle than the chassis. Further faulty points are seen at the connection of the two outer members where the Heim joint connects to the steering knuckle on both arms. This connection point was designed as a separate part as opposed to being part of one of the outer members, leading to a lot of play in these points, requiring duct tape to hold them together. Based on this new info, the offset in the upper arm is going to be moved closer to the chassis to accommodate for the shock, and the Heim connection points are going to be integrated into one of the outer members of both arms to create an overall more robust system.

6.2.3 Steering

During the initial prototyping stage of the steering system, the primary questions I wanted to answer were whether the calculated Ackermann Steering angles were accurate, whether the selected tie-rod lengths gave the correct wheel motion, and how well the steering box fit spatially within the front chassis. through physical testing, I confirmed that my inner wheel angle was nearly exact, with a calculated 49.3° and a measured 49° at full lock. The outer wheel angle measured 31°, slightly higher than the calculated 28.9°, which indicated a small deviation but still acceptable performance for the prototype stage. The prototype also revealed that my original 17-inch tie rods were too long, causing excessive knuckle rotation even without steering input.

After re-measuring the setup, I updated the tie-rod length to 14 inches, which provided the proper steering response and correct wheel angles. Finally, the spatial evaluation showed that the steering box fits comfortably within the front assembly, leaving sufficient room for other systems such as the front differential. These findings will guide the next iteration by refining tie-rod geometry and making minor adjustments to improve steering accuracy and overall system integration. The figures below show the initial prototype of the steering subsystem.

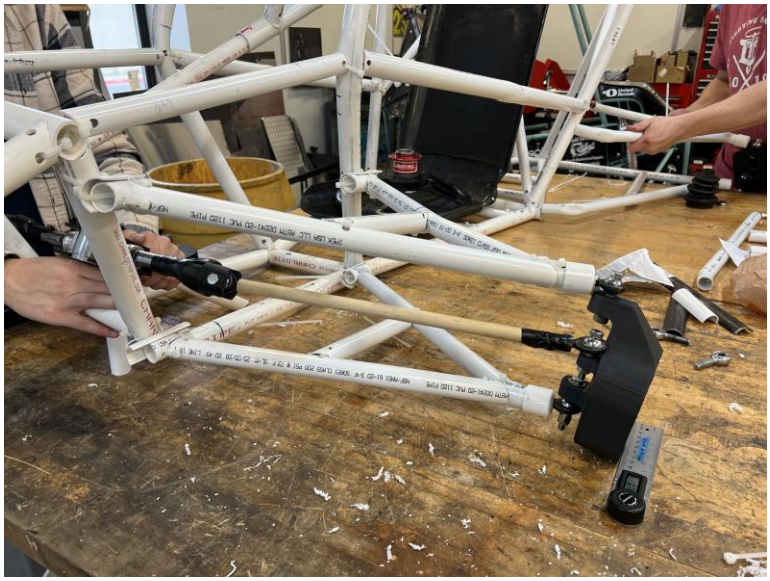

Figure 6.2.3-1: Side View of Tie Rod Connection

Figure 6.2.3-2: Front View of Steering Assembly

6.2.4 Rear Suspension

The prototype answered the question of how much travel the arms have, verifying that the design will fit within the racing rules. The prototype also showed that the rear knuckle needs an additional connection point to lock in the tow angle, using Heim joints rather than a pipe with an insert. Adding the tie rod to the design with Heim joints lets us adjust the angles to better fit the competition, whether it's a rock crawl or an endurance race.

The prototype showed that the members needed to be shortened by 2 inches on either side to give spacing for the portal hub connection to the tire. While shortening the arms slightly reduces rear-suspension travel, we can still meet our goal of 12-15 inches of travel measured from the center wheel.

Figure 6.2.4-1: Rear Suspension

6.2.5 Brakes

A physical model of the rotor and caliper assembly was installed on the prototype frame system, as shown in Figure 6.2.5-1. The brake assembly was attached to a prototyped CV axle and frame at the approximate location in relation to the differential within the toe box, using zip ties to answer the question of whether there is enough spatial allowance for an inboard installation of the front brake system.

Figure 6.2.5-1: Physical Modeling of the Front Brake System

Despite the lack of a physical model for the front differential, it became apparent that there was very little room on the toe box that would allow for a rule-compliant inboard installation of the front brake system. Due to the minimal space present for the inboard brake, an additional design of the front brake system was initiated, where the brakes are to be attached to the hub of the wheel alongside the portal hubs and the suspension knuckles. Further analysis requires the knuckle and portal hub assembly to be corrected to allow for the brakes to be addressed. Though the space within the wheel hub may also pose a problem. If an insistence on inboard installation for the front brake system were to continue, reconfiguration of the differential is required to accommodate an inboard brake system installation, as well as changing the framing and paneling for the outside portion of the toe box.

6.3 Other Engineering Calculations

6.3.1 Steering Knuckle

All other calculations performed since the last report have been finite element analysis to check the factors of safety with the growing force loads. Karston Kluth on the Drivetrain sub-team oversees the portal hub gear reduction system that is now inside of the knuckle design. These gears will create force loads that will affect the steering knuckle. The analysis of the knuckle also used the 10,000 Newton load or 2,248 pound-force load for the bump load to examine an extreme load case. The finite element analysis of the rear knuckle was done to focus on the integrity of the suspension member mounting locations. This is seen in Figure 6.3.1-1. There were issues with the load case affecting the bolt holes for the heim joints as well as some critical points on the upper part of the knuckle. This design also had some stress factors reach critical inside of the casing on the bearing walls. All of these stress locations had to be reduced to continue towards the manufacturing of a knuckle so a new design was made.

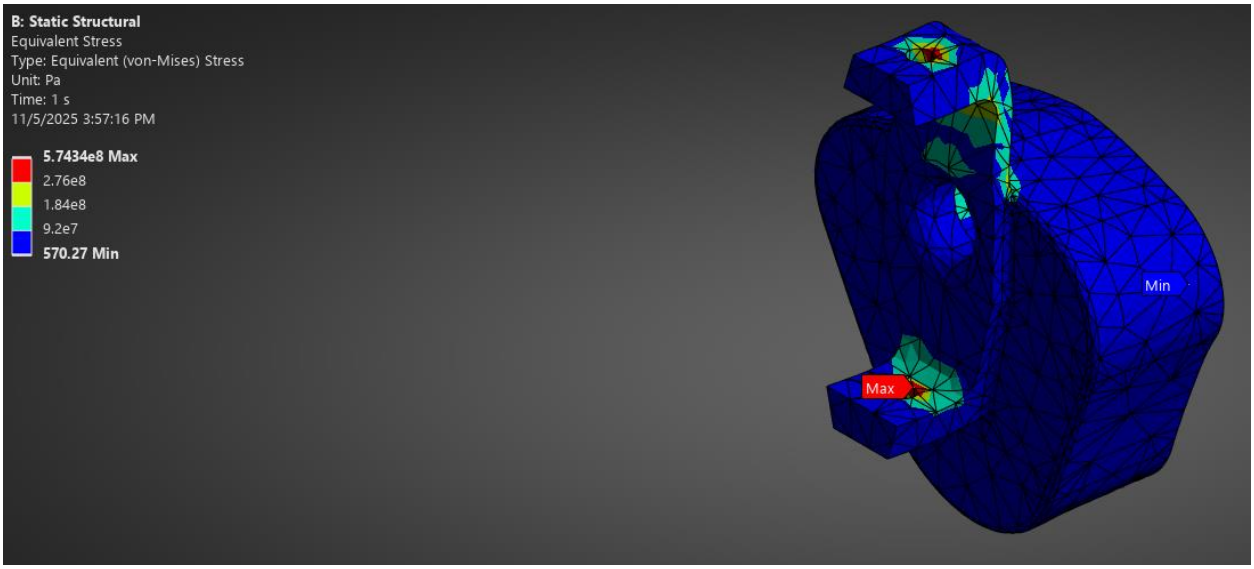

Figure 6.3.1-1: Rear Knuckle with Portal ANSYS Analysis

Two design iterations were completed since an additional component was changed to be mounted onto the knuckles. The brake calipers are going to be mounted on the front knuckles, and they are going to be placed above the portal hubs, so the mounting is going to be inside the structure of the casing. This is seen in Figure 6.3.1-2.

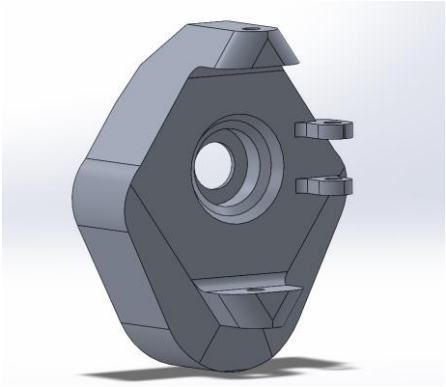

Figure 6.3.1-2: Front Steering Knuckle with Portal Hub Casing and Brake Mounting

Another ANSYS analysis was done on the knuckle to test the structural integrity of the new knuckle. There is now more material to support the suspension member mounting locations as well as a relocation of a bearing to have more material on the inside of the portal hub casing. The tie rod connection has changed to a fork design to improve the structural integrity of the Heim placement and move any critical point off the knuckle. The same testing was done to this knuckle design but there was an addition of the steering forces. The assumed force for testing is 500 newtons or 112 pound-force split between the directions of the tie rods. The assumed angle of the tie rod was 30 degrees, so the forces are split to 17.3 pound-force in the x and 111 pound-force in the z. The ANSYS analysis of the new knuckle design is shown in Figure 6.3.1-3 below.

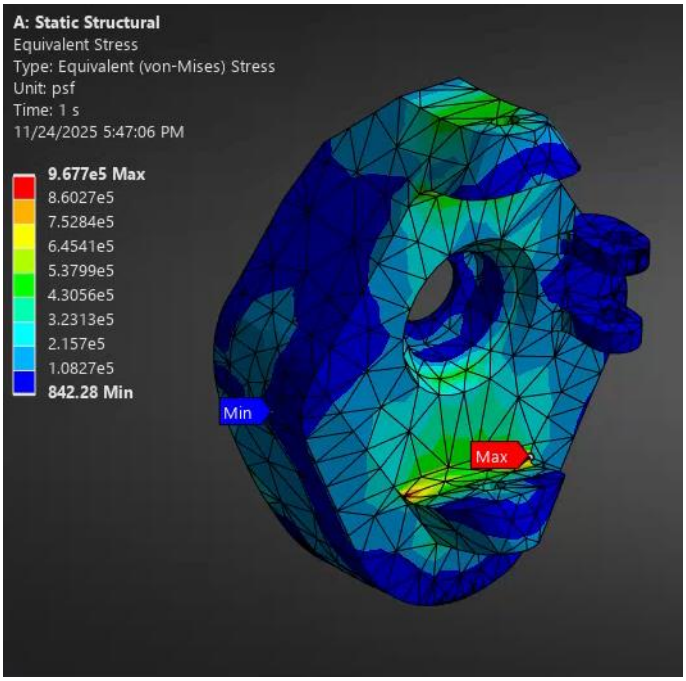

Figure 6.3.1-3: ANSYS Analysis of Figure 6.3.1-2 Knuckle Design

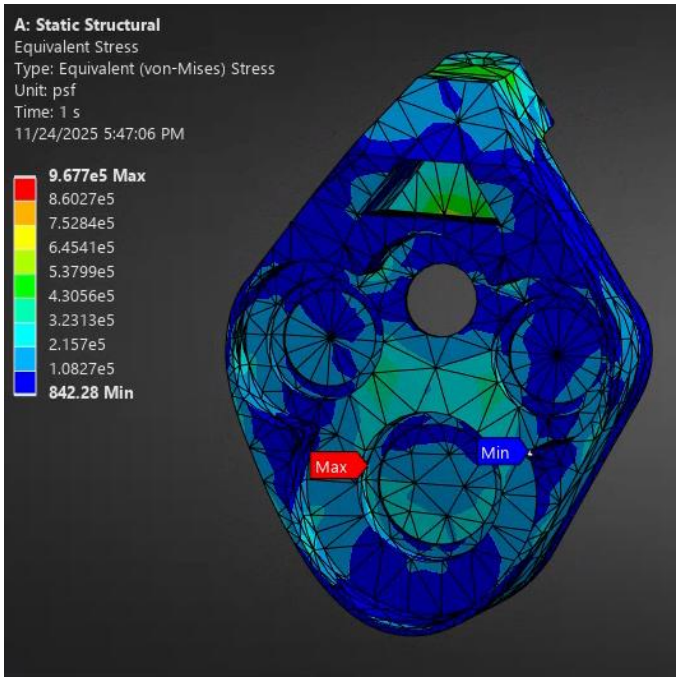

Figure 6.3.1-4: ANSYS Analysis of Figure 6.3.1-2 Knuckle Design

This design had a factor of safety above 5 so it can be used for manufacturing. The design has some issues like the brake components have yet to be implemented so the torque from the brake calipers was not added to the load case as well as cv axle dimension have yet to be found

so design changes may still have to occur. Each design change will come with a new ANSYS analysis to confirm that the factor of safety will remain above 3. For now, the steering knuckle designs are shown in Figure 6.3.1-5 through Figure 6.3.1-7 below.

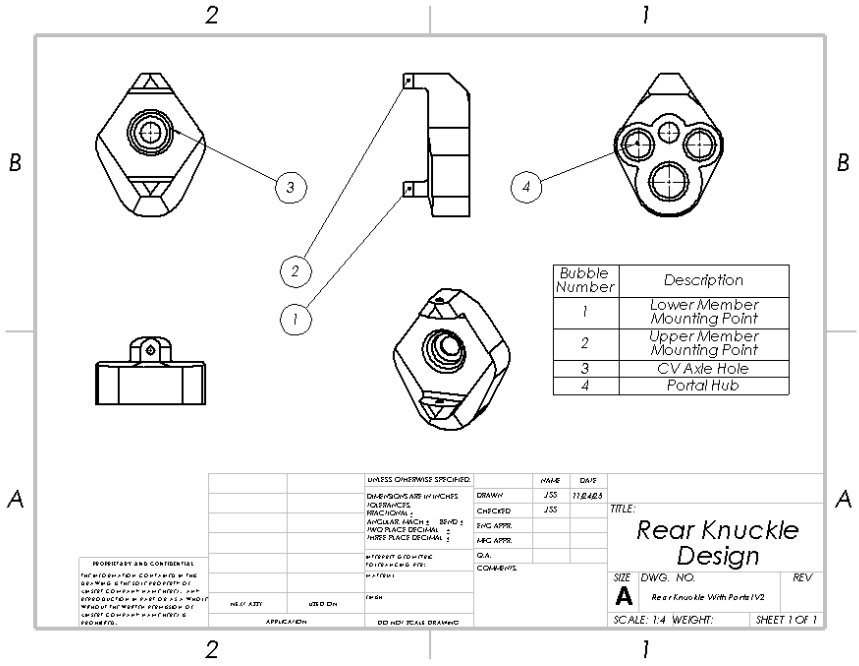

Figure 6.3.1-5: Rear Knuckle Design

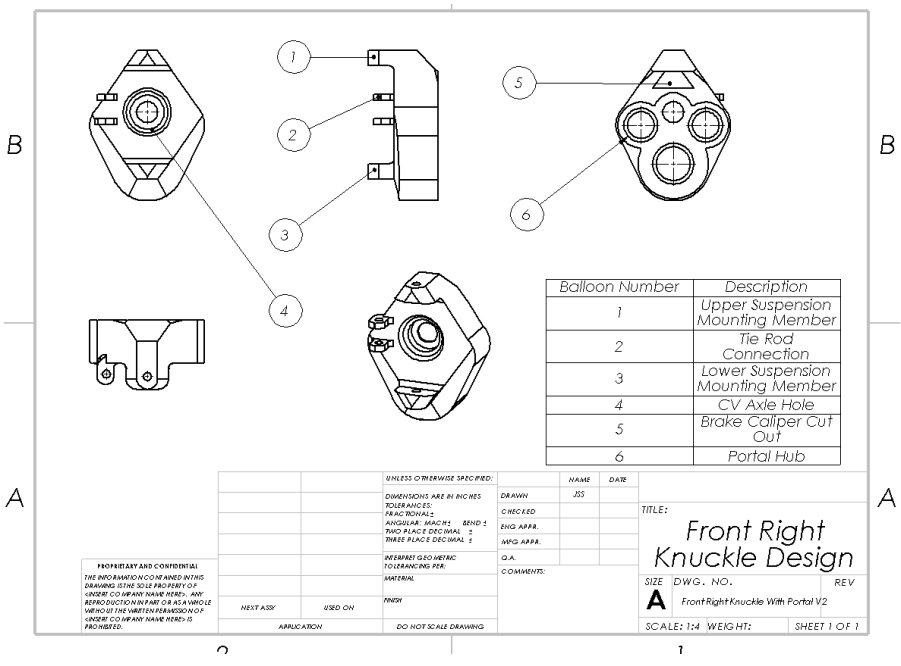

Figure 6.3.1-6: Front Right Knuckle Design

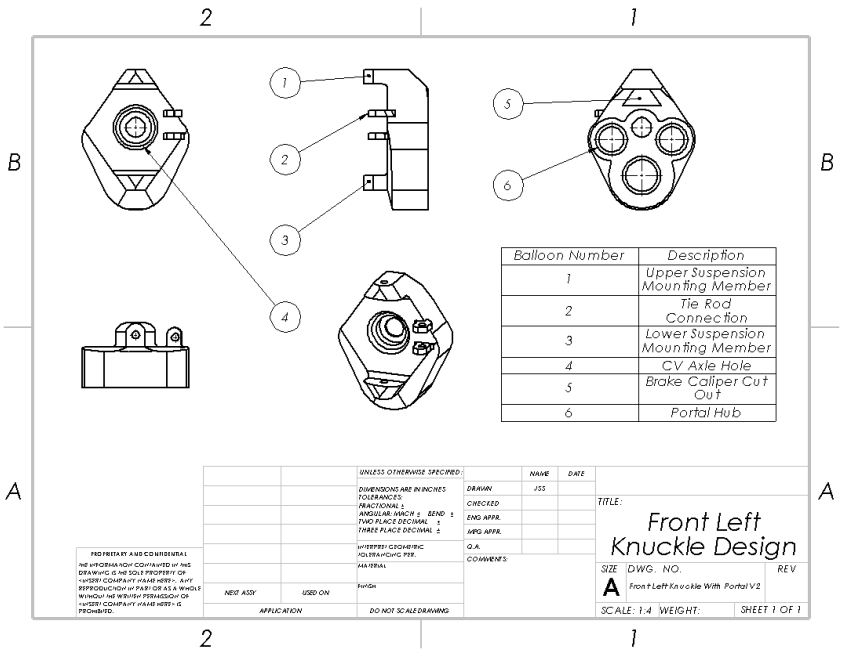

Figure 6.3.1-7: Front Left Knuckle Design

6.3.2 Front Suspension

The calculations that have been performed since the concept selection phase have been updates to the previously performed stress analysis with updated dimensions to ensure that the new designs are still valid options. Since the original stress analysis was a static one, the new analysis accounts for the forces applied to the members during the competition to produce more realistic results. The factors of safety were also calculated to ensure that they were above 1.2, a value taken to ensure the safety of the vehicle. The results of the updated design yielded factors of safety of 1.47, 1.23, and 1.36, for the offset members, other upper members, and the lower members of the control arms. These calculations were done by assuming a force of four times the static loading acts on the members evenly throughout the competition. Since this analysis neglects the middle member of each A-arm, these factors of safety are actually lower than the actual values, providing further confirmation that the design is safe. These factors of safety were calculated by dividing the yield strength of the material, 4130 chromoly steel, by the resulting stress values.

6.3.3 Steering

There have been additional engineering calculations and analyses performed since selecting the rack-and-pinion steering system. For each analysis, a load of 2,928 lbf was applied per tie rod to verify that the rack, Heim joints, and tie rods could withstand a worst-case crash load.

The first analysis conducted was for the tie rods. Euler buckling calculations were performed on the 14-in 6061-T6 aluminum tie rods to ensure adequate stability under compressive crash loading. The minimum required inner diameter was determined to be 0.667 in and was confirmed through a slenderness-ratio evaluation. The selected 0.652-in inner diameter satisfies this requirement and remains within the elastic buckling regime.

The next analysis evaluated the minimum geometric requirements and thread-shear capacity of the Heim joints. Axial stress calculations determined that the minimum required shank diameter was 0.288 in, well below the size of the selected 3/8-24 alloy-steel Heim joints. Thread-shear analysis yielded a factor of safety of 10.24, indicating substantial margin against thread stripping and confirming that the joints can safely transmit the design load.

The final analysis performed was a finite element analysis (FEA) of the steering subsystem to validate the hand calculations and assess the structural behavior under the same 2,928-lbf crash load. An ANSYS static structural simulation was conducted with loads applied through each tie rod in their correct orientations. The results showed a maximum deformation of approximately 0.9 in occurring at the tie-rod ends near the steering-knuckle connections, consistent with elastic bending under extreme loading. Stress concentrations were observed at the steering-rack connection points, which is expected due to geometric transitions and simplified modeling assumptions. While some peak stresses were higher than physically realistic because of mesh limitations and idealized geometry, the FEA results confirmed that the overall steering assembly remains structurally stable under the applied crash load and highlighted areas where geometry or mesh refinement could further improve accuracy. The figures below show the results of the static analysis for deformation and stress.

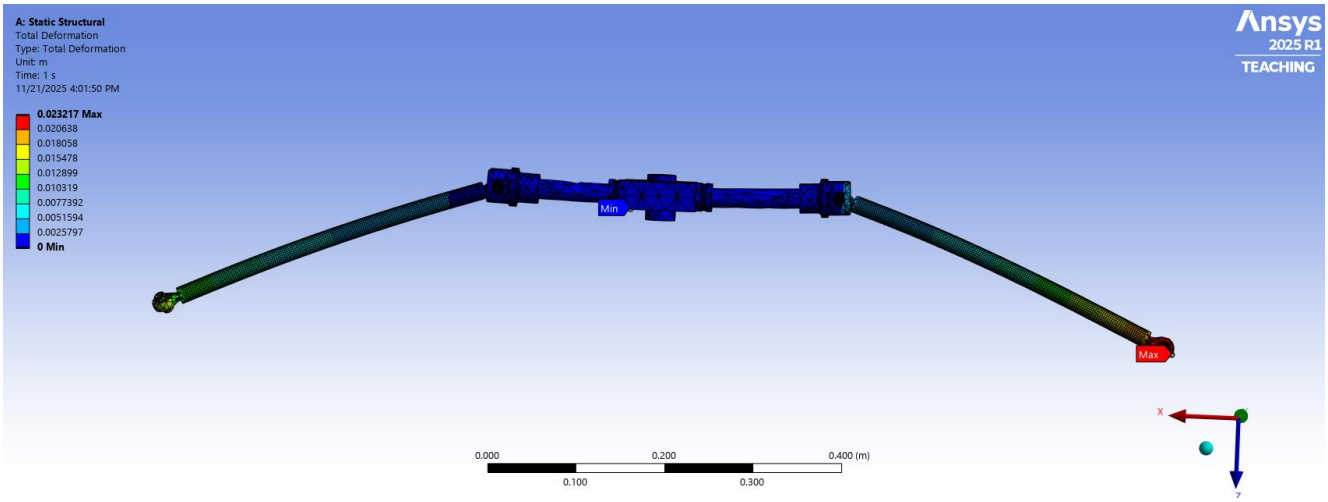

Figure 6.3.3-1: Top View of FEA Deformation Model

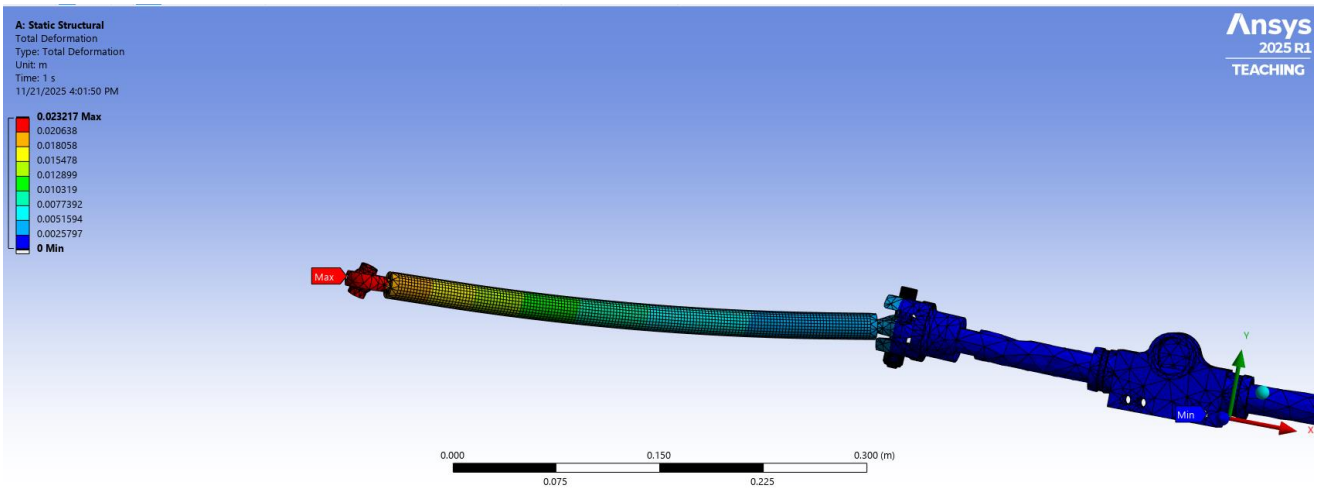

Figure 6.3.3-2: Tie Rod Deformation View

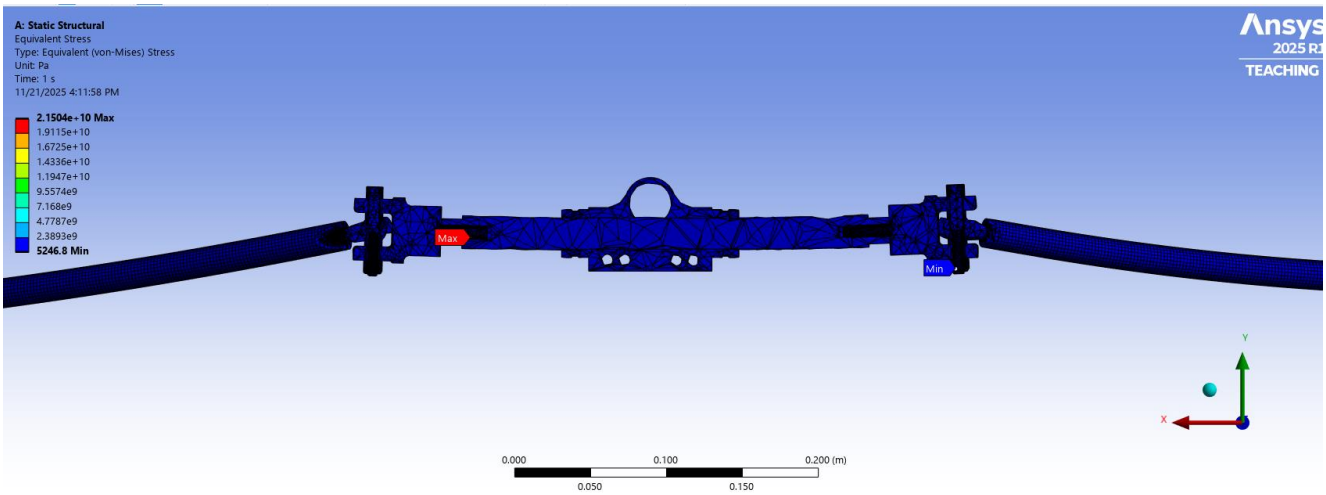

Figure 6.3.3-3: Maximum and Minimum Stress Location

6.3.4 Rear Suspension

6.3.4.1 Colby Brett

The Rear suspension control arms needed minor changes before performing calculations. After the prototype, it became apparent that the control arms were too long to be compliant with the competition regulations. To make the width of the car comply with the rules, each control arm was shortened by 2.5”. After making these design changes, ANSYS was used to perform total deformation and maximum stress calculations.

The boundary conditions are set to isolate the large bend by making the face that is connected to the Heim joint that connects the control arm to the body, as a fixed support, the cylindrical support on the right side, and a force of 1287 lbf is placed on the connection to the knuckle with a load of 1000 lbf vertically, 300 lbf towards the rear and 700 lbf in compression. These boundary conditions are applied to both upper and lower control arms, shown in the figures below.

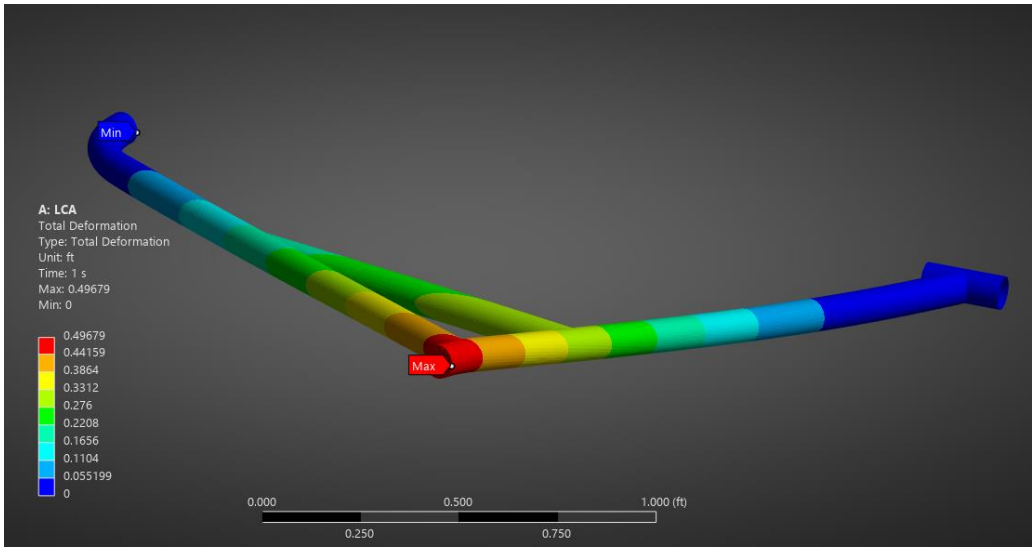

Figure 6.3.4-1: Lower Control Arm Deformation

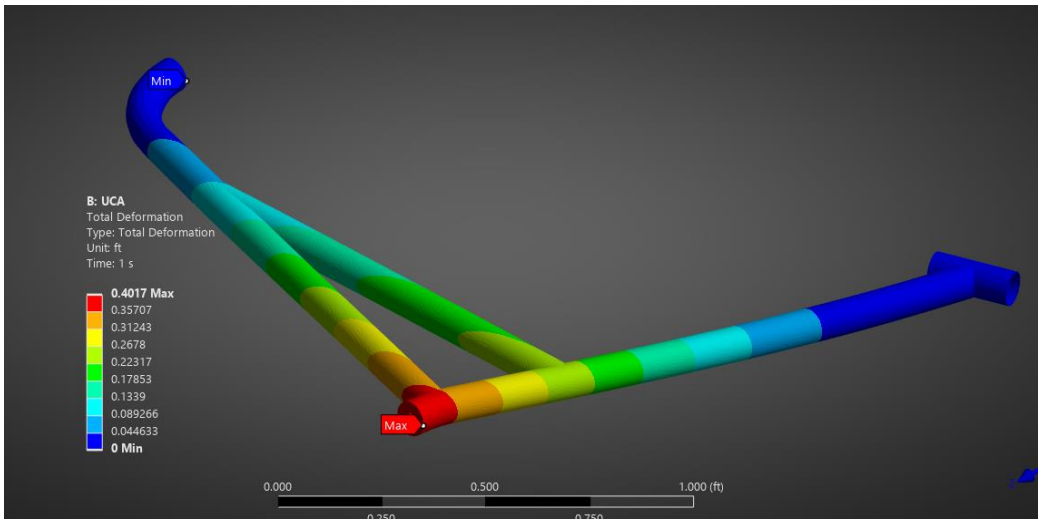

Figure 6.3.4-2: Upper Control Arm Deformation

The maximum deformation for each arm under these loading conditions is 0.5” on the lower control arm and 0.4" on the upper control arm. The maximum deformation is located near the connection of the knuckle.

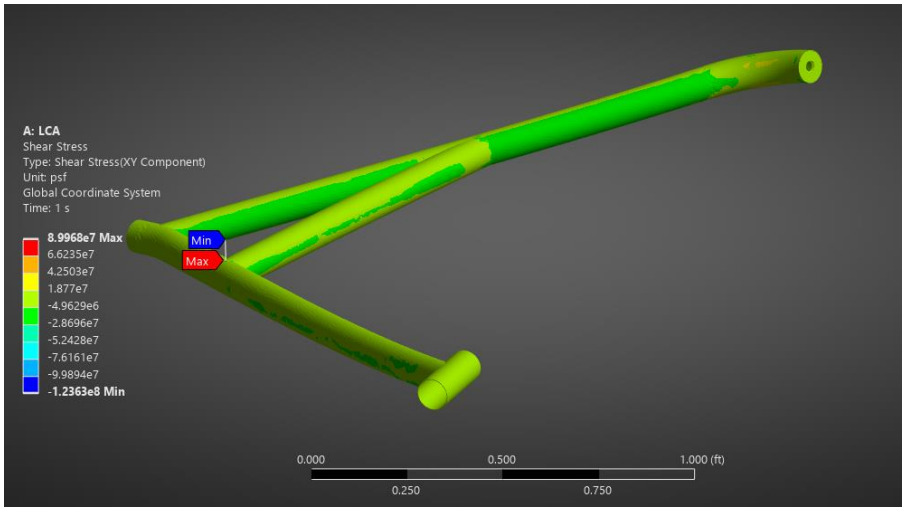

Figure 6.3.4-3: Lower Control Arm Shear Stress

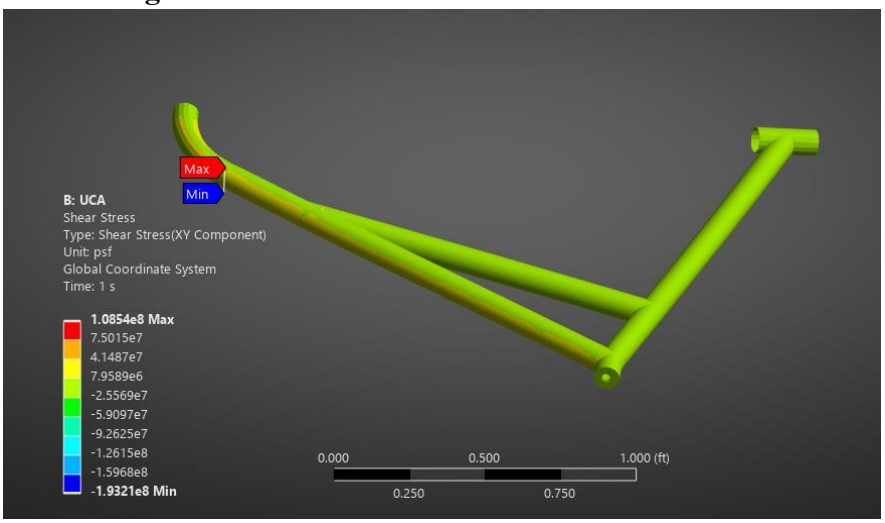

Figure 6.3.4-4: Upper Control Arm Shear Stress

The lower control arm has a max shear stress of 624.2 ksi at the connection of the support member. Where the upper control arm has a maximum shear stress near the predicted area, it is 753.75 ksi. Utilizing the material properties of chromoly 4130, the shear modulus of 11,600 ksi, the lower control arm has a safety factor of 18.5, and the upper control arm has a safety factor of 15.38.

6.3.4.2 Jose Avitia

Since the concept selection phase, there has been no change in the calculation methodology, only the use of more advanced software providing detailed results and analysis of different geometry configurations to maintain the ideal -1 to -2 degrees camber angle for the wheels. The calculations began with formulas found in the literature review [11], then progressed to the 2-D VSusp software for preliminary suspension geometry. Although VSusp could not

determine individual A-arm member lengths, it provided a useful tool for quickly establishing suitable suspension geometry.

The primary analysis was performed using Optimum Kinematics software, which provides 3-D comprehensive modeling and motion simulations. This software uses the suspension attachment points in a coordinate system to evaluate accurate suspension behavior. The simulations demonstrated excellent camber stability across all motion conditions. Heave motion showed a maximum camber change of 1.226°, while roll motion was highly symmetrical with a maximum of 0.127° on the left wheel and -0.077° on the right wheel. Pitch motion simulation revealed a nearly negligible change of -0.0178°, and steering motion maintained constant 0.0° camber with no deviation, confirming no rear steering interference.

The calculations confirmed that our A-arm geometry achieves the target camber angles with minimal variation across all motion conditions. This will provide good tire performance and handling for the vehicle during the Baja SAE competition.

6.3.5 Brakes

A refinement of the clamping forces on the brake systems involved was performed to determine accurate loads involved. Calculations of the clamping forces, hydraulic pressures, and brake dimensions were performed to gain an accurate insight into the brake system requirements, particularly on what parts of the brakes need changes and reconfiguration before purchasing.

Table 6.3.5-1 summarizes a more refined controlled variables than the initially presented calculation. The following variables incorporate worst-case scenarios into the vehicle's brake design that allow for proper margins to be introduced.

Table 6.3.5-1: Summary of Controlled Variables

Variable	Value	Units	Notes
COF_{TIRE}	1		Worst Case Value for Tire Coefficient of Friction (Real<1)
H_{COG}	25	in	Estimated center of gravity height
WB	63	in	Estimated wheelbase
W	750	lbf	Worst-case estimated weight w/ driver (Target < 620 lbf)
r_{TIRE}	11.5	in	Current tire radius
$r_{rotor\text{-}front}$	3	in	Rotor radius from the center of the wheel to the center of the caliper/pad
$r_{rotor\text{-}rear}$	3	in	Rotor radius from the center of the wheel to the center of the caliper/pad
r_{PEDAL}	5		Pedal Length / Pushrod Arm Length (adjust higher depending on space)
F_{PEDAL}	100	lbf	Input force by the driver to lock the brakes
D_{MC}	0.63	in	Temporary master cylinder diameter
COF_{PAD}	0.5		Using Willwood's BP-Q Ceramic Compound

Table 6.3.5-2 displays the calculated values from the mathematical analysis of the brake system. These values can be controlled using the controlled variables from Table 6.3.5-1, allowing the team to select the appropriate brake kits for purchase. The results presented are also for the worst-case scenario that the team can anticipate (push from the front test, a coefficient of friction of 1 for the tires, etc.) to allow for some margin of error.

Table 6.3.5-2: Summary of Calculated Variables

Variable	Value	Units	Notes
F_{COG}	750.00	lbf	Normal force applied to the center of gravity
$F_{NORM\text{-}FRONT}$	672.62	lbf	Force from the moment of the rear (worst case for the front, where the push is from the rear)
$F_{NORM\text{-}REAR}$	77.38	lbf	
$F_{CAL\text{-}FRONT}$	2578.37	lbf	Force needed to lock the front wheels (worst case for front wheels)
$F_{CAL\text{-}REAR}$	296.63	lbf	The force needed to lock the rear wheels
$F_{NORM\text{-}FRONT}$	77.38	lbf	
$F_{NORM\text{-}REAR}$	672.62	lbf	Force from the moment of the front (worst case for the rear, where push is from the front)
$F_{CAL\text{-}FRONT}$	296.63	lbf	
$F_{CAL\text{-}REAR}$	2578.37	lbf	
$F_{CAL\text{-}FRONT\text{-}MIN}$	2578.37	lbf	Minimum required force for brake lockout for the front caliper
$F_{CAL\text{-}REAR\text{-}MIN}$	2578.37	lbf	Minimum required force for brake lockout for the rear caliper
Bias	0.50		Calculated from max forces (can be changed depending on target deceleration and other variables)
$P_{CYL\text{-}FRONT}$	651.90	psi	Master Cylinder Pressure Rating (multiply by 4-5 times for emergencies) (40/60 rear bias)
$P_{CYL\text{-}REAR}$	977.85	psi	Master Cylinder Pressure Rating (multiply by 4-5 times for emergencies) (40/60 rear bias)
$A_{PISTON\text{-}FRONT}$	3.96	in^2	Running a 1 piston per Caliper on a 2 Caliper system
$A_{PISTON\text{-}REAR}$	2.64	in^2	Running a 2-piston per Caliper on a 1 Caliper system

The calculations provided factor in margins to calculate the necessary forces to lock out all four wheels of the vehicle. Currently, due to the weight concerns with the vehicle, the front and rear brakes require a force of 2579.37 lbf to pass inspection. With an input pedal force of 100 lbf, which is already high, the cylinder pressures are 651.90 and 977.85 psi for the front and rear, respectively, which are within the rating for the previous years' master cylinders. However, these forces and pressures are quite high, and further improvements on the vehicle are necessary to lower these loads. Due to the high loads present, the piston areas for the front and rear systems are quite high for the current single piston and double caliper for the front, and the double piston and single caliper on the rear configurations. There are no current caliper configurations for the current solved piston area for the front brake system on Willwood's catalog (where the team hopes to purchase). The calculated brake bias is also even due to the rotors used for the front and the rear being of the same diameter, which could result in forgoing the incorporation of a bias bar to the brake system. However, as a precaution, a braking bias was introduced on the calculation of the pressures involved to allow for early rear lock-up, particularly with running a single inboard caliper for the rear brake system. Further analysis on the brake bias, particularly when the team has decided on the final installation location for the brakes, is needed.

The results calculated allow for reflection on the current design of the brake system and of the overall vehicle, particularly on how the brakes would behave with the current direction of the team's design. Currently, the team is increasing the weight of the vehicle significantly, and the car might go over the target weight with the driver's weight added on; thus, it is prudent to allow for margins on the brake forces involved and involve an overestimate on the forces to ensure that the brakes pass the static and dynamic brake tests of the competition. Due to the increase in load, a reconfiguration of the brake system for both front and rear should be considered to allow for proper braking forces introduced into the system, which would allow for better vehicle control and safety.

6.4 Future Testing Potential

6.4.1 Steering Knuckle

The steering knuckle has many tests that still need to be run. These tests are constant iterations of finite element analysis to refine the part and confirm the factor of safety is passing with the addition of more force loads. The knuckle design could also have some possible topology optimization done. If the factor of safety is high enough that some material could be removed, it could save on weight and money.

6.4.2 Front Suspension

Some potential testing procedures that can be performed on the front suspension system in the near future include performing a finite element analysis on the members in order to identify any weak points that may exist. By simulating the forces that will act on the members during the competition, a prediction of their behaviors can be observed. This analysis can also be performed on several iterations of the design to aid in the determination of the final design that the team will be moving forward with. Loading the individual members of the arms in

compression and tension until failure would also allow for the identification of any potential failure modes and the verification of the finite element analysis results.

6.4.3 Steering

Further testing is planned to validate component performance under competition conditions. This includes additional ANSYS modeling to refine stress and deformation predictions, verification of the steering mounting system for shear and load transfer, and confirmation that the tie rods maintain sufficient strength under worst-case crash loads. These tests will ensure the steering and suspension systems are robust, safe, and reliable prior to dynamic on-vehicle evaluation.

6.4.4 Rear Suspension

Future testing will include additional Optimum Kinematics simulations with combined motions, where more than one motion occurs simultaneously, such as heave motion while steering. This will ensure the geometry maintains proper dimensions and performance under realistic driving conditions. The analysis will also examine other parameters, such as toe angle, to validate overall suspension behavior. Additionally, the front and rear suspension systems will be modeled together to evaluate their interaction as a complete vehicle system. This will provide a comprehensive analysis tool for the entire vehicle's suspension performance.

Physical testing methods include full range-of-motion testing and measurement of camber and tow angles. Once the angles are verified, we can start the physical testing of the vehicle.

6.4.5 Brakes

Future testing will include a finite element analysis (FEA) of the rotor-caliper assembly and, after the purchasing and installation of the brakes, several braking trials for both static and dynamic conditions. The FEA of the rot-caliper assembly will analyze the forces involved in the brake systems to determine that the configuration will not be subjected to too many forces that would rip the brake system apart from cyclic loading. The braking trials would also determine the efficiency of the purchased and installed brake in providing control to the steering of the vehicle. Before the suggested testing, a spatial analysis through computer and physical modeling is to be performed to determine that the spatial allowance is enough for either outboard or inboard installation of the brake system for the front and the back for the selected brake assembly.

7 CONCLUSIONS

The suspension system is the foundation of the SAE Baja's performance and reliability. The three systems of suspension, steering, and braking will work together to make sure the car can withstand any competition challenge and perform at its absolute best. Each part must either withstand all the forces applied or be able to have quick maintenance done so the vehicle is operational again. The sub-team will make sure each part operates efficiently with the other sub-team's assembly. There needs to be a focus on reducing weight while maintaining strength inside of our members. The steering system must have a highly responsive steering while also reducing the vibrations inside of the gearbox. The brakes must have full functionality while also having the flexibility to be located at different locations in the car. There also needs to be seamless integration with the other sub-team to allow the suspension, steering and brake systems to operate as smoothly as possible. The outcome of this semester is to have a complete suspension system while also having any other systems being integrated into the other sub-team's assemblies.

8 REFERENCES

Colby's Sources

[1] W. F. Milliken and D. L. Milliken, Race car vehicle dynamics. Warrendale, Pa, U.S.A.: Sae International, 1995. Chapter 17

[2] F. Luo, "Double Wishbone Suspension: Precision and Performance," Aaastand.com, Jul. 23, 2025. https://www.aaastand.com/blog/double-wishbone-suspension/ (accessed Sep. 11, 2025).

[3] D. J. B and S. P. R, "Design and calculation of double arm suspension of a car," Journal of Mechanical Engineering, Automation and Control Systems, vol. 1, no. 1, pp. 25-30, Jun. 2020, doi: https://doi.org/10.21595/jmeacs.2020.21436.

[4] M. Abe, "Chapter 6 - Vehicle Body Roll and Vehicle Dynamics," ScienceDirect, Jan. 01, 2015. https://www.sciencedirect.com/science/article/abs/pii/B9780081003909000063

[5] D. Hathaway, "Tech 03: Spring spacing, Roll Stiffness and Transverse Weight Transfer." Accessed: Sep. 13, 2025. [Online]. Available: https://www.ismasupers.com/wp-content/uploads/2021/11/Tech-03-Springs-Roll-Stiffness-4.pdf

[6] "Understanding Spring Rate: Calculations & Selection Guide for Car Suspension," Qa1.net, 2024. https://qa1.net/resources/spring-rate/

[7] M. H. Mujavar, A. Ahmed, M. Akbar, and M. S. Dakhani, "Design and Analysis of Double Wishbone Suspension System using FEA and MATLAB," *International Journal of Engineering Research & Technology (IJERT)*, vol. 7, no. 05, May 2018. [Online]. Available: https://www.ijert.org/research/design-and-analysis-of-double-wishbone-suspension-system-using-fea-and-matlab-IJERTV7IS050255.pdf

[8] S. Lee, "Optimizing Vehicle Handling with Trailing Arms," Numberanalytics.com, 2025. https://www.numberanalytics.com/blog/optimizing-vehicle-handling-trailing-arms (accessed Sep. 11, 2025).

[9] D. Jebaraj B and S. Prasanna R, "Design and calculation of double arm suspension of a car," Journal of Mechanical Engineering, Automation and Control Systems, vol. 1, no. 1, pp. 11–25, Jun. 2020, doi:10.21595/jmeacs.2020.21436

[10] Shane, ," *MFG Shop*, Apr. 24, 2025. [Online]. Available: https://shop.machinemfg.com/sae-aisi-4130-chromoly-steel-properties-composition-and-applications/ (shop.machinemfg.com)

Jose's Sources

[11] R. N. Jazar, Vehicle Dynamics: Theory and Applications, 3rd ed. Springer, 2017. Chapter 7.

[12] J. C. Dixon, Suspension Geometry and Computation. Hoboken, NJ: Wiley, 2009. Chapters 7, 12.

[13] J. Fetter, "Active Suspension for a Baja SAE car," Cornell Univ., Dept. Computer Science, Ithaca, NY, Tech. Rep., Jan. 2018. Accessed: Sep 12, 2025. Available: https://people.ece.cornell.edu/land/courses/eceprojectsland/STUDENTPROJ/2017to2018/jdf258/MEng_Report_Final.pdf

[14] J. DeBoer, H. Hirsch, P. Pang, and S. Cappos, "Baja SAE Semi-Active Suspension Final Design Review Report," California Polytechnic State Univ., Mechanical Engineering Dept., San Luis Obispo, CA, Tech. Rep., Mar. 2022. Accessed: Sep 12, 2025. Available: https://digitalcommons.calpoly.edu/cgi/viewcontent.cgi?article=1727&context=mesp

[15] P. A. Bennett, "Zips SAE Baja Brakes and Throttle System," Honors Research Projects, The Dr. Gary B. and Pamela S. Williams Honors College, University of Akron, Akron, OH, Spring 2015. Accessed: Sep 12, 2025. Available: https://ideaexchange.uakron.edu/cgi/viewcontent.cgi?article=1145&context=honors_research_projects

[16] "Design of a suspension system," Engineering Cheat Sheet. [Online]. Accessed: Sep. 13, 2025. Available: https://engineeringcheatsheet.com/requirements-cascade-and-interface-analysis-for-suspension-system/

[17] "4130 Steel (AISI, ASTM, UNS)," ASTM Steel. [Online]. Accessed: Oct. 18, 2025. Available: https://www.astmsteel.com/product/4130-steel-aisi-25crmo4-7218-scm430/.

[18] R. Beardsley, "VSusp: Vehicle Suspension Geometry Calculator/Simulator - Default Values Configuration," VSusp, 2009. Online. Available: http://vsusp.com/. [Accessed: Oct. 01, 2025].

[19] OptimumG, LLC, "OptimumKinematics: Suspension and Design Analysis," ver. 2.3.207,Laguna Beach, CA, USA, 2017. [Computer software]. Available: https://www.optimumg.com

[20] SAE International, "2026 Baja SAE Rules," Warrendale, PA: SAE International, 2025. [Online]. Available: https://www.bajasae.net/. [Accessed: Oct. 20, 2025].

James S' Sources

[21] "Home - Baja Racing at Cornell," Cornell.edu, 2025. https://baja.mae.cornell.edu/ (accessed Sep. 16, 2025).

[22]"Seasons – Blue Jay Racing," Jhu.edu, 2025. https://baja.jhu.edu/seasons-2/ (accessed Sep. 16, 2025).

[23]"Baja ÉTS," Bajaets.com, 2017. https://www.bajaets.com/ (accessed Sep. 16, 2025).

[24] C. Rebeyka, G Pontarolo, M. Arceno, R. Filho, S. Lajarin, “Design for Manufacturing and Assembly of a BAJA Steering Knuckle,” International Research Journal of Engineering and Technology, vol. 11, Issue 09, 2008, Accessed: Sep. 12, 2025. [Online]. Available: https://www.irjet.net/archives/V11/i9/IRJET-V11I919.pdf

[25] B. Saravanan, H. Kebin, V. Mani, A. Nirmal Bharath, “STRUCTURAL ANALYSIS OF STEERING KNUCKLE.” International Journal of Scientific Development and Research, vol. 4, issue 3, Accessed: Sep. 12, 2025. [Online]. Available: https://ijsdr.org/papers/IJSDR1903040.pdf

[26] S. Srivastava, S. Salunkhe, S. Pande, B. Kapadiya, "Topology optimization of steering knuckle structure," International Journal for Simulation and Multidisciplinary Design Optimization, vol 11, issue 4, 2020, Accessed: Sep. 12, 2025. [Online]. Available: https://www.researchgate.net/publication/338792811_Topology_optimization_of_steering_knuckle_structure

[27] B. A. Saputro, Ubaidillah, D. A. Triono, D. R. Pratama, S. I. Cahyono, and F. Imaduddin, “Static load simulation of steering knuckle for a formula student race car,” AIP Conference Proceedings, 2018, doi: https://doi.org/10.1063/1.5024108.

[28] J. Sandeep, Reddy, S. Sai, Dheeraj, and S. Upendar Reddy, “Design and Structural Analysis of Steering Knuckle for An Electric All-Terrain Vehicle -E Baja.” International Journal of Engineering Research and Technology, vol. 8, issue 08, 2019, Accessed: Sep. 12, 2025. [Online]. Available: https://www.ijert.org/research/design-and-structural-analysis-of-steering-knuckle-for-an-electric-all-terrain-vehicle-e-baja-IJERTV8IS080029.pdf

[29] J. Bracco, C. DeAnda, J. Deschenes, T. Olson, and A. Sabbagha, “SAE Baja Front Suspension,” The George Washington University School of Engineering and Applied Sciences, May 2018. Available: https://scholarspace.library.gwu.edu/downloads/9880vr219?locale=en

[30] S. Patel, “2013 Baja Car Rear Suspension Redesign,” Department of Mechanical and Materials Engineering College of Engineering and Applied Science University of Cincinnati, 2014. Accessed: Sep. 12, 2025. [Online]. Available: https://drc.libraries.uc.edu/server/api/core/bitstreams/71ce9bd4-9ef7-47c6-a501-306c2c961809/content

[31] AMSQQA200/8A, *Aluminum Alloy 6061, Bar, Rod, Shapes, Tube, and Wire, Extruded A96061*. 2015.

[32] “Steering Knuckle Design & FEA Simulation (Static),” YouTube, May 12, 2024. [Online]. Available: https://www.youtube.com/watch?v=2TunTUlTvPM. [Accessed: Nov. 25, 2025].

[33] “Structural Analysis of a Knuckle of a Student Car using Altair Inspire,” YouTube, Apr. 27, 2021. [Online]. Available: https://www.youtube.com/watch?v=k_KjnR4kZCQ. [Accessed: Nov. 25, 2025].

[34] “Tutorial: XYZ (starting at ~16:00),” YouTube, [date unknown]. [Online]. Available: https://www.youtube.com/watch?v=8LtBWZPLJKw. [Accessed: 25 Nov. 2025].

Jakob’s Sources

[35] W. F. Milliken and D. L. Milliken, Race car vehicle dynamics. Warrendale, Pa, U.S.A.: Sae International, 1995. Chapter 19

[36] D. Choate, “UC SAE Baja Steering Rack Design and Analysis,” Accessed: Sep. 12, 2025. [Online]. Available: https://arches.union.edu/do/52090/iiif/677b57ac-aac7-4791-81d7-bf3e6f06b0ec/full/full/0/2023_ChoateD.pdf

[37] E. O’Neill and Dr. C. Jobes, “A Study of Ackerman Steering and Its Applicability to SAE Mini Baja.” 2024 Accessed: Sept.12, 2025
Available: https://www.google.com/url?sa=t&source=web&rct=j&opi=89978449&url=https://peer.asee.org/a-study-of-ackerman-steering-and-its-applicability-to-sae-mini-baja.pdf&ved=2ahUKEwjE5bu21tSPAxVjJEQIHUOpJNUQFnoECB4QAQ&usg=AOvVaw2WvoqyAkNkRLagC10HEfx6

[38] E. Wessels, “2017 Bearcats Baja SAE – Steering System,” 2017. Accessed: Sept.12, 2025
Avaliable: https://www.google.com/url?sa=t&source=web&rct=j&opi=89978449&url=https://scholar.uc.edu/downloads/bc388285m&ved=2ahUKEwiLyObH-dSPAxXBJUQIHbFuG4cQFnoECBsQAQ&usg=AOvVaw3iNdhlHt1uePAOO2UdS7lE

[39] J. Knapczyk, M. Maniowski, and Institute of Automobiles and Internal Combustion Engines, Cracov University of Technology, “EXPERIMENTAL RIG STUDY ON RESISTANCE FORCES IN CAR STEERING SYSTEM WITH RACK AND PINION,” journal-article.
Acessed: Sept.12, 2025
Avaliable: https://www.researchgate.net/publication/325999795_Experimental_rig_study_on_resistance_forces_in_car_steering_system_with_rack_and_pinion

[40] SAE International, M. Allwin, and V. D. Tamilarasan, “Design and Analysis of an Ackermann Steering System for an Off-Road Electric Vehicle,” Aug. 2024. doi: 10.47953/SAE-PP-00402. Acsessed: Sept.12,2025 Avaiable:https://mobilityrxiv.sae.org/preprint/design-and-analysis-of-an-ackermann-steering-system-for-an-off-road-electric-vehicle--sae-pp-00402

[41] "SAE J670_202206" Acsessed:Sept.12, 2025
Avaliable: https://www.sae.org/standards/content/j670_202206/

[42] “49 CFR 393.209 -- Steering wheel systems.” Available: https://www.ecfr.gov/current/title-49/subtitle-B/chapter-III/subchapter-B/part-393/subpart-J/section-393.209 [Accessed: Nov. 24, 2025]

[43] S. T. Team, “Steering Shaft and U-Joint selection guide,” *Speedway Motors*. Avaliable: https://www.speedwaymotors.com/the-toolbox/steering-shaft-and-u-joint-selection-guide/28638?srsltid=AfmBOopaIFYlYu5nDHHPoDW8IFjFM6fXQHAOAqhqsvJ1zfwEhdgiV4Ey [Accessed: Nov. 24, 2025]
[44] D. Oza *et al.*, “Analysis of steering system in FSAE vehicle,” *NanoWorld Journal*, vol. 9, Nov. 2023, doi: 10.17756/nwj.2023-s4-023. [Accessed: Nov, 24, 2025]

Marc’s Source

[45] W. F. Milliken and D. L. Milliken, Race car vehicle dynamics. Warrendale, Pa, U.S.A.: Sae International, 1995. Chapter 20
[46] R. Limpert, Brake Design and Safety. Warrendale, Pa. (400 Commonwealth Dr, Warrendale PA USA): Society of Automotive Engineers, 2011. Chapter 4.3
[47] Design and analysis of Double Piston Brake Caliper for SAE baja vehicle, https://www.sae.org/publications/technical-papers/content/2023-01-5152/ (accessed Sep. 12, 2025).
[48] “Going rock crawling?,” PowerStop Brakes, https://www.powerstop.com/resources/what-brakes-are-best-for-rock-crawling/ (accessed Sep. 12, 2025).
[49] Irjet, IRJET-V7I227.pdf (accessed Sep. 12, 2025).
[50] Fundamentals of brake design, https://www.sae.org/publications/technical-papers/content/250042/ (accessed Sep. 12, 2025).
[51] Brake System Regulations and Standards Review and comparison focused on Europe, NA and sa markets, https://www.sae.org/publications/technical-papers/content/2017-01-2534/ (accessed Sep. 12, 2025).
[52] “Wilwood disc brakes - specialty OEM, racing, and street performance bolt-on Brake Kits,” Wilwood Disc Brakes - Specialty OEM, Racing, and Street Performance Bolt-On Brake Kits, https://www.wilwood.com/ (accessed Nov. 26, 2025).

[53] “5.1.1 brake systems (part 393 subpart C)>,” The Motor Carrier Safety Planner, https://csa.fmcsa.dot.gov/safetyplanner/MyFiles/SubSections.aspx?ch=22&sec=64&sub=130 (accessed Nov. 26, 2025).

[54] Code of Federal Regulation, https://www.ecfr.gov/current/title-49/subtitle-B/chapter-V/part-571/subpart-B/section-571.105 (accessed Nov. 26, 2025).

James C’s Sources

[55] W. F. Milliken and D. L. Milliken, Race car vehicle dynamics. Warrendale, Pa, U.S.A.: Sae International, 1995. Chapter 21 (accessed Sep. 13, 2025).

[56] Tires, suspension and handling. Chapter 5, https://staff.emu.edu.tr/alexanderchefranov/Documents/CMSE443/CMSE443%20Fall%202023/pdfcoffee.com_tires-suspension-and-handling-1-56091-831-4-pdf-free.pdf (accessed Sep. 13, 2025).

[57] C. Rouelle, Of springs and dampers, https://optimumg.com/wp-content/uploads/2021/10/racecar-2020_11.pdf (accessed Sep. 13, 2025).

[58] (PDF) design of Double Stage Springs for baja SAE type vehicles, https://www.researchgate.net/publication/374319341_Design_of_double_stage_springs_for_Baja_SAE_type_vehicles (accessed Sep. 13, 2025).

[59] IJCRT, https://www.ijcrt.org/papers/IJCRT2502631.pdf (accessed Sep. 13, 2025).

[60] Trinity Auto Care, "The science of suspensions: How they work and why they matter," Trinity Auto Care, https://trinityautomn.com/the-science-of-suspensions-how-they-work-and-why-they-matter/ (accessed Sep. 13, 2025).

[61] Springs and Spring Suspensions, https://www.sae.org/publications/technical-papers/content/200004/ (accessed Sep. 13, 2025).

[62] J. K. Nisbett and R. G. Budynas, Shigley's Mechanical Engineering Design. New York, NY: McGraw-Hill, 2024. Chapter 03

[63] A. Sierra, O. A. González-Estrada, and P. A. C. Santamaría, "Stress analysis of a suspension control arm," *ResearchGate*, Jan. 2018, doi: 10.13140/rg.2.2.12817.28007.

[64] SAE International Recommended Practice, Measurement of Vehicle and Suspension Parameters for Directional Control Studies, SAE Standard J1574/1_201801, Stabilized January 2018, Revised October 2012, Issued May 1994, https://doi.org/10.4271/J1574/1_201801.

9 APPENDICES

9.1 Appendix A: VSusp ("Vehicle Suspension")[35]

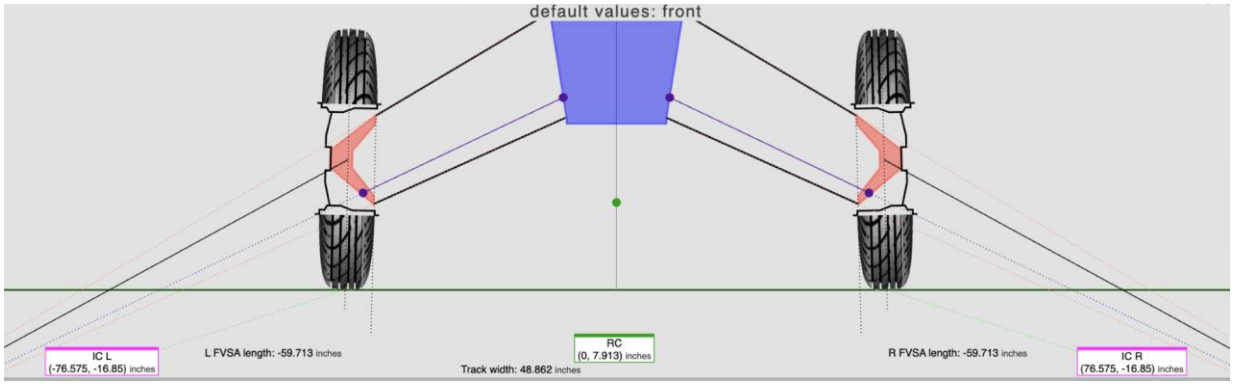

Figure 9.1-1

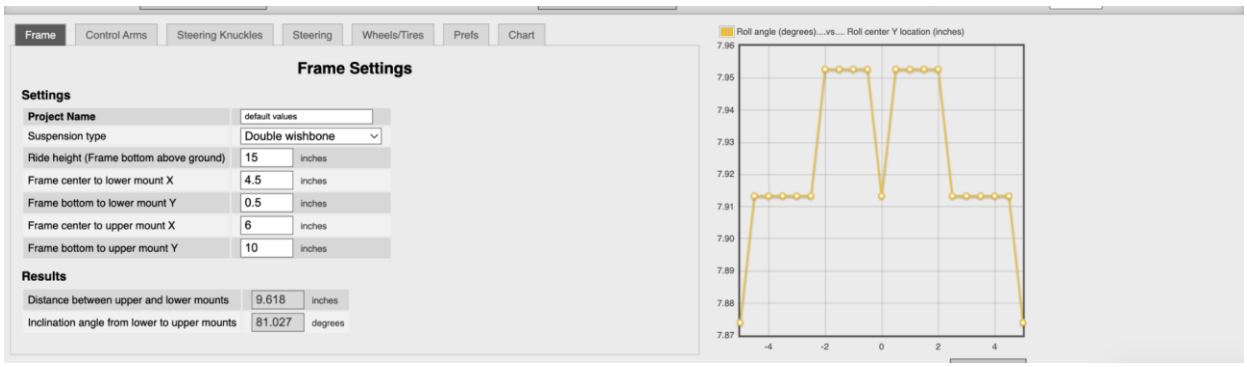

Figure 9.1-2

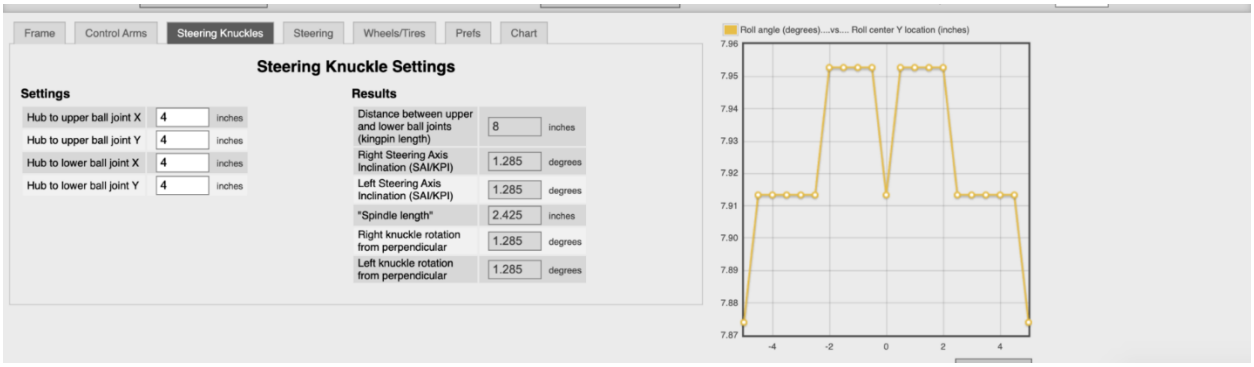

Figure 9.1-3

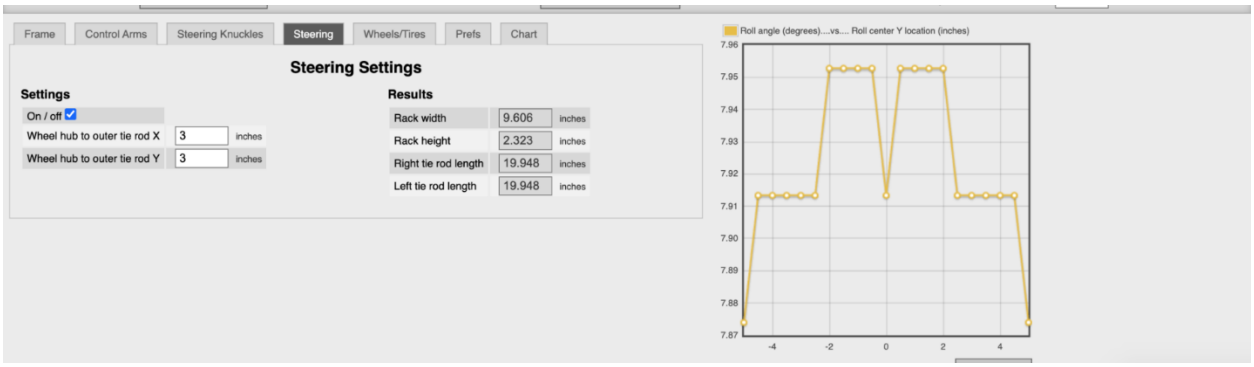

Figure 9.1-4

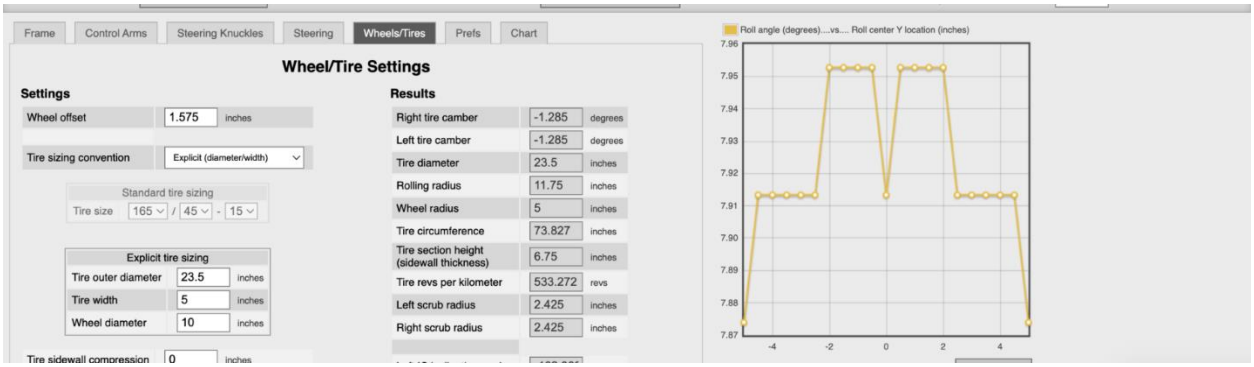

Figure 9.1-5

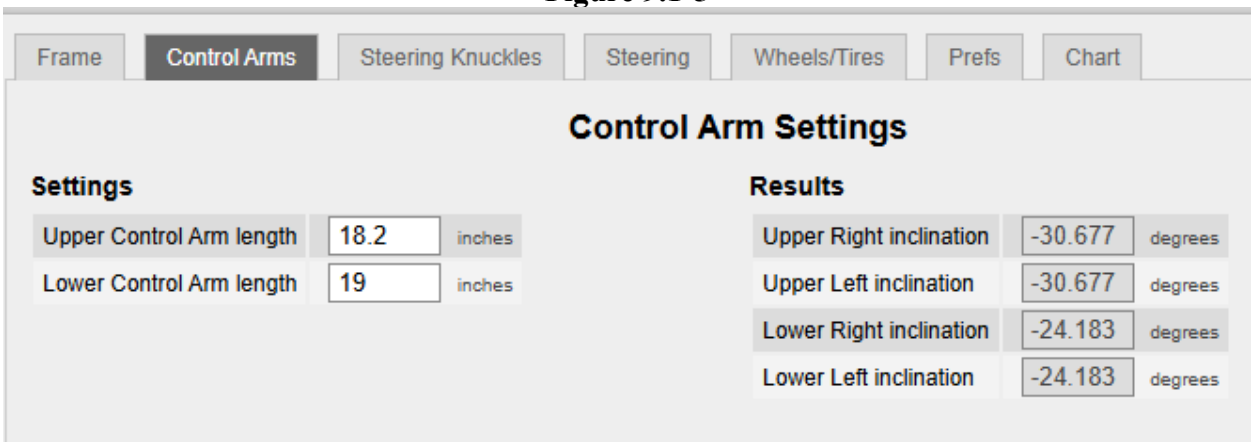

Figure 9.1-6

9.2 Appendix B: FMEA Charts

9.2.1 Steering Knuckle FMEA Chart

Product Name: NAU SAE BAJA		Development Team: James Sundeen				Page No 1 of 1			
System Name: Suspension						FMEA Number			
Subsystem Name: Knuckles						Date: 11/25/25			
Component Name: Front and Rear Knuckle									
Part # and Functions	Potential Failure Mode	Potential Effect(s) of Failure	Severity (S)	Potential Causes and Mechanisms of Failure	Occurance (O)	Current Design Controls Test	Detection (D)	RPN	Recommended Action
P1: Knuckle/Portal Hub Casing	Deformation/Destruction	Wheel is no longer supported, Car no longer competes	10	Extreme Applied Force/ Crash	3	FEA on Structural Integrity	1	30	Keep Factor of Safety of the design as high as possible to avoid deformation
P2: Bearings	Lock Up/Fall out	Axle or portal gears struggle to spin	5	debris, lack of lube	2	CAD or Visual inspection	5	70	design lock for the bearing to avoid slip and clearance to avoid rub
P3: CV Axles	Deformation/Destruction	Wheel is no longer supported, Car no longer competes	9	Extreme Applied Force/ Crash	1	visual inspection	4	36	keep axles inside of other parts like suspension members and frame supports
P4: Casing Bolts	Shear	Opening or portal hub	7	Debris/ extreme applied force	4	visual inspection	1	28	Change bolts regularly or check regularly for damage after a hit

9.2.2 Front Suspension FMEA Chart

Product Name: NAU SAE BAJA		Development Team: James Cole				Page No 1 of 1			
System Name: Suspension						FMEA Number			
Subsystem Name: Front Arms						Date: 11/04/2025			
Component Name									
Part # and Functions	Potential Failure Mode	Potential Effect(s) of Failure	S	Potential Causes and Mechanisms of Failure	Occurance (O)	Current Design Controls Test	Detection (D)	RPN	Recommended Action
P1 – Upper Arms (Guides Wheel Movement)	Cracking or bending of the pipe, especially at the bend	Change in camber angle, uneven vehicle, less stability, reduced clearance	7	Poor material selection, thi pipes, repeated use, installation errors	4	Visual observation, check mounting points	2	56	Ensure proper installation prior to use, use mathematical modeling to ensure material properties and geometry will suffice
P2 – Lower Arms (Guides Wheel Movement)	Cracking or bending of the pipe	Change in camber angle, uneven vehicle, less stability, reduced clearance	7	Poor material selection, thin pipes, repeated use, installation errors	4	Visual observation, check mounting points	2	56	Ensure proper installation prior to use, use mathematical modeling to ensure material properties and geometry will suffice
P3 – Heim Joints (Increase Range of Motion of Control Arms)	Ball wear, angle of rotation being exceeded	Looseness of the joint, the angle of rotation being exceeded may cause sudden failure	6	Repeated use, harsh use, installation errors, corrosion	6	Visual observation, test the angle of rotation, check for corrosion, audible observation	1	36	Ensure full thread engagement, have frequent inspections, add lubrication

9.2.3 Steering FMEA Chart

Product Name: NAU SAE BAJA		Development Team: Jakob Martinez				Page No 1 of 1			
System Name: Suspension						FMEA Number			
Subsystem Name: Steering						Date: 11/04/2025			
Component Name									
Part # and Functions	Potential Failure Mode	Potential Effect(s) of Failure	S	Potential Causes and Mechanisms of Failure	Occurrence (O)	Current Design Controls Test	Detection (D)	RPN	Recommended Action
P1- Steering Wheel (Provides Driver Input)	Loose or detaches from hub	Loss of driver input (Total loss of steering	10	Insufficient torque on fasteners, worn splines, failed retention pin	2	Visual QA at assembly, Assembly Torque spec	3	60	Desing secure hub/Connection point with steering column
P2 — Steering Column (transmits torque to gearbox)	Shaft fracture or spline connector failure	Loss of torque transmission; possible loss of steering	10	Fatigue f, overload, poor material, defective connection points	3	Material spec & visual inspection; design strength check	4	120	Use strong material, make sure connections are torqued to spec, visual QA during assembly
P3 — Rack & Pinion (converts rotation to linear motion)	Gear wear, excessive backlash, seizure	Increased play , reduced precision , locked steering	9.5	Inadequate lubrication, contamination, incorrect materials for gear/rack, seal failure	4	Verify material strength QA on seals, lubrication during assembly	4	152	Improve material hardness & seals; add dust boots; schedule lubrication, maintenance
P4 — Tie Rods (transfer rack motion to knuckle)	Bending, thread failure, or fracture	Wheel misalignment, reduced control, potential steering loss	9	Impact/overload, improper thread engagement, improper length	3	SOF for design, CAD to ensure proper lengths	4	108	Increase rod diameter for strength; implement inspection intervals
P5 — Heim Joints (rod-end bearings)	Wear, loosening, or excessive play	Steering play, imprecise control, accelerated wear in linkage	7	Poor lubrication, contamination, undersized joint, cyclic wear	5	Selected rod-ends, occasional greasing	6	210	Use sealed or maintenance-free joints; add grease fittings/shields
P6 — Steering Knuckle (wheel pivot interface)	Fracture, bearing failure, or spindle wear	Wheel collapse, total loss of control (safety hazard)	10	Impact damage, poor material, bearing preload loss3	2	Design checks (FEA), bearing selection, visual inspection	4	80	Validate with FEA & proof-load testing; specify impact-tolerant materials

9.2.4 Rear Suspension FMEA Chart

Product Name NAU SAE BAJA						Page No 1 of 1			
System Name Rear Suspension						FMEA Number			
Subsystem Name Control arms and shocks						Date			
Component Name									
Part # and Functions	Potential Failure Mode	Potential Effect(s) of Failure	Severity (S)	Potential Causes and Mechanisms of Failure	Occurance (O)	Current Design Controls Test	Detection (D)	RPN	Recommended Action
LCA	Bending/ Welding failure	Changes to castor, camber& tow	7	Rough impacts at odd angles	2		1	14	Properly install, verify with engineering models
UCA	Bending/ Welding failure	Pipe Bending and Cracking	7	Rough impacts at odd angles	2		2	28	Properly install, verify with engineering models
Heim Joints	Bolt shear/ Ball wear, exceexing max angle of rotation	Shear force. Ball wear	8	Sharp impact forces	5		1	40	Have extra, easy to replace, verify with saftey factor of 1.2
Shocks	Bolt failure	Shear force	8	fatigue/ shear	3		1	24	Have extra, easy to replace, verify with saftey factor of 1.2

9.2.5 Brakes FMEA Chart

Product Name: NAU SAE BAJA		Development Team: Marc Angelo Maquiling				Page No 1 of 1			
System Name: Suspension						FMEA Number			
Subsystem Name: Brakes						Date: 11/05/2025			
Component Name									
Part # and Functions	Potential Failure Mode	Potential Effect(s) of Failure	S	Potential Causes and Mechanisms of Failure	Occurrence (O)	Current Design Controls Test	Detection (D)	RPN	Recommended Action
P1- Rotor (Converts Motion to Thermal Energy)	Fading, Warping, Cracking	Reduction of Break Power, Vibration	9	Overheating, Heavy Braking, Terrain, Contamination	4	Visual, Hearing, Braking at Speed, Thickness Check, Heat Measurement	5	180	Wear and Warping Check, Proper Material Choice, QAs
P2 — Caliper (Clamps Pads Into Rotor)	Wear, Sticking, Leaking	Brake Pressure Reduction, Uneven Breaking	9	Poor Maintenance, Corrosion	3	Hearing, Braking at Speed, Leaking Check	3	81	Cleaning, Lubrication, and Checking Actuation
P3 — Caliper Pad (Provides Friction to Stop Car)	Wear and Glazing	Increased Stopping Distance, Disc Damage	9	Damaged Rotor, Heavy Braking	7	Braking at Speed & Static, Hearing, Wear Check	2	126	Checking for Wear, Replace Timely
P4 — Master Cylinder (Provides Hydraulic Pressure to Caliper)	Leaking	Brake Failure, Reduced Pedal Actuation	10	Terrain, Poor Maintenance, Contamination	4	Leak Test, Pressure Check	1	40	Seal and Fluid Checks, Immediately Repair for Any Leaks
P5 — Brake Lines(Carry the Hydraulic Pressure)	Corrosion, Leaking	Brake Failure, Reduced Pedal Actuation	10	Age, Corrosion, Terrain	2	Leak Test, Pressure Test, Visual	1	20	Regular Visual Inspection, Replace Timely
P6 — Brake Pedal (Converts User Force to Brake Control)	Sinking, Bending	Delayed Pedal, Reduced Control	9	Misalignment, Hydraulic Issues, Age	2	Force Input Check, Link Check	3	54	Check links, Adjust for Proper Ergonomics

9.3 Appendix C: MATLAB Code

```
function portal4_bearing_analysis()
% portal4_bearing_analysis.m
% 4-gear portal (driver -> two identical idlers -> driven), 20 deg, DP=12
% Fixed tooth counts: Z1=18, Zi=22 (x2), Z4=36
% Layout with backlash, OD clearance checks, mesh forces, bearing reactions, optional L10 life.
%% ========================= USER INPUTS =========================
% Geometry system (use DP OR module)
DP        = 12;                % [1/in]; set [] if using module
modul     = [];                % [mm];  set [] if using DP
phi_deg   = 20;                % pressure angle [deg]
% Tooth counts (fixed per request)
Z1 = 18; Zi = 22; Z4 = 36;
% Shaft centers (units follow DP/module). Keep on x-axis for simplicity.
p1 = [0.000, 2.48];            % driver center
p4 = [0, 0.000];           % driven center  <-- set to your hardware C14
% Backlash targets (fraction of module; typical 0.04 to 0.10)
jt_frac_1i = 0.06;             % driver–idler backlash at pitch
jt_frac_i4 = 0.06;             % idler–driven backlash at pitch
% OD clearance required for NON-mating pairs (idler–idler, driver–driven)
od_clearance_allow = 0.06;      % [in]
% Strength (Lewis bending)
T_in      = 250;               % driver torque [in-lbf]
b         = 1;             % face width [in]
K_service = 1.50;              % service factor
eta_split = 0.48;              % load share per idler (0.45–0.50)
sigma_allow = 75000;           % allowable bending stress [psi]
min_SF_req  = 1.20;
% Bearing model: two bearings per shaft (simple beam split).
% Bearings at x=0 and x=L_s, gear load applied at x=xg_s along the span.
L_drv  = 1.80;  xg_drv  = L_drv/2;   % driver
L_idlA = 1.25;  xg_idlA = L_idlA/2;  % idler A
L_idlB = 1.25;  xg_idlB = L_idlB/2;  % idler B
L_drvn = 2.20;  xg_drvn = L_drvn/2;  % driven
% Optional L10 life (set C_rating=[] to skip)
rpm_drv     = 3000;            % driver RPM
bearing_type = "ball";         % "ball" (p=3) or "roller" (p=10/3)
C_rating    = [];              % dynamic rating C [lbf]; [] => skip L10
%% ================================================================
% ----- Units & basic geometry -----
phi = deg2rad(phi_deg);
if ~isempty(DP) && isempty(modul)
```

```
  m = 1/DP;            % [in]
elseif isempty(DP) && ~isempty(modul)
  m = modul; DP = [];  % [mm]
else
  error('Specify exactly one of DP or module.');
end
pitchR = @(Z) 0.5*m*Z;
R1 = pitchR(Z1); Ri = pitchR(Zi); R4 = pitchR(Z4);
C14 = norm(p4 - p1);
% Backlash -> center-distance opening
jt_1i = jt_frac_1i * m;
jt_i4 = jt_frac_i4 * m;
delta_a1 = jt_1i/(2*tan(phi));   % driver–idler center opening
delta_a2 = jt_i4/(2*tan(phi));   % idler–driven center opening
% Assembly center distances (use these in CAD)
a1 = R1 + Ri + delta_a1;         % driver–idler
a2 = Ri + R4 + delta_a2;         % idler–driven
% Place idlers at the two circle–circle intersections
[pA, pB, ok] = circle_circle_intersections(p1, a1, p4, a2);
if ~ok
  error('No feasible idler locations. Check C14=%.4f vs a1=%.4f, a2=%.4f (and backlash).', C14,
a1, a2);
end
% OD clearance checks for NON-mating pairs
a_add = m;                       % full-depth addendum
if norm(pA - pB) < ( (Ri+a_add) + (Ri+a_add) + od_clearance_allow )
  error('Idler–idler OD clearance too small. Increase C14 or reduce Zi.');
end
if C14 < ( (R1+a_add) + (R4+a_add) + od_clearance_allow )
  error('Driver–driven OD clearance too small. Increase C14 or adjust sizes.');
end
% ----- Strength (Lewis bending) -----
% Tangential load at driver pitch: Ft_total = 2*T_in / d1 = T_in / R1
Ft_total = T_in / R1;
Ft_each  = eta_split * Ft_total;      % per idler
Ft_eff   = K_service * Ft_each;       % include service factor
Fr_each  = Ft_each * tan(phi);        % radial (separating) per mesh
Y1 = lewisY20(Z1); Yi = lewisY20(Zi); Y4 = lewisY20(Z4);
sig_drv  = Ft_eff/(b*m*Y1);
sig_idlr = Ft_eff/(b*m*Yi);           % idler tooth (max of two meshes; same Ft here)
sig_drvn = Ft_eff/(b*m*Y4);
SF_drv = sigma_allow/sig_drv;
SF_idl = sigma_allow/sig_idlr;
```

```
SF_out = sigma_allow/sig_drvn;
SF_min = min([SF_drv, SF_idl, SF_out]);
% ----- Force vectors at each gear center (use actual geometry) -----
% For pair i(at Pi) vs j(at Pj): e_ij=(Pj-Pi)/|...|, t_ij=[-e_y, e_x]
% Force on gear i from gear j (power i->j): F_i = -(Ft*t_ij + Fr*e_ij)
% Driver vs Idler A
e1A = (pA - p1) / norm(pA - p1);   t1A = [-e1A(2), e1A(1)];
% Driver vs Idler B
e1B = (pB - p1) / norm(pB - p1);   t1B = [-e1B(2), e1B(1)];
% Idler A vs Driven
eA4 = (p4 - pA) / norm(p4 - pA);   tA4 = [-eA4(2), eA4(1)];
% Idler B vs Driven
eB4 = (p4 - pB) / norm(p4 - pB);   tB4 = [-eB4(2), eB4(1)];
% Forces on each center (lbf)
F1A = -(Ft_each*t1A + Fr_each*e1A);   % on driver from A
F1B = -(Ft_each*t1B + Fr_each*e1B);   % on driver from B
F_driver = F1A + F1B;
FA_from1 = -F1A;                      % on A from driver
FA_to4   = -(Ft_each*tA4 + Fr_each*eA4);   % on A from driven (power to driven)
F_idlerA = FA_from1 + FA_to4;
FB_from1 = -F1B;
FB_to4   = -(Ft_each*tB4 + Fr_each*eB4);
F_idlerB = FB_from1 + FB_to4;
F4_fromA = -(FA_to4);                 % opposite of force on A from driven
F4_fromB = -(FB_to4);
F_driven = F4_fromA + F4_fromB;
% ----- Bearing reactions (two bearings per shaft) -----
Drv  = split_two_supports(F_driver, L_drv,  xg_drv);
IdlA = split_two_supports(F_idlerA, L_idlA, xg_idlA);
IdlB = split_two_supports(F_idlerB, L_idlB, xg_idlB);
Out  = split_two_supports(F_driven, L_drvn, xg_drvn);
% ----- Reports -----
fprintf('\n=== Geometry (DP=%g, PA=%g deg) ===\n', DP, phi_deg);
fprintf('Pitch diameters: d1=%.3f, di=%.3f, d4=%.3f in\n', 2*R1, 2*Ri, 2*R4);
fprintf('Centers: a1(driver-idler)=%.4f, a2(idler-driven)=%.4f, C14=%.4f in\n', a1, a2, C14);
fprintf('Backlash (circumferential): jt_1i=%.4f, jt_i4=%.4f in\n', jt_1i, jt_i4);
fprintf('\n=== Lewis bending (per-mesh Ft=%.2f lbf, Fr=%.2f lbf) ===\n', Ft_each, Fr_each);
fprintf('SF_driver=%.3f, SF_idler=%.3f, SF_driven=%.3f  |  SF_min=%.3f\n', SF_drv, SF_idl,
SF_out, SF_min);
if SF_min < min_SF_req
   fprintf(2,'WARNING: SF_min < %.2f. Consider wider face, lower K_service, or different
sizes.\n', min_SF_req);
end
```

```
fprintf('\n=== Resultant gear-center forces (lbf) ===\n');
prnVec('Driver ', F_driver);
prnVec('Idler A', F_idlerA);
prnVec('Idler B', F_idlerB);
prnVec('Driven ', F_driven);
fprintf('\n=== Bearing reactions (two supports per shaft) ===\n');
prnBear('DRIVER',  L_drv,  xg_drv,  Drv);
prnBear('IDLER A', L_idlA, xg_idlA, IdlA);
prnBear('IDLER B', L_idlB, xg_idlB, IdlB);
prnBear('DRIVEN ', L_drvn, xg_drvn, Out);
% Optional L10 life
if ~isempty(C_rating)
   p = 3; if lower(string(bearing_type))=="roller", p = 10/3; end
   fprintf('\n=== L10 life (C=%.0f lbf, type=%s, rpm=%g) ===\n', C_rating, bearing_type,
rpm_drv);
   L10_block('Driver ', Drv,  C_rating, p, rpm_drv);
   L10_block('Idler A', IdlA, C_rating, p, rpm_drv);
   L10_block('Idler B', IdlB, C_rating, p, rpm_drv);
   L10_block('Driven ', Out,  C_rating, p, rpm_drv);
end
% ----- Simple plot -----
figure('Name','Portal 4-gear Layout + Forces'); hold on; axis equal; grid on;
draw_circle(p1, R1, 'LineWidth',1.4); draw_circle(pA, Ri, 'LineWidth',1.4);
draw_circle(pB, Ri, 'LineWidth',1.4); draw_circle(p4, R4, 'LineWidth',1.4);
draw_circle(p1, R1+m, 'LineStyle','--'); draw_circle(pA, Ri+m, 'LineStyle','--');
draw_circle(pB, Ri+m, 'LineStyle','--'); draw_circle(p4, R4+m, 'LineStyle','--');
plot(p1(1),p1(2),'ko','MarkerFaceColor','k'); text(p1(1),p1(2),'  Driver');
plot(pA(1),pA(2),'ko','MarkerFaceColor','k'); text(pA(1),pA(2),'  Idler A');
plot(pB(1),pB(2),'ko','MarkerFaceColor','k'); text(pB(1),pB(2),'  Idler B');
plot(p4(1),p4(2),'ko','MarkerFaceColor','k'); text(p4(1),p4(2),'  Driven');
scale = 0.004;  % arrow scale for visibility
quiver(p1(1),p1(2), scale*F_driver(1), scale*F_driver(2), 0, 'r','LineWidth',1.6);
quiver(pA(1),pA(2), scale*F_idlerA(1), scale*F_idlerA(2), 0, 'r','LineWidth',1.6);
quiver(pB(1),pB(2), scale*F_idlerB(1), scale*F_idlerB(2), 0, 'r','LineWidth',1.6);
quiver(p4(1),p4(2), scale*F_driven(1), scale*F_driven(2), 0, 'r','LineWidth',1.6);
title(sprintf('Z1=%d, Zi=%d(x2), Z4=%d  |  DP=%g, PA=%g deg', Z1, Zi, Z4, DP, phi_deg));
xlabel('X [in]'); ylabel('Y [in]'); hold off;
end % main
% ============================ HELPERS ============================
function [pA, pB, ok] = circle_circle_intersections(c1, r1, c2, r2)
d = norm(c2 - c1);
if d > r1 + r2 || d < abs(r1 - r2) || (d==0 && r1==r2)
   pA=[NaN,NaN]; pB=[NaN,NaN]; ok=false; return;
```

```
end
ex = (c2 - c1)/d;
x  = (r1^2 - r2^2 + d^2)/(2*d);
h2 = max(r1^2 - x^2, 0); h = sqrt(h2);
ey = [-ex(2), ex(1)];
p_mid = c1 + x*ex;
pA = p_mid + h*ey;  pB = p_mid - h*ey;  ok = true;
end
function Y = lewisY20(Z)
% 20 deg full-depth spur (no shift) – common approximation
Y = 0.175 - 0.841./Z; Y = max(Y, 0.05);
end
function S = split_two_supports(F, L, xg)
% Split a 2D point load F=[Fx,Fy] at x=xg along a span [0..L] between two supports.
if L <= 0, error('Bearing span L must be > 0'); end
a = xg; b = L - xg;  if a<0 || b<0, error('xg must be within [0,L]'); end
Rx1 = F(1) * b / L;  Rx2 = F(1) * a / L;
Ry1 = F(2) * b / L;  Ry2 = F(2) * a / L;
Rmag1 = hypot(Rx1, Ry1); Rmag2 = hypot(Rx2, Ry2);
S = struct('Rx1',Rx1,'Ry1',Ry1,'Rmag1',Rmag1,'Rx2',Rx2,'Ry2',Ry2,'Rmag2',Rmag2);
end
function prnVec(lbl, F)
fprintf('%s: Fx=%.2f, Fy=%.2f  |  |F|=%.2f\n', lbl, F(1), F(2), hypot(F(1),F(2)));
end
function prnBear(name, L, xg, S)
fprintf('%s: L=%.3f, x=%.3f\n', name, L, xg);
fprintf('  B1: (Rx,Ry)=(%.2f, %.2f) | |R|=%.2f lbf\n', S.Rx1, S.Ry1, S.Rmag1);
fprintf('  B2: (Rx,Ry)=(%.2f, %.2f) | |R|=%.2f lbf\n', S.Rx2, S.Ry2, S.Rmag2);
end
function L10_block(name, S, C, p, rpm)
P1 = S.Rmag1; P2 = S.Rmag2;
L10_1_Mrev = (C/P1)^p;  L10_2_Mrev = (C/P2)^p;
hrs1 = L10_1_Mrev*1e6 / (60*rpm);  hrs2 = L10_2_Mrev*1e6 / (60*rpm);
fprintf('%s: L10 @B1 = %.2f Mrev (%.0f h),  @B2 = %.2f Mrev (%.0f h)\n', ...
  name, L10_1_Mrev, hrs1, L10_2_Mrev, hrs2);
end
function draw_circle(c, R, varargin)
th = linspace(0,2*pi,360);
plot(c(1)+R*cos(th), c(2)+R*sin(th), varargin{:});
end
```

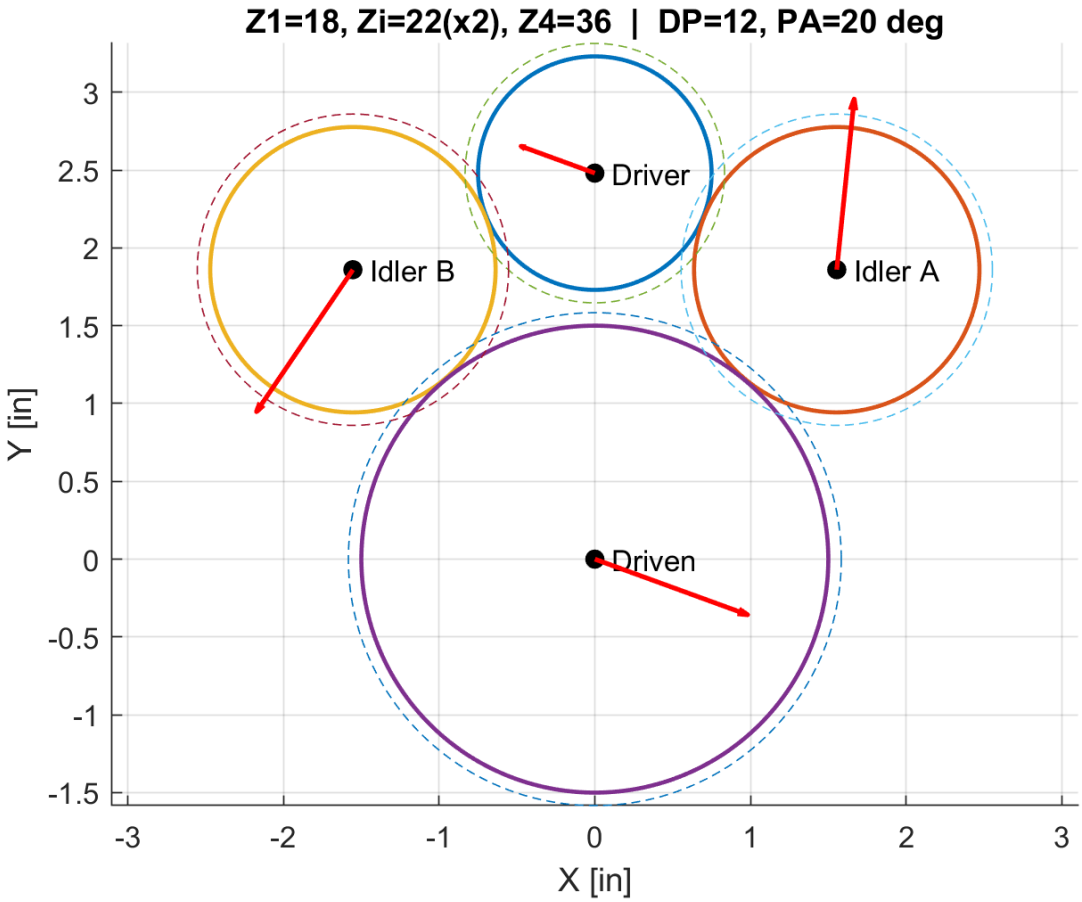

Figure 9.3-1: Gear Forces Vectors

9.4 Appendix D: Optimum Kinematics

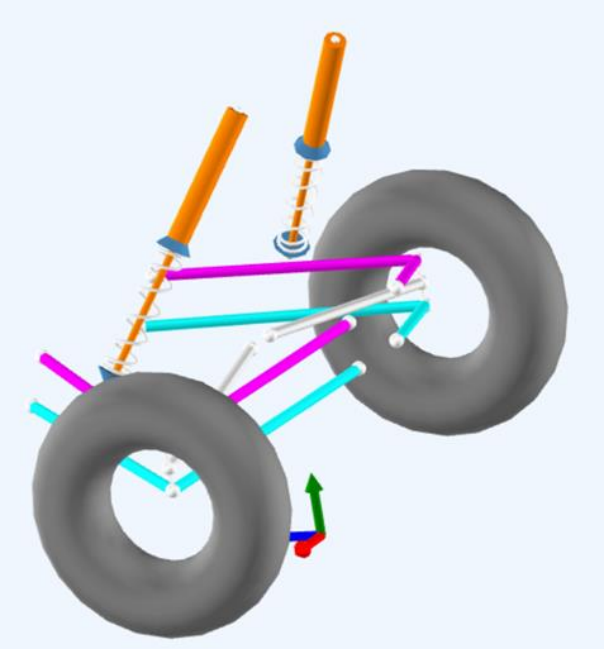

Figure 9.4-1: Rear Suspension

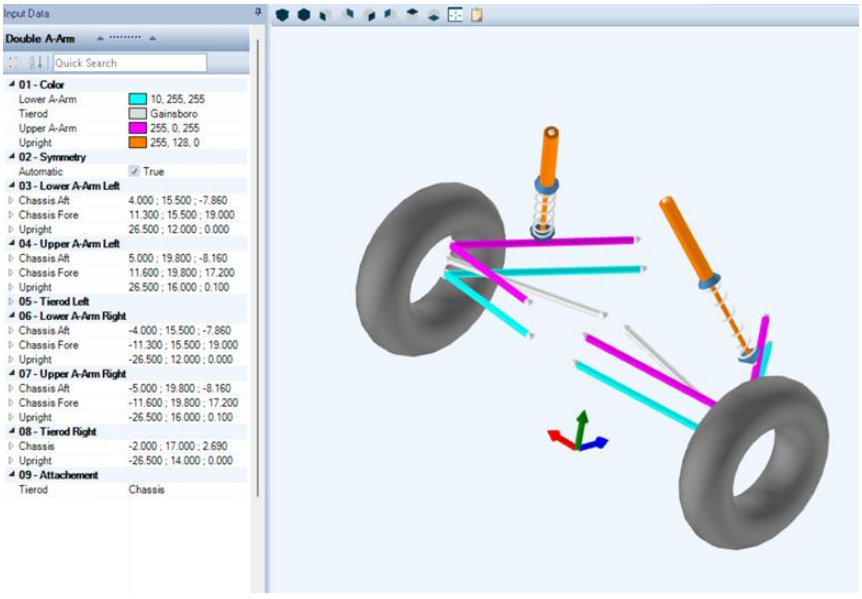

Figure 9.4-2: Rear suspension configuration

	Camber Angle Gain in Heave [Left] [Rear] (in/deg)	Camber Angle Gain in Roll [Left] [Rear] (-)	Camber Angle Gain in Pitch [Left] [Rear] (-)	Camber Angle [Left] [Rear] (deg)	Camber Angle [Right] [Rear] (deg)	Motion [Heave] (in)	Motion [Roll] (deg)	Motion [Pitch] (deg)
Maximum Value	-1.355	1.639	3.23E-1	1.226	1.226	6.44E-1	0.00	0.00
Minimum Value	-3.092	-2.75E-1	-8.98E-1	-3.76E-1	-3.76E-1	-2.68E-1	0.00	0.00
Average Value	-1.707	-1.34E-2	-1.56E-1	2.1E-1	2.1E-1	1.1E-1	0.00	0.00
Start Value	-1.469	-2.54E-1	0.00	0.00	0.00	0.00	0.00	0.00
End Value	-1.469	-2.54E-1	0.00	0.00	0.00	0.00	0.00	0.00
Max Absolute Value	3.092	1.639	8.98E-1	1.226	1.226	6.44E-1	0.00	0.00
Variance Value	2.2E-1	2.2E-1	1.42E-1	2.34E-1	2.34E-1	7.99E-2	0.00	0.00
Std Deviation Value	4.69E-1	4.69E-1	3.77E-1	4.83E-1	4.83E-1	2.83E-1	0.00	0.00
Step [0]	-1.469	-2.54E-1	0.00	0.00	0.00	0.00	0.00	0.00
Step [1]	-1.589	-1.76E-1	-1.99E-1	2.36E-1	2.36E-1	1.55E-1	0.00	0.00
Step [2]	-1.771	-2.49E-2	-4.06E-1	4.95E-1	4.95E-1	3.09E-1	0.00	0.00
Step [3]	-2.067	2.45E-1	-6.24E-1	7.9E-1	7.9E-1	4.64E-1	0.00	0.00
Step [4]	-2.786	8.86E-1	-8.58E-1	1.153	1.153	6.19E-1	0.00	0.00
Step [5]	-3.092	1.639	-8.98E-1	1.226	1.226	6.44E-1	0.00	0.00
Step [6]	-2.253	4.14E-1	-7.14E-1	9.21E-1	9.21E-1	5.25E-1	0.00	0.00
Step [7]	-1.936	1.25E-1	-5.41E-1	6.74E-1	6.74E-1	4.06E-1	0.00	0.00
Step [8]	-1.740	-5.16E-2	-3.76E-1	4.57E-1	4.57E-1	2.88E-1	0.00	0.00
Step [9]	-1.603	-1.66E-1	-2.17E-1	2.59E-1	2.59E-1	1.69E-1	0.00	0.00
Step [10]	-1.503	-2.36E-1	-6.38E-2	7.5E-2	7.5E-2	5.05E-2	0.00	0.00
Step [11]	-1.430	-2.7E-1	8.48E-2	-9.88E-2	-9.88E-2	-6.82E-2	0.00	0.00
Step [12]	-1.379	-2.73E-1	2.28E-1	-2.65E-1	-2.65E-1	-1.87E-1	0.00	0.00
Step [13]	-1.355	-2.59E-1	3.23E-1	-3.76E-1	-3.76E-1	-2.68E-1	0.00	0.00
Step [14]	-1.365	-2.67E-1	2.79E-1	-3.24E-1	-3.24E-1	-2.3E-1	0.00	0.00
Step [15]	-1.377	-2.73E-1	2.34E-1	-2.71E-1	-2.71E-1	-1.91E-1	0.00	0.00
Step [16]	-1.391	-2.75E-1	1.88E-1	-2.18E-1	-2.18E-1	-1.53E-1	0.00	0.00
Step [17]	-1.408	-2.75E-1	1.42E-1	-1.65E-1	-1.65E-1	-1.15E-1	0.00	0.00
Step [18]	-1.426	-2.71E-1	9.5E-2	-1.11E-1	-1.11E-1	-7.65E-2	0.00	0.00
Step [19]	-1.446	-2.64E-1	4.78E-2	-5.58E-2	-5.58E-2	-3.83E-2	0.00	0.00
Step [20]	-1.469	-2.54E-1	0.00	0.00	0.00	0.00	0.00	0.00

Figure 9.4-3: Heave analysis

	Camber Angle Gain in Heave [Left] [Rear] (in/deg)	Camber Angle Gain in Roll [Left] [Rear] (-)	Camber Angle Gain in Pitch [Left] [Rear] (-)	Camber Angle [Left] [Rear] (deg)	Camber Angle [Right] [Rear] (deg)	Motion [Heave] (in)	Motion [Roll] (deg)	Motion [Pitch] (deg)
Maximum Value	-1.444	1.274	3E-1	1.27E-1	1.17E-1	0.00	4.76E-1	0.00
Minimum Value	-1.863	-1.558	-2.86E-1	-7.82E-2	-7.81E-2	0.00	-5.39E-1	0.00
Average Value	-1.578	-1.73E-1	9.27E-3	1.4E-2	6.07E-3	0.00	-2.49E-2	0.00
Start Value	-1.469	-2.54E-1	0.00	0.00	0.00	0.00	0.00	0.00
End Value	-1.469	-2.54E-1	0.00	0.00	0.00	0.00	0.00	0.00
Max Absolute Value	1.863	1.558	3E-1	1.27E-1	1.17E-1	0.00	5.39E-1	0.00
Variance Value	1.78E-2	9.37E-1	3.97E-2	5.72E-3	5.21E-3	0.00	1.19E-1	0.00
Std Deviation Value	1.33E-1	9.68E-1	1.99E-1	7.56E-2	7.22E-2	0.00	3.45E-1	0.00
Step [0]	-1.469	-2.54E-1	0.00	0.00	0.00	0.00	0.00	0.00
Step [1]	-1.444	1.92E-1	9E-2	4.13E-2	-3.75E-2	0.00	-1.57E-1	0.00
Step [2]	-1.460	6.04E-1	1.71E-1	7.85E-2	-6.38E-2	0.00	-3.02E-1	0.00
Step [3]	-1.500	9.44E-1	2.37E-1	1.06E-1	-7.63E-2	0.00	-4.22E-1	0.00
Step [4]	-1.542	1.179	2.82E-1	1.22E-1	-7.81E-2	0.00	-5.05E-1	0.00
Step [5]	-1.562	1.274	3E-1	1.27E-1	-7.7E-2	0.00	-5.39E-1	0.00
Step [6]	-1.547	1.206	2.87E-1	1.23E-1	-7.79E-2	0.00	-5.14E-1	0.00
Step [7]	-1.508	9.93E-1	2.46E-1	1.09E-1	-7.72E-2	0.00	-4.39E-1	0.00
Step [8]	-1.466	6.72E-1	1.84E-1	8.43E-2	-6.71E-2	0.00	-3.26E-1	0.00
Step [9]	-1.444	2.77E-1	1.07E-1	4.92E-2	-4.37E-2	0.00	-1.87E-1	0.00
Step [10]	-1.460	-1.54E-1	2.04E-2	9.11E-3	-8.92E-3	0.00	-3.52E-2	0.00
Step [11]	-1.518	-5.83E-1	-6.83E-2	-2.85E-2	3.07E-2	0.00	1.17E-1	0.00
Step [12]	-1.615	-9.71E-1	-1.52E-1	-5.67E-2	6.72E-2	0.00	2.57E-1	0.00
Step [13]	-1.729	-1.282	-2.21E-1	-7.23E-2	9.49E-2	0.00	3.71E-1	0.00
Step [14]	-1.825	-1.487	-2.69E-1	-7.75E-2	1.11E-1	0.00	4.49E-1	0.00
Step [15]	-1.863	-1.558	-2.86E-1	-7.82E-2	1.17E-1	0.00	4.76E-1	0.00
Step [16]	-1.825	-1.485	-2.69E-1	-7.75E-2	1.11E-1	0.00	4.48E-1	0.00
Step [17]	-1.734	-1.293	-2.24E-1	-7.27E-2	9.58E-2	0.00	3.75E-1	0.00
Step [18]	-1.626	-1.005	-1.59E-1	-5.88E-2	7.04E-2	0.00	2.69E-1	0.00
Step [19]	-1.532	-6.48E-1	-8.21E-2	-3.38E-2	3.69E-2	0.00	1.4E-1	0.00
Step [20]	-1.469	-2.54E-1	0.00	0.00	0.00	0.00	0.00	0.00

Figure 9.4-4: Roll analysis

	Camber Angle Gain in Heave [Left] [Rear] (in/deg)	Camber Angle Gain in Roll [Left] [Rear] (-)	Camber Angle Gain in Pitch [Left] [Rear] (-)	Camber Angle [Left] [Rear] (deg)	Camber Angle [Right] [Rear] (deg)	Motion [Roll] (deg)	Motion [Heave] (in)	Motion [Pitch] (deg)
Maximum Value	-1.469	2.49E-1	8.09E-2	0.00	0.00	0.00	0.00	2.91E-1
Minimum Value	-1.798	8.61E-2	4.88E-2	-1.78E-2	-1.78E-2	0.00	0.00	0.00
Average Value	-1.631	1.69E-1	6.43E-2	-8.19E-3	-8.19E-3	0.00	0.00	1.43E-1
Start Value	-1.469	2.49E-1	4.88E-2	0.00	0.00	0.00	0.00	0.00
End Value	-1.469	2.49E-1	4.88E-2	0.00	0.00	0.00	0.00	0.00
Max Absolute Value	1.798	2.49E-1	8.09E-2	1.78E-2	1.78E-2	0.00	0.00	2.91E-1
Variance Value	1.07E-2	2.64E-3	0.00	0.00	0.00	0.00	0.00	8.36E-3
Std Deviation Value	1.03E-1	5.14E-2	1.01E-2	5.59E-3	5.59E-3	0.00	0.00	9.14E-2
Step [0]	-1.469	2.49E-1	4.88E-2	0.00	0.00	0.00	0.00	0.00
Step [1]	-1.580	1.94E-1	5.91E-2	-5.13E-3	-5.13E-3	0.00	0.00	9.68E-2
Step [2]	-1.690	1.4E-1	6.98E-2	-1.11E-2	-1.11E-2	0.00	0.00	1.94E-1
Step [3]	-1.798	8.61E-2	8.09E-2	-1.78E-2	-1.78E-2	0.00	0.00	2.91E-1
Step [4]	-1.790	8.97E-2	8.01E-2	-1.73E-2	-1.73E-2	0.00	0.00	2.84E-1
Step [5]	-1.771	9.95E-2	7.81E-2	-1.6E-2	-1.6E-2	0.00	0.00	2.66E-1
Step [6]	-1.751	1.09E-1	7.6E-2	-1.48E-2	-1.48E-2	0.00	0.00	2.48E-1
Step [7]	-1.731	1.19E-1	7.4E-2	-1.35E-2	-1.35E-2	0.00	0.00	2.31E-1
Step [8]	-1.711	1.29E-1	7.2E-2	-1.23E-2	-1.23E-2	0.00	0.00	2.13E-1
Step [9]	-1.691	1.39E-1	7E-2	-1.12E-2	-1.12E-2	0.00	0.00	1.95E-1
Step [10]	-1.671	1.49E-1	6.8E-2	-1E-2	-1E-2	0.00	0.00	1.77E-1
Step [11]	-1.651	1.59E-1	6.6E-2	-8.89E-3	-8.89E-3	0.00	0.00	1.6E-1
Step [12]	-1.631	1.69E-1	6.41E-2	-7.79E-3	-7.79E-3	0.00	0.00	1.42E-1
Step [13]	-1.611	1.79E-1	6.21E-2	-6.72E-3	-6.72E-3	0.00	0.00	1.24E-1
Step [14]	-1.591	1.89E-1	6.02E-2	-5.68E-3	-5.68E-3	0.00	0.00	1.06E-1
Step [15]	-1.571	1.99E-1	5.83E-2	-4.67E-3	-4.67E-3	0.00	0.00	8.87E-2
Step [16]	-1.551	2.09E-1	5.64E-2	-3.68E-3	-3.68E-3	0.00	0.00	7.1E-2
Step [17]	-1.530	2.19E-1	5.44E-2	-2.72E-3	-2.72E-3	0.00	0.00	5.32E-2
Step [18]	-1.510	2.29E-1	5.26E-2	-1.79E-3	-1.79E-3	0.00	0.00	3.55E-2
Step [19]	-1.490	2.39E-1	5.07E-2	0.00	0.00	0.00	0.00	1.77E-2
Step [20]	-1.469	2.49E-1	4.88E-2	0.00	0.00	0.00	0.00	0.00

Figure 9.4-5: Pitch analysis

	Camber Angle Gain in Heave [Left] [Rear] (in/deg)	Camber Angle Gain in Roll [Left] [Rear] (-)	Camber Angle Gain in Pitch [Left] [Rear] (-)	Camber Angle [Left] [Rear] (deg)	Camber Angle [Right] [Rear] (deg)	Motion [Heave] (in)	Motion [Roll] (deg)	Motion [Pitch] (deg)	Motion [Steering] (deg)
Maximum Value	-1.469	-2.54E-1	0.00	0.00	0.00	0.00	0.00	0.00	4.02E-1
Minimum Value	-1.469	-2.54E-1	0.00	0.00	0.00	0.00	0.00	0.00	0.00
Average Value	-1.469	-2.54E-1	0.00	0.00	0.00	0.00	0.00	0.00	2E-1
Start Value	-1.469	-2.54E-1	0.00	0.00	0.00	0.00	0.00	0.00	0.00
End Value	-1.469	-2.54E-1	0.00	0.00	0.00	0.00	0.00	0.00	0.00
Max Absolute Value	1.469	2.54E-1	0.00	0.00	0.00	0.00	0.00	0.00	4.02E-1
Variance Value	0.00	0.00	0.00	0.00	0.00	0.00	0.00	0.00	1.63E-2
Std Deviation Value	0.00	0.00	0.00	0.00	0.00	0.00	0.00	0.00	1.28E-1
Step [0]	-1.469	-2.54E-1	0.00	0.00	0.00	0.00	0.00	0.00	0.00
Step [1]	-1.469	-2.54E-1	0.00	0.00	0.00	0.00	0.00	0.00	1.3E-1
Step [2]	-1.469	-2.54E-1	0.00	0.00	0.00	0.00	0.00	0.00	2.6E-1
Step [3]	-1.469	-2.54E-1	0.00	0.00	0.00	0.00	0.00	0.00	3.9E-1
Step [4]	-1.469	-2.54E-1	0.00	0.00	0.00	0.00	0.00	0.00	4.02E-1
Step [5]	-1.469	-2.54E-1	0.00	0.00	0.00	0.00	0.00	0.00	3.77E-1
Step [6]	-1.469	-2.54E-1	0.00	0.00	0.00	0.00	0.00	0.00	3.52E-1
Step [7]	-1.469	-2.54E-1	0.00	0.00	0.00	0.00	0.00	0.00	3.27E-1
Step [8]	-1.469	-2.54E-1	0.00	0.00	0.00	0.00	0.00	0.00	3.01E-1
Step [9]	-1.469	-2.54E-1	0.00	0.00	0.00	0.00	0.00	0.00	2.76E-1
Step [10]	-1.469	-2.54E-1	0.00	0.00	0.00	0.00	0.00	0.00	2.51E-1
Step [11]	-1.469	-2.54E-1	0.00	0.00	0.00	0.00	0.00	0.00	2.26E-1
Step [12]	-1.469	-2.54E-1	0.00	0.00	0.00	0.00	0.00	0.00	2.01E-1
Step [13]	-1.469	-2.54E-1	0.00	0.00	0.00	0.00	0.00	0.00	1.76E-1
Step [14]	-1.469	-2.54E-1	0.00	0.00	0.00	0.00	0.00	0.00	1.51E-1
Step [15]	-1.469	-2.54E-1	0.00	0.00	0.00	0.00	0.00	0.00	1.26E-1
Step [16]	-1.469	-2.54E-1	0.00	0.00	0.00	0.00	0.00	0.00	1E-1
Step [17]	-1.469	-2.54E-1	0.00	0.00	0.00	0.00	0.00	0.00	7.53E-2
Step [18]	-1.469	-2.54E-1	0.00	0.00	0.00	0.00	0.00	0.00	5.02E-2
Step [19]	-1.469	-2.54E-1	0.00	0.00	0.00	0.00	0.00	0.00	2.51E-2
Step [20]	-1.469	-2.54E-1	0.00	0.00	0.00	0.00	0.00	0.00	0.00

Figure 9.4-6: Steering analysis

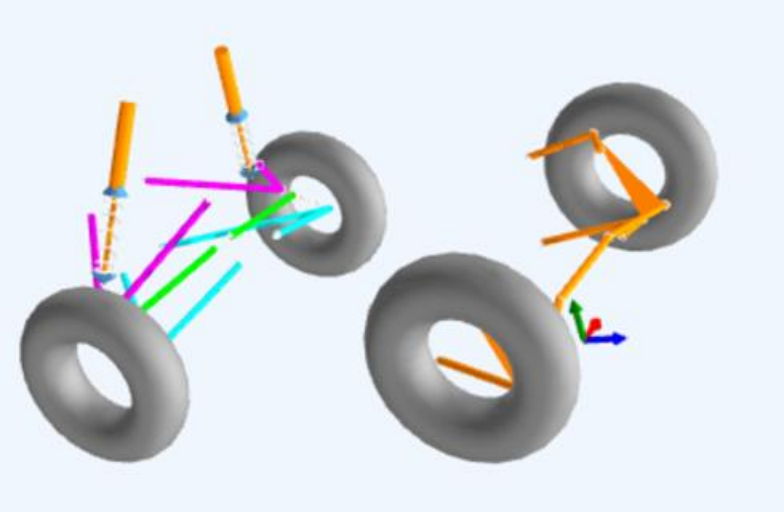

Figure 9.4-7: Rear and front suspension

9.5 Appendix E: Bill of Materials

Bill of Materials

Item #	Item Name	Description	Part #	Supplier	Website	Type	Quantity	Unit	Unit Cost	Total	Action
1	Heim Joints	Suspension Member Connection To Front Knuckle	JMX12T	Summit	Link	Component	4	ea	$ 43.99	0	In stock
2	3in x 6in x 48in Alumir	Steering Knuckle Material	F436	MetalsDepot	Link	Raw Material	2	ea	$ 659.20	1318.4	
3	3/4 in Bolts	Suspension Member Connection To Rear Knuckle	G8HB3431	Menards	Link	Component	4	ea	$ 4.35	17.4	
4	Screws	Screws that will attach steering housing to car (comes in pacl	90044A129	McMaster-Carr	link	Component	1	ea	$ 10.71	10.71	
5	Steering rack	Steering rack	2932N1	McMaster-Carr	Link	Component	1	ea	$ 150.00	0	Using in house
6	Steering bearing	Bearing that connects to pinion to allow for smooth roation	2780T65	McMaster-Carr	Link	Component	1	ea	$ 38.36	38.36	
7	U - Joints	Steering U-joints				Component	2	ea	$ 50.00	100	
8	Optimum Kinematics	Student edition software for suspension design and analysis		Optimum G	Link	Software	1	ea	$ 295.00	295	Purchased
9	4130 Chromoly 1.25"x	Chassis & Suspension tubing	CMR1049	Advanced Metal Sales		Raw Material	20	ft	$ 112.93	0	Donated
10	4 x Tires	Tires and rims 23"		BBWheels	link	Finished Good	4	ea	$ 148.47	593.88	
11	4 x Disc Brakes			Point Karting	Link	Finished Good	4	ea	$ 143.12	572.48	
12	4X Calipers			Wilwood	Link	Finished Good	4	ea	$ 171.42	685.68	
13	1" PVC tubing	1 in. x 10 ft. PVC Schedule 40 Tubing DWV Pipe	PVC40 PEPIP	Homedepot	Link	Raw Material	3	ft	$ 8.91	26.73	Purchased by Chasis
14	Vibration-damping bushing	Neoprene Vibration-Damping Bushing, 1.09" Diameter, 140 lbs	8109N14	McMaster-Carr	Link	Component	2	ea	$ 11.43	22.86	
15	Wooden 3/8 Dowels	Wooden Dowels for temperary tie rods		Home Depot	Link	Raw Material	3	ea	$ 11.09	33.27	Purchased
									Total	3714.77	